Departamento de Biología Molecular
Facultad de Ciencias
Universidad Autónoma de Madrid

A NETWORK OF ACTOMYOSIN REGULATORS CONTROLS APICAL MATURATION IN EPITHELIA

UNA RED DE REGULADORES DE ACTOMIOSINA CONTROLA LA MADURACION APICAL EN EPITELIOS

MADRID, 2018

Mariam Hachimi

Memoria presentada por Mariam Hachimi, licenciada en Biología, para optar al título de doctora en Biociencias Moleculares

Director de la tesis:

Dr. Fernando Martín Belmonte, PhD

Esta tesis ha sido realizada en el Centro de Biología Molecular Severo Ochoa (CSIC-UAM) bajo la supervisión del Dr. Fernando Martín Belmonte, Investigador Científico del CSIC.

La realización de esta Tesis ha sido posible gracias a una beca predoctoral FPI concedida a Mariam Hachimi por el Ministerio de Economía y Competitividad de España.

SUMMARY

One of the critical questions in cell biology is how tissues acquire their shape and function during development. Dynamic remodeling of the actin cytoskeleton has been largely established to be one of the principal causes of these morphological changes. For instance, during intestinal morphogenesis, the actin cortex undergoes massive changes, polarizing towards the apical domain, where it forms the terminal web, an intricate meshwork of actin filaments and actin-binding proteins that connects cell-cell junctions and anchors microvilli.

Decades of work have shown that epithelial actin remodeling is triggered by junction formation and maturation. However, dynamic actin remodeling in epithelia has rarely been explained by changes in gene expression, especially in vertebrates.

In this thesis, we report that the least characterized member of the Smoothelin protein family, Smoothelin-like 2, is induced during epithelial morphogenesis and is required for lumen formation. We also generate and describe a mutant allele for *smtnl,* the Smtnl2 zebrafish homolog. *Smtnl* is induced during intestinal morphogenesis, and is required for maturation of the apical F-actin cortex, and the successful formation of microvilli.

Using proximity biotinylation assays, we describe that Smtnl2 forms part of an apicojunctional network of actin binding proteins that is required for epithelial morphogenesis. We show that SMTNL2 binds to Cortactin and Coronin-1B (an inhibitor of Cortactin function), which, is sufficient and required to induce apical F-actin polymerization and actomyosin contraction in epithelial cells.

One of the key questions in mammalian epithelial biology is how the branched actin networks formed by initial cell-cell contacts transition into parallel actin arrays required for actomyosin-mediated cell shape changes that take place during cell spreading and apical-junction maturation. Here, we demonstrate that SMTNL2 is transcriptionally induced during epithelial morphogenesis to mediate this process through regulation of Cortactin and Coronin-1B.

Una de las preguntas más importantes en biología cellular es como los tejidos adquieren su forma y función durante el desarrollo. Una de las causas principales de estos cambios morfológicos es la renovación dinámica del citoesqueleto de actina. Por ejemplo, durante la morfogénesis intestinal, el córtex de actina atraviesa cambios masivos, polarizándose hacia el dominio apical, donde constituye la red terminal, formada por filamentos de actina y proteínas de unión a actina estrechamente conectados, y anclando las uniones célula-célula y las microvellosidades.

La renovación dinámica de la actina apical en las células epiteliales está regulada por la formación y maduración de las uniones célula-célula. Sin embargo, pocos estudios en vertebrados han explicado estos cambios a través de la expresión dinámica de genes reguladores de actina.

En este trabajo de tesis, hemos caracterizado a la proteína Smoothelin-like 2, la cual se encuentra inducida durante la morfogénesis epitelial y es necesaria para la correcta formación de lúmenes y la maduración apical. En este mismo trabajo hemos generado y descrito un mutante nulo de SMTNL2 en pez cebra. *Smtnl* se expresa en el intestino y es necesaria para la correcta formación y maduración de la membrana apical junto con la organización de las microvellosidades en enterocitos.

Empleando ensayos de biotinilación proximal, descubrimos que SMTNL2 forma parte de una red apical de proteínas de unión de actina, las cuales son necesarias para la morfogénesis epitelial. Hemos demostrado que SMTNL2 interacciona con Cortactina y Coronina-1B, un inhibidor de la actividad de Cortactina, para la correcta polimerización y la contractilidad de la actomyosina apical.

Una de las preguntas clave en biología epitelial es cómo se estructura la actina ramificada a lo largo del inicio de los contactos célula-célula, y como se organiza la actomyosina de forma paralela para permitir cambios en la arquitectura de la célula, como pueden surgir durante la migración o a lo largo de la maduración de las uniones y membrana apical. En este trabajo, demostramos que SMTNL2 se induce transcripcionalmente durante la morfogénesis epitelial y es necesaria junto con Cortactina y Coronina-1B para mediar este proceso.

INDEX

GLOSSARY

2D: 2-dimensional

3D: 3-dimensional

HPF: Hours Post Fertilization

DPF: Days Post Fertilization

ABP: Actin-Binding Protein

TAGNL2: Transgelin-2

SMTNL2: Smoothelin like 2

SMTNL1: Smoothelin like1

SMTN-A: Smoothelin A

SMTN-B: Smoothelin B

CORO1B: Coronin-1B

CTTN: Cortactin

AJs: Adherens Junctions

TJs: Tight junctions

AMIS: Apical Membrane Initiating Site

PAP: Pre Apical Patch

β-cat: β-catenin

ECIS: Electric Cell-substrate Impedance System

ECM: Extracellular Matrix

EMT: Epithelial-to-Mesenchymal Transition

FAs: Focal Adhesions

FBS: Fetal Bovine Serum

FRAP: Fluorescence Recovery After Photobleaching

GFP: Green Fluorescent Protein

RFP: Red Fluorescent Protein

ZA: Zonula Adherens

IF: Immunofluorescence

KD: Knock-down

CRISPR: Clustered Regularly Interspaced Short Palindromic Repeats

Cas9: CRISPR-associated protein-9 nuclease

LRP2: Low density lipoprotein-related protein 2

MG: Matrigel

MDCK: Madin-Darby Canine Kidney II

p-MLC: Phosphorylated NMII Regulatory Light Chain

RLC: Non-muscular Myosin II Regulatory light chains

ELC: Non-muscular Myosin II Essential light chains

PIP2: Phosphatidylinositol(4,5)-bisphosphate

PIP3: Phosphatidylinositol(3,4,5)-trisphosphate

PCP: Planar Cell Polarity

Gp135: Podocalyxin

Podxl: Podocalyxin

qPCR: Quantitative real-time PCR

SHH: Sonic Hedgehog

siRNA: small interfering RNA molecules

TER: Trans-epithelial resistance

TEM: Transmission Electronic Microscopy

ZO-1: Zonula Occludens 1

BP: BP clonase II enzyme

LR: LR clonase II enzyme

EPP: epithelial polarity programme

Sdt: Stardust

Crb: Crumbs

CaCo2: Caucasian Colon Adenocarcinoma cell line 2

CFTR: cystic fibrosis transmembrane conductance regulator

F-actin: Filamentous actin

G-actin: Globular actin

NPF: Nucleation Promoting Factors

Abp1: Actin-binding protein 1

NMII: Non-muscular myosin class II proteins

CH: Calponin Homology

TBL: TnT binding like domain

CBD: Calmodulin binding domain

CHASM: Calponin Homology-Associated Smooth Muscle Protein

ER: Estrogen Receptor

PR: Progesterone Receptor

WGA: Wheat Germ Agglutinin

INTRODUCTION

1. The origin and architecture of epithelial tissues

Most epithelial tissues are essentially large sheets of cells covering all the surfaces of the body exposed to the outside environment and lining the outward of organs. Epithelial cells derive from all three major embryonic layers (Figure I-1). The epithelia lining the skin, including parts of the mouth and nose, and the anus develop from the ectoderm. Cells lining the airways and most of the digestive system originate from the endoderm and finally the epithelium that lines vessels in the lymphatic and cardiovascular system, which derive from the mesoderm.

Epithelial tissues protect the entire body from physical, chemical, and biological wear and tear. The cells of an epithelium act as gatekeepers controlling permeability and allowing selective transfer of materials across a physical barrier. Some epithelia, such us tubular epithelia often include structural features that allow the selective transport of molecules and ions across their cell membranes. Epithelia are the most archetypal type of polarized tissue in metazoa, with ~60% of the cells in mammals being epithelial. Epithelial morphogenesis encircles all the processes that result in organ formation and the establishment of a determined body shape, comprising the molecular mechanisms that trigger cell shape changes, cell migration, cell division and correct cell differentiation. These morphogenetic changes are genetically regulated in time and in space and are attended by differentiation of the cells within the epithelia into different identities. It is crucial to understand these processes to elucidate the mechanisms that drive the cellular rearrangement of epithelial tissues. Epithelial morphogenesis is orchestrated by a variety of signaling molecules and transcription factors that coordinate changes in cell shape, cell rearrangement and cell migration (Gilmour et al., 2017; Rauzi et al., 2015). Morphogenesis of epithelial, or epithelial-derived, tubular organs such as the gut and vasculature requires the generation of apico-basal polarity, and the formation of a central lumen (Bryant and Mostov, 2008). One fundamental feature of epithelial cells is that they are well polarized. Cell polarity is defined by an apico-basal axis, that is, the existence of an apical domain lining the central lumen and a basolateral domain attached to adjoining cells and to the estroma (Bryant and Mostov, 2008; Rodriguez-Fraticelli and Martin-Belmonte, 2013). These domains are characterized by their different composition in proteins and lipids, which develop different functions. The establishment of membrane polarization

requires the coordination of several cellular processes, including polarized vesicular transport, polarization of the cytoskeleton and the establishment of cell adhesion and junction complexes. The mechanisms that promote the establishment of epithelial cell polarity are not completely understood, and can differ among different types of mammalian epithelial cells and model organisms. The establishment and the control of this tissue architecture are fundamental not only for the understanding of epithelial organogenesis but also because the loss of tissue polarity is associated with different diseases, such us polycystic kidney diseases, which are due to an increase in tube size, spina bifida, associated to a failure in neural tube closure, and one of the most studied diseases, carcinomas (cancers derived from epithelial tissues) in which it can lead to tumor progression invasion and metastasis (Landy et al., 2016; Martin-Belmonte and Perez-Moreno, 2011).

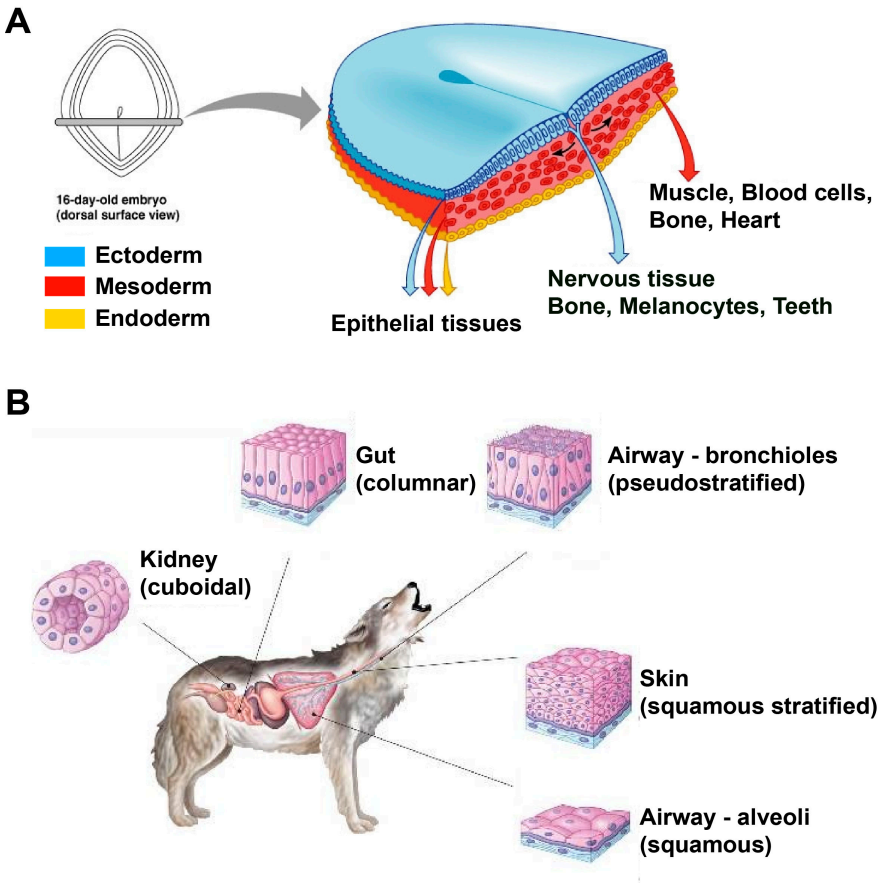

Figure I-1. Origin and diversity of epithelial tissues. A) Epithelial tissues are derived from all embryonic layers (ectoderm, mesoderm and endoderm). **B)** Epithelial cells can acquire different morphologies in each organ, adapted to the functions and necessities of the tissue they form.

2. Epithelial Cell polarity

Cell polarity is vital for the structure and function of epithelial tissues. Epithelial polarization requires the interposition of several fundamental cell processes that must be tightly regulated in space and time (Roignot et al., 2013). The establishment and maintenance of a polarized epithelial cell with apical, basolateral and ciliary surface domains, is directed by an epithelial polarity programme (EPP), which is controlled by a network of protein and lipid regulators. The EPP is organized in response to extracellular cues and requires the establishment of an apical–basal axis, intercellular junctions, cytoskeletal rearrangements and polarized trafficking (Rodriguez-Boulan and Macara, 2014).

2.1 Apical and basolateral domains

The partitioning of apical and basolateral domains that define cell asymmetry is achieved by the coordination of three main polarity complexes, which are highly conserved among metazoans (Figure I-2). **The Par/aPKC complex**, consisting in Par3, Par6 and atypical protein kinase C (aPKC), together with Cdc42, controls cell polarity in different contexts, and maintains the integrity of the apical domain by the recruitment of proteins from the Crumbs and Scribble complexes (Goldstein and Macara, 2007). **The Crumbs complex** consisiting of Crb, Stardust (Sdt), PATJ and Lin-7, is localized apically and controls mainly the extension of the apical domain (Bulgakova and Knust, 2009). **The Scribble complex** consisting of Scribble, Lethal giant larvae (Lgl) and Discs large (Dlg), which are well conserved across species, is localized to the lateral membrane and restricts tight junction formation to the apical domain by inhibiting Par3 recruitment to the lateral domain (Rodriguez-Boulan and Macara, 2014; Yamanaka and Ohno, 2008). All these complexes are regulating each other by negative and positive feedback loops and impairment of any of their functions causes changes in cell polarity that lead to defective epithelial layers and disrupted morphogenesis.

2.2 Cell-cell junctions

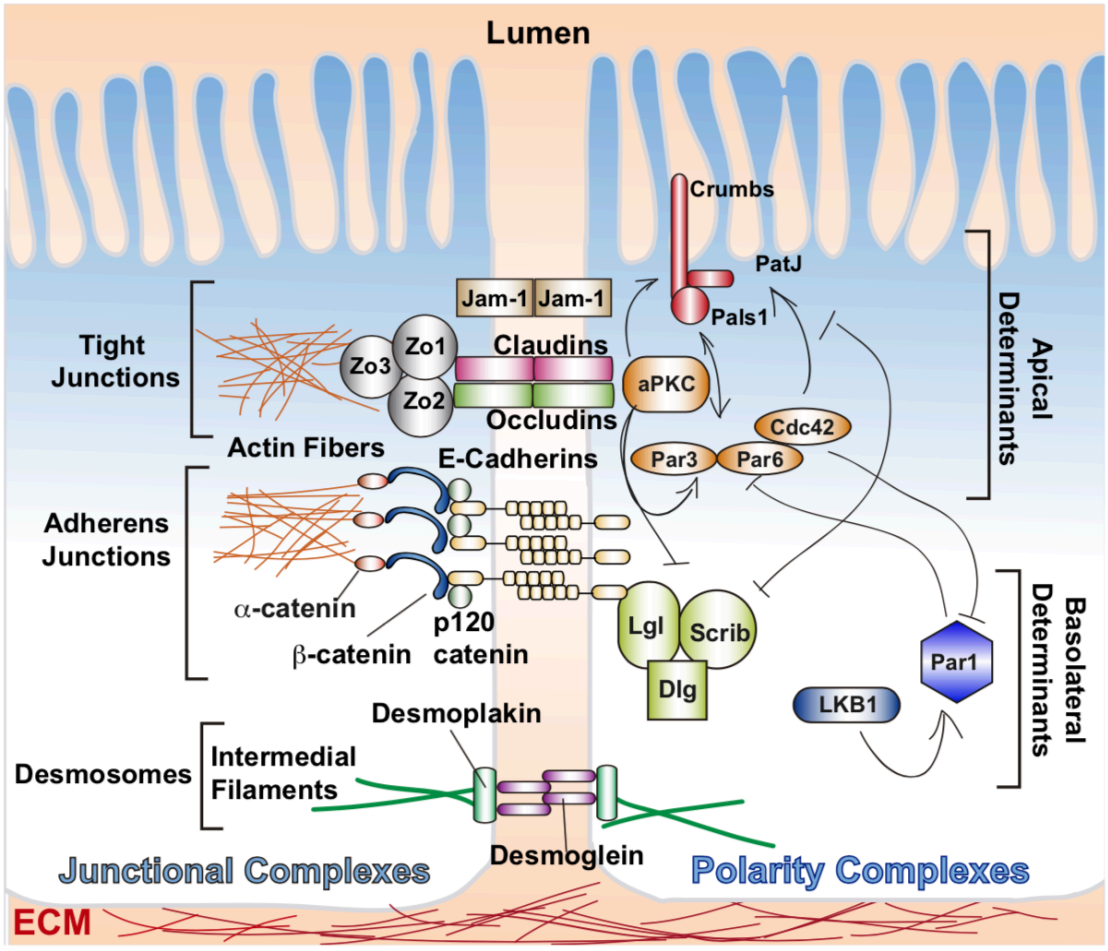

Figure I-2. Cell junctions and polarity complexes. Epithelial organization is initiated and maintained through the formation of junctional complexes (tight junctions, adherens junctions and desmosomes). These junctional complexes recruit polarity protein complexes, which define the identity of each domain. Apical determinants are the aPKC and Crumbs complexes. Basolateral determinants are the LKB1/Par1 and Scribble complexes.

The initial step in the assembly and function of the polarity proteins is the organization of the junctional complexes. In epithelia, these complexes can be divided into tight junctions (TJs), adherent junctions (AJs), and desmosomes, in the lateral side (Figure I-2). Since TJs and AJs are tightly associated and localized in the apical end of the lateral domain they are often referred to as "the apical junctional complex" (except in the endothelial cell, in which both complexes are found to be intercalated). The apical junctional complexes define the apicobasal axis by restricting the apical and basal membrane domains. The TJs encompass a large

number of transmembrane proteins, of which their main function is to control the paracelullar permeability, that is, the passive transport of molecules across the tissue. In addition, TJs restrict the exchange of membrane components between apical and basolateral domains, also known as the “fence function” (Zihni et al., 2016). AJs perform multiple functions including initiation and stabilization of cell–cell adhesion, regulation of the actin cytoskeleton, intracellular signaling, and transcriptional regulation. The AJs in epithelia are formed mainly by E-cadherins, which are the most commonly studied cadherins. E-cadherins are homotypic cell adhesion receptors. The cytoplasmic domain of cadherins interacts with β-catenin (β-cat), which in turn is bound to actin filaments via α-catenin and via other scaffolding and nucleating proteins to the cytoskeleton and can respond to extracellular stimuli. E-cadherins mediate many facets of tissue morphogenesis. In response to extracellular signals they control cell sorting, cell rearrangements and cell movements, and not only during the development of new tissues, but likewise in the adult by controlling tissue growth and homeostasis (Gumbiner, 2000). Together TJs and AJs, help the epithelial cells form a tight, polarized cell layer that can perform barrier and transport function.

2.3 The cytoskeleton

The cytoskeleton founds the pillars that sustain the epithelial cells. The cytoskeleton of epithelial tissues is mainly composed of actin, microtubules and intermediate filaments (keratins). Actin and microtubules provide a structural basis for cell polarization because of their intrinsic structural polarity along the polymer networks (Bornens, 2008). Additionally, the cytoskeleton has a crucial role in targeting and membrane sorting of proteins and organelle positioning in polarized epithelial cells (Bornens, 2008; Mays et al., 1994). For an epithelial cell to achieve a polarized columnar shape, both the actin and microtubule cytoskeleton have to be polarized (Figure I-3). To succeed this morphology, microtubules are organized in bundles that are polarized along the apico-basal axis, with the minus end pointed toward the apical membrane and the plus end towards the basal membrane. This divergence is paramount for the targeting of transport vesicles between the different membrane compartments and therefore to maintain the

identity of the apical and basolateral domain. Disruption of microtubules with nocodazole or colchicine results in a missorting of apical proteins to the basolateral domain together with a decrease in delivery of apical cargos (Bornens, 2008; Chifflet and Hernandez, 2012; Mays et al., 1994). On the other hand, the most conspicuous actin structure in epithelial cells is the actin belt (also known as the terminal web), a bundle of three-dimensional meshwork located beneath the apical domain, which recruits several acting-binding proteins, forming "the apical cell cortex". This actin network is tightly associated with the apical junctions complex and determines cell shape and function on this domain (Gottlieb et al., 1993). Furthermore, actin filaments extending from the terminal web constitute the core of the microvilli, which are essential for increasing the surface area for diffusion, developing several functions such as membrane secretion and absorption of salts and nutrients (Fath et al., 1993; Nelson et al., 1990). Therefore, the association of actin filaments to the plasma membrane is crucial not only to sustain cell architecture but also for the correct cell function. Ultimately, the major component of the epithelial cell cytoskeleton is the intermediate filaments or

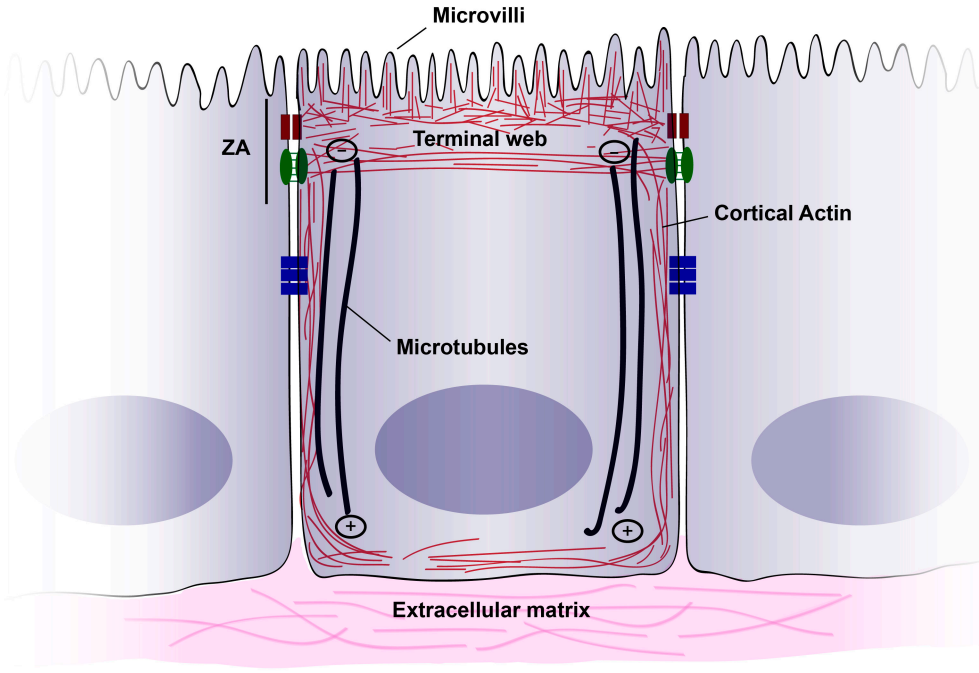

Figure I-3. Cytoskeletal polarity. The cytoskeleton in epithelial cells is highly polarized. Beyond the intrinsic polarity of the cytoskeletal filaments, which contain a positive and a negative end, actin is accumulated in the apical domain, where it forms a dense network interconnected with the zonula adherens (ZA). Cortical microtubules are also polarized along the apicobasal axis, with their minus ends pointing towards the apical domain.

keratins, which, in contrast to actin and microtubule filaments, present no intrinsic polarization. Still, their distribution is often polarized, for example in intestinal epithelial cells they form a strip below the apical terminal web region and localized within the apical junction complex (Coch and Leube, 2016).

3. The emergence of epithelial tubes or lumens

The emerging properties of the tissue result from the combined roles of the individual cells that are involved (DM Bryant - 2008). During the morphogenesis of an epithelial tissue, cells often organize forming tubes. There are several biological ways to achieve a tube but they all lead to the same path, by forming an enclosed and open lumen. Strategies for making tubes can be classified according to whether the joining cells are already polarized or whether such polarity is achieved in response to local clues (Hogan and Kolodziej, 2002; Lubarsky and Krasnow, 2003; Sigurbjornsdottir et al., 2014). Sheets of polarized cells generate hollow lumens through two different processes: wrapping and budding, both processes involving actomyosin-mediated apical constriction (Figure I-4). In the case of wrapping, the polarized epithelial sheet curves to enclose a hollowed cavity. For instance, during budding, the formation of tubes relies on an invagination process. Two examples of wrapping are the formation of the neural tube in vertebrates and gastrulation in *Drosophila* (Dessaud et al., 2008; Leptin, 2005). Otherwise, the mammalian lung and mammary ducts, as well as the formation of the tracheal system in *Drosophila,* are achieved primarily through a budding process of new sprouts (Bryant and Mostov, 2008; Lubarsky and Krasnow, 2003). Non-polarized cells can also convert into polarized epithelial tubes and create lumens ‘‘de novo” between the cells, usually through a process of mesenchymal to epithelial transition (MET) (Bernascone et al., 2017; Datta et al., 2011; Thiery, 2009). Making tubes from unpolarized cells can be divided into two main patterns: hollowing and cavitation (Figure I-4). In hollowing, the lumen is formed by membrane separation and repulsion, whereas in the process of cavitation the central lumen emerges from a mass of cells where the inner cells start to undergo apoptosis. The 3D-MDCK system can develop both processes depending on culture conditions (Martin-Belmonte and Mostov, 2008; Martin-

Belmonte et al., 2008). One example of cord hollowing is the process of lumen formation in the zebrafish gut and vasculature (Herwig et al., 2011; Horne-Badovinac et al., 2001), whereas a clear example of cavitation is the formation of the mammary gland terminal end bud (Debnath et al., 2002). Due to the subsistence of diverse routes that epithelial organs follow to form tubes, many *in vitro* and *in vivo* models have been used, each one providing different insights into lumen and tube formation. Even so, in all systems, lumen formation involves the structured expansion of the apical plasma membrane through general mechanisms of vesicle transport and the regulation of microtubule and actin cytoskeleton (Sigurbjornsdottir et al., 2014).

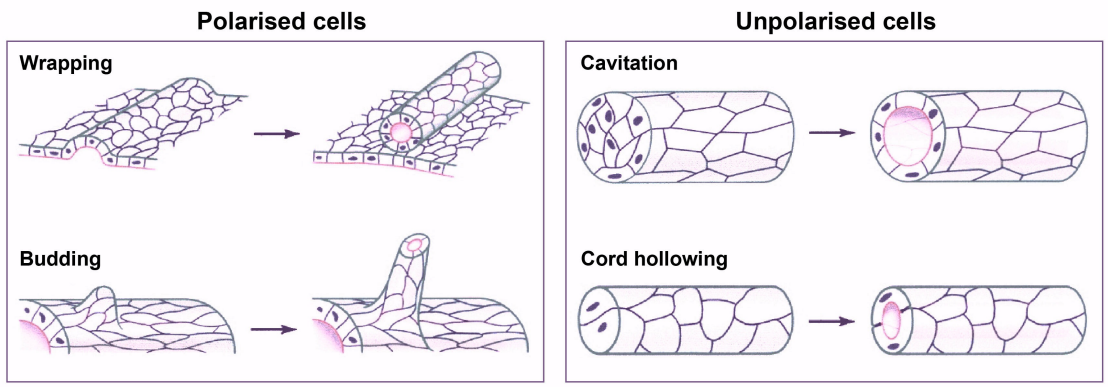

Figure I-4. Mechanisms of lumen formation. Epithelial tubes can be formed from a previous epithelium (wrapping and budding), or from a rod of cells lacking distinct apical and basal domains (cavitation and hollowing). (Adapted from Lubarsky and Krasnow 2003)

3.1 In vitro models

Epithelial cell lines have been cultured in 2D monolayers to study epithelial behavior, vesicle trafficking or polarity. However, these types of cultures are far from recapitulating what happens *in vivo*. In the last years three dimensional cultures (3D) have been developed, which allow the molecular study of cellular events necessary for the formation of epithelial organs. Although many epithelial cell lines have been cultured in 3D, the 3D-MDCK system is perhaps the most indebted and widely used *in vitro* model to investigate cell polarity during epithelial morphogenesis (Apodaca et al., 2012; Bryant et al., 2010; Bryant and Mostov, 2008; Datta et al., 2011; Gassama-Diagne et al., 2006; Martin-Belmonte et al., 2008; O'Brien et al., 2001; O'Brien et al., 2002; Rodriguez-Fraticelli et al., 2010;

Roland et al., 2011; Yu et al., 2005). In this system, MDCK cells, which are canine kidney cells from distal tubule, are cultured embedded in ECM (collagen or Matrigel) where they grow forming cysts (Figure I-5). These cysts are spherical structures consisting of a sheet of polarized epithelial cells enclosing a central liquid-filled lumen, reminding the structure of an acini or alveoli, and mimicking the transversal section of a kidney or gut tube. Besides the 3D-MDCK model, there are several organotypic models of different epithelial tissues that have been used: CaCo2 cells from human colon carcinoma (Ivanov et al., 2008; Jaffe et al., 2008; Townley et al., 2012) primary luminal mammary epithelial cells (MECs) and other cell lines derived from mammary glands (Akhtar and Streuli, 2013; Lo et al., 2012; Schmeichel and Bissell, 2003). Additionally, new techniques of organotypic cell culture have been developed based on micropatterns and other microarchitecture based models (Rodriguez-Fraticelli et al., 2012). These micropatterns have brought the possibility of interacting mechanistically with the cells, which provided new insights in the biomechanics of lumen formation (Madsen et al., 2015; Tozluoglu et al., 2013). In parallel, many other laboratories have developed promising 3D cell culture system of primary stem and progenitor cells, denominated organoids. Some of these organoid cultures combine stem cells with animal explants or cell lines, and specific culture conditions, to recreate an organ-like structure in a low scale. Organoids derived from kidney (Takasato et al., 2015; Takasato and Little, 2016; Xia et al., 2013), guts (Sato et al., 2009), mammary glands (Nguyen-Ngoc et al., 2015) or optic cups (Eiraku et al., 2011) have arisen, creating a powerful tool to study differentiation and morphogenesis *in vitro.*

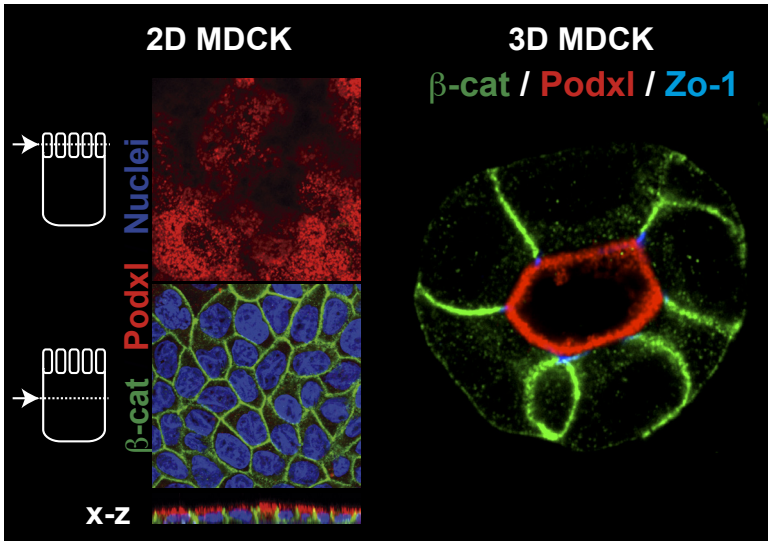

Figure I-5. In vitro models of epithelial morphogenesis. MDCK cells can be cultured in transwells, forming a polarized epithelial layer, in which we can detect apical membranes (Gp135/Podxl) and basolateral membranes (β-catenin). In presence of extracellular matrix (3D cultures), MDCK cells grow into organoid-like spheres, or cysts, through the process of hollowing.

3.2 *In vivo models*

There are many animal models that have been used for the study of epithelial tube morphogenesis, including *Drosophila, C. elegans, zebrafish* and *mouse*. Each of these models present different patterns, strengths and weaknesses, so the studies made on them are often complementary. Because of its powerful genetics, the *Drosophila* trachea and salivary gland are widely studied model systems for wrapping and budding tubes, respectively. Both organs begin as polarised epithelial placodes, which through coordinated cell shape changes, cell rearrangements, and cell migration form tubes (Kerman et al., 2006). The mouse model has provided insights in the processes of branching of mammary ducts or the ureteric bud using *ex vivo* cultures (Iruela-Arispe and Beitel, 2013; Johnson and Mueller, 2013). In the case of zebrafish, this model has been traditionally oriented to the study of the angiogenesis, including the patterning of the dorsal aortal and intersegmental vessels (Xu and Cleaver, 2011; Xu et al., 2011). However, the mechanisms of lumen formation in other organs are increasingly under scrutiny (Figure I-6). For

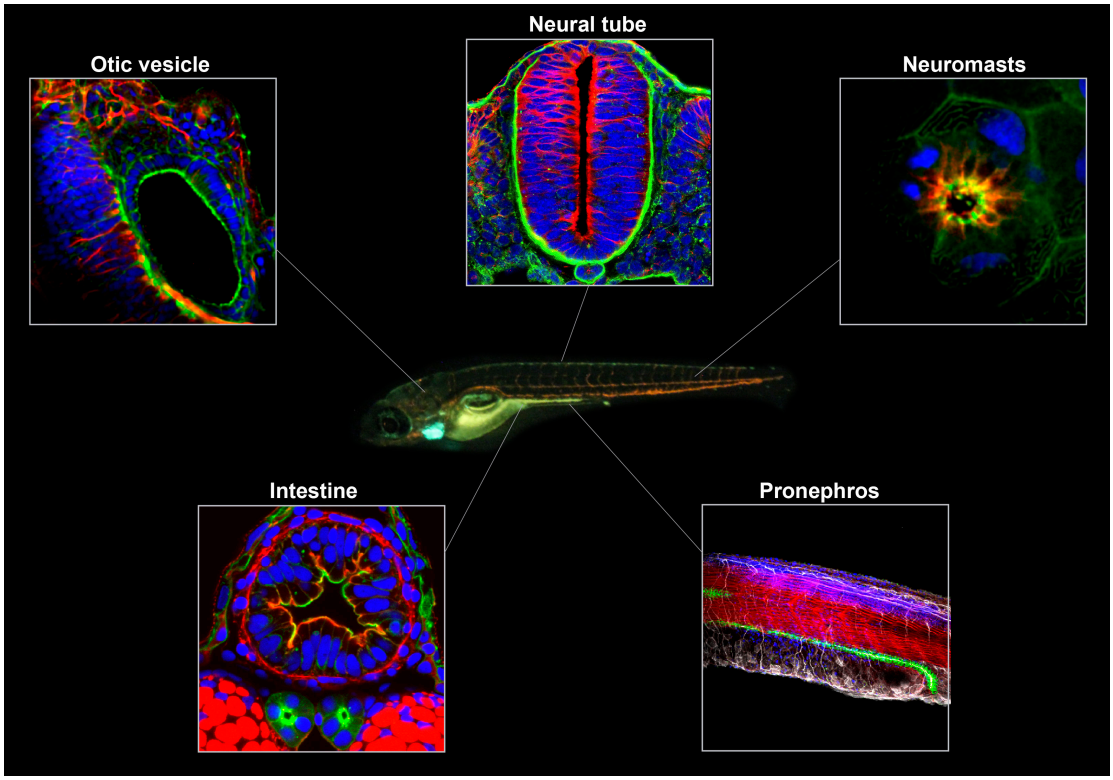

Figure I-6. Models to study lumen formation in zebrafish. The otic vesicle, the neuromasts of the lateral line, the intestine and the pronephros form their lumens by hollowing. In contrast, the lumen of the neural tube is formed by wrapping.

instance, genetic analysis using the zebrafish has led to the identification of mutations in molecules that are required for gut morphogenesis (Pack et al., 1996). Lumen formation in the zebrafish gut occurs by '*de novo*' apical polarisation, and the developmental steps have been recently characterized (Alvers et al., 2014; Bagnat et al., 2007; Ng et al., 2005; Wallace et al., 2005). In the case of the pronephros, the primordial kidney, it is known that flux from the glomerulus, driven by motile cilia, is necessary for cell migration and thus for elongation of the pronephric duct (Vasilyev and Drummond, 2012). However, less is known about how the pronephros builds its central lumen.

4. " De novo" lumen formation

To understand the origin of cell organization first requires to appreciate how the self-organizing physical and biochemical properties of cellular constituents can convert simple sequential changes in gene expression levels into complex changes in physical and three dimensional structures (Rafelski and Marshall, 2008). The generation of epithelial organs from unpolarized cells can be simplified in four key events: first, the extracellular environment provides the initial cues for the cell to orient the polarization axis and to recognize neighboring cells (Figure I-7). Second, a polarized vectorial membrane trafficking is induced together with the polarization of the cytoskeleton to originate the first signs of an apical domain. Third, a small lumen appears. Then, through collaboration with paracellular transport of ions to the luminal space, electrostatic repulsion of proteins in the membrane and apical acto-myosin contractility, an open and mature luminal space will form. Finally, this lumen will be sustained by orientated cell division (Lubarsky and Krasnow, 2003; Martin-Belmonte et al., 2008)(Figure ale). If any of these events are perturbed, different defects on lumen formation can be acquired, resulting in many human diseases, such us carcinomas or polycystic kidney diseases, among others. So, the understanding and control of these processes are crucial for the comprehension of epithelial development and to come up with novel therapy strategies.

4.1 Initial polarization

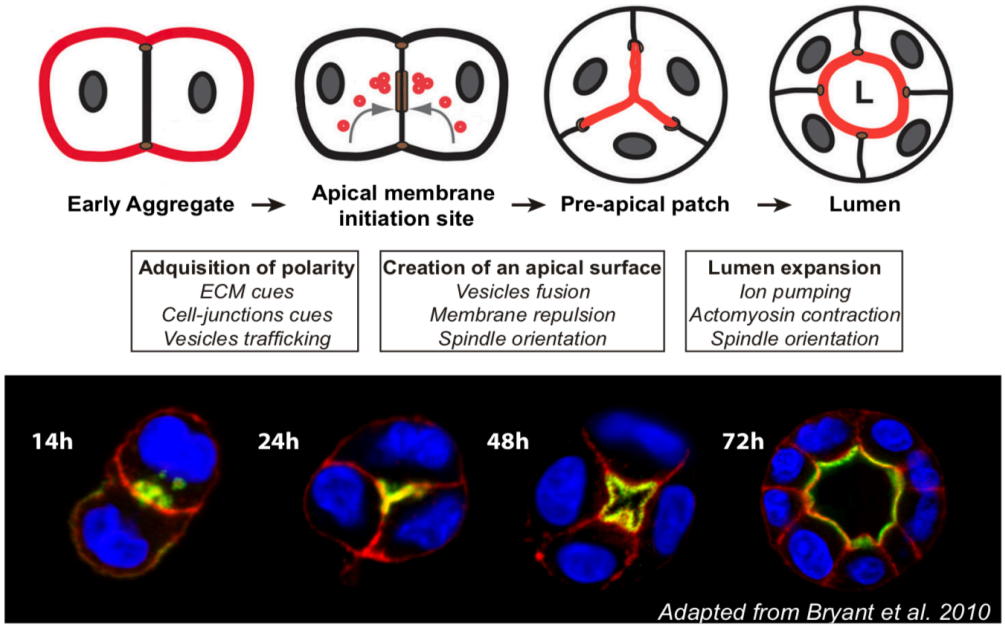

Figure I-7. Mechanisms for de novo lumen formation. *De novo* lumen formation in 3D MDCK can be subdivided into four stages. First, early aggregates orient apicobasal polarity through positioning of ECM and cell-cell junction cues. Then, apical membranes are inserted between cell-cell contacts and lumens are formed by apical membrane repulsion and actomyosin contraction. Importantly, single lumens are maintained through controling mitotic spindle orientation to position daughter cells within the plane of the monolayer. Finally, lumen expansion requires osmotic movement of water and ions through the tight junctions.

In the kidney tubular epithelium, lumens form perpendicular to the ECM-contacting surface. One axis is provided through the interaction of the cell with the ECM components. Afterwards, the cell needs to recognize neighboring cells and establish cell-cell contacts, which will provide the second axis. These inputs will afford molecular cues, and thus spatial coordinates, for the generation and the positioning of apical membranes between two cells. In 3D-MDCK β1-integrin seems to be critical for the correct orientation of cell polarity and lumen formation. β1-integrin has the ability to interact with collagen I, resulting in an internal signal transduction response entailed in the activation of the Rac1 pathway. In turn, Rac1 activation induces the secretion and assembly of laminin to the ECM, generating a positive feedback loop, which reinforces the orientation signaling pathway (Naylor et al., 2005; O'Brien et al., 2001; Wu et al., 2009; Zhang et al., 2009). The

mechanism of β1-integrin seems to relay on the orientation of the microtubule cytoskeleton, through the ILK-integrin module (integrin-linked kinases plus β1-integrins) (Akhtar and Streuli, 2013). Moreover, β1-integrin deficiency perturbs the normal orientation of the apical surface, through the inappropriate activation of RhoA–ROCKI–myosin II pathway, suggesting that the ECM provides mechanical cues, which are required for the correct lumen formation through the regulation of cytoskeletal tension.

4.2 Determining membrane identity

The aforementioned polarity defining cues induce the segregation of membrane phosphoinositide types, which are implicated in specifying membrane identity (Di Paolo, 2006). Diverse phosphoinositides are enriched in specific subcellular compartments, concentrated at the cytosolic surface of cellular membranes. In MDCK cells Phosphatidylinositol (3,4,5)-trisphosphate (PIP3) determines the basolateral membrane, whereas Phosphatidylinositol (4,5)-bisphosphate (PIP2) is required for apical membrane identity (Eaton and Martin-Belmonte, 2014; Gassama-Diagne et al., 2006; Rodriguez-Boulan et al., 2005). It has been proposed that the signalling mediated by the balance of PIP2 and PIP3 at the plasma membrane controls many important cellular processes such as growth, polarity, migration, and proliferation, (Carracedo and Pandolfi, 2008) all of which are regulated by the enzymes Phosphatase and tensin homolog deleted in chromosome 10 (PTEN) and Phosphatidylinositol-3-kinase (PI3K). PTEN can recruit and activate the RhoGTPase Cdc42 to the cell cortex through specific apical enrichment of PIP2, maintaining the activity of the Par6-aPKC complex (Martin-Belmonte et al., 2007; Martin-Belmonte and Mostov, 2007) and contributing to the generation of apical membrane identity.

4.3 Vectorial trafficking

Epithelial cells have to ensure proper delivery of apical and basolateral cargoes to their respective membrane domains to maintain cell polarity. Protein trafficking is regulated by sorting signals contained within the proteins

themselves, which are recognised by the specific sorting machinery (Folsch, 2008; Rodriguez-Boulan et al., 2005). The different trafficking routes and sorting mechanisms in epithelial cells include biosynthetic, endocytic, recycling, and transcytotic pathways. The biosynthetic pathway delivers newly synthesised proteins to the apical and basolateral membranes. Once these proteins reach the plasma membrane, they can also be endocytosed and delivered to the early endosomes where they follow the endocytic route for degradation in the lysosomes (Eaton and Martin-Belmonte, 2014; Rodriguez-Fraticelli et al., 2015). Proteins in the plasma membrane can also follow the recycling route by passing through recycling endosomes, which can sort them back to the original cell surface (Desclozeaux et al., 2008; Langevin et al., 2005). These proteins can also be transported across the cell to the opposite plasma membrane through the transcytotic pathway (Bryant et al., 2010; Madrid et al., 2010). All these routes must be finely regulated in order to induce and maintain apicobasal cell polarity. Trafficking of vesicles is also linked to microtubule elongation and stabilization, since vesicles move along microtubules attached to motor proteins. Remarkably, actin cytoskeleton is also important in this process, providing the driving force for apical vesicle formation and transport. Two clear examples are the processes of endocytosis and phagocytosis, which both requires actin polymerization to drive the extension of the plasma membrane around the particle surface (Goley and Welch, 2006). For instance, Myosin-Vb, is required for epithelial polarity, recycling and brush border formation (Gidon et al., 2012; Muller et al., 2008; Szperl et al., 2011; Thoeni et al., 2014). Curiously, little is known about the role of actin or actin regulators in this process.

4.4 Lumen opening and expansion

Once the apical membrane is delivered to the cell surface, an extracellular space must be generated between neighboring cells. The first sign of an apical domain is known as the apical membrane initiation site (AMIS). Apical vesicles fuse at the cell-cell junctions, forming two layers of apical membranes that are very close to each other. In this situation, the secretion of proteins that helps to prevent membranes from sticking plays a significant role *in vitro* (3D cysts) and *in vivo*

(Meder et al., 2005; Schottenfeld et al., 2010; Strilic et al., 2010; Strilic et al., 2009). Glycoproteins and polysaccharides such us mucin 1, Crumbs and Gp135 (also known as podocalyxin) among others, induce membrane detachment by steric hindrance of cell-cell adhesion. This structure where the apical plasma membranes are separated but the lumen is still closed is called the pre-apical patch (PAP). In addition, Gp135 also controls subapical recruitment of an F-actin–ERM–RhoA–myosin-II network, which may generate the force required for lumen expansion and maintenance (Datta et al., 2011; Lammert and Axnick, 2012). This apical actin network, together with the Diaphanous family of formins, polymerize parallel actin tracks required for subsequent secretion during lumen maturation (Massarwa et al., 2009). Additionally, the apical actomyosin belt orientates the centrosome to the apical pole (Rodriguez-Fraticelli et al., 2012), which in turn organizes the microtubule cytoskeleton and therefore the traffic of vesicles. Besides membrane repulsion and apical contractility, filling of the cavity with liquid is also contributing to lumen expansion (Figure I4). In this scenario, TJ proteins play an important role. It is known that Claudin-2 is required for epithelial morphogenesis (Galvez-Santisteban et al., 2012; Krupinski and Beitel, 2009). Claudins form selective pores that allow the interchange of different ions, thereby controlling the permeability of epithelial junctions. In zebrafish, Claudin-15a controls lumen coalescence in the gut, whereas the claudin-15-like b regulates intrahepatic biliary duct morphogenesis (Bagnat et al., 2007; Cheung et al., 2012). Other components such ion pumps are required as well. The cystic fibrosis transmembrane conductance regulator (CFTR) channel increases the luminal concentration of chloride ions, resulting in the net pumping of fluid into the luminal cavity (Bagnat et al., 2010; Yang et al., 2008).

4.5 Orientation of cell division

The orientation of cell divisions plays an important role in controlling differentiation and morphogenesis in many animal models, including the morphogenesis of the central nervous system and the skin (Clarke, 2009; Siller and Doe, 2009; Williams et al., 2011). The orientation of cell division is controlled by capture of astral microtubules by the GaI, Pins (LGN) and NuMa, that form a

complex initially described to be necessary for regulation of asymmetric cell division in Drosophila neuroblast (Cai et al., 2003; Schaefer et al., 2000; Yu et al., 2000) and vertebrates (Blumer et al., 2006; Du et al., 2001; Morin et al., 2007; Peyre et al., 2011). More recently the role of this complex has been identified in epithelial morphogenesis in 3D-MDCK cells (Hao et al., 2010; Rodriguez-Fraticelli et al., 2010; Zheng et al., 2010). Furthermore, we have found that an EGF-IQGAP1 module regulates the mitotic spindle orientation, probably through the initial attachment of the microtubules (Banon-Rodriguez et al., 2014). Curiously, Cdc42 not only regulates membrane trafficking but also the orientation of the mitotic spindle through the GEFs Intersectin-2, Tuba and Graf1 (Kieserman and Wallingford, 2009; Qin et al., 2010; Rodriguez-Fraticelli et al., 2010; Vidal-Quadras et al., 2017).

5. Zebrafish gut development

In the zebrafish gut, as mentioned before, lumen formation occurs by de novo apical polarization, providing an approachable *in vivo* model to study this process (Figure I-8). During zebrafish gut morphogenesis, endoderm-derived intestinal progenitors converge in the medial line forming a rod-like structure consisting of about 1000 cells at 36 hours post-fertilization (hpf), which already present intercellular junctions. After a single division cycle, tight junctions become apparent at multiple sites in the rod. These sites accumulate apical polarity markers and later expand into small microlumens, which rapidly become fluid filled near 55-60 hpf. Then, around 72 hpf lumens start progressively coalescing with anterior-to-posterior directionality through a mechanism that requires removal of interluminal junctions. Interestingly, the genetic program required for lumen coalescence is dependent on Hedgehog signaling, and its crosstalk with the underlying smooth muscle is essential for gut integrity (Alvers et al., 2014; Seiler et al., 2012).

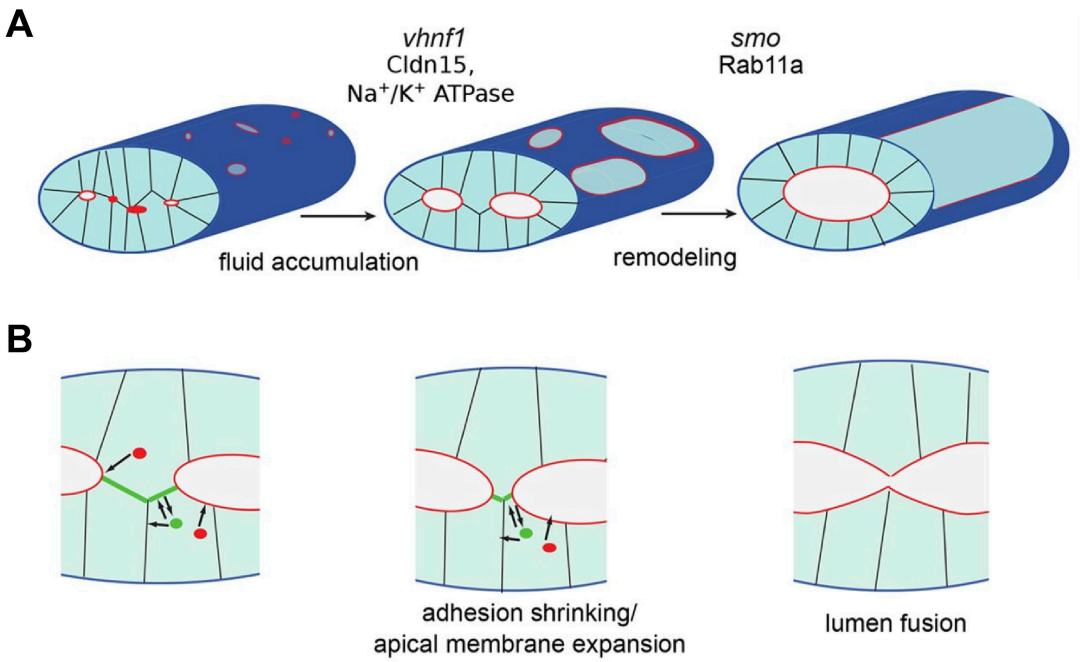

Figure I-8. De novo lumen formation in zebrafish. A) *De novo* lumen formation in the zebrafish gut occurs by cord hollowing. The genetic program regulating single lumen formation is controlled by Hedgehog signaling and transcription factor *vhnf1*. This in turn results in the upregulation of junction remodeling genes, such as Rab11a, and leaky tight junction proteins, such as Cldn15. **B)** Rab11 expression results in recycling of E-cadherin from interluminal cell-cell contacts, to facilitate apical membrane fusion, enabling lumen resolution. (Adapted from Alevers et al. 2014)

5.1 Apical membrane maturation in the intestine

The zebrafish epithelial layer of the gut lacks intestinal crypts, but it presents fingerlike protrusions known as villi (Wallace and Pack, 2003). The epithelium that lines each villus is composed of several cell types including goblet, paneth enteroendocrine, and enterocyte cells. Among these, enterocytes are the most abundant cell type and the one responsible for nutrient absorption (Brugman, 2016). To achieve their correct function, these absorptive epithelial cells must remodel their apical surface during differentiation to form a highly polarized and differentiated structure known as the brush border (Figure I-9). This structure is comprised by an array of actin-supported membrane protrusions named microvilli, which, according to their density, will define the degree of apical membrane maturation (Wallace et al., 2005). The microvilli are sustained by actin-based microfilaments and are anchored in an apical network of actomyosin and intermediate filaments known as the terminal web (Fath et al., 1993). To generate

microvilli, epithelial cells must overcome physical forces that oppose membrane deformation including membrane bending, stiffness and surface tension (Nambiar et al., 2010; Sheetz, 2001). To do so, cells employ cytoskeletal dynamics to generate forces that push against cellular membranes and to drive membrane deformation (Atilgan et al., 2006; Theriot, 2000). In the case of intestinal microvilli, the origin of the deforming force remains unclear but is prone to be generated by

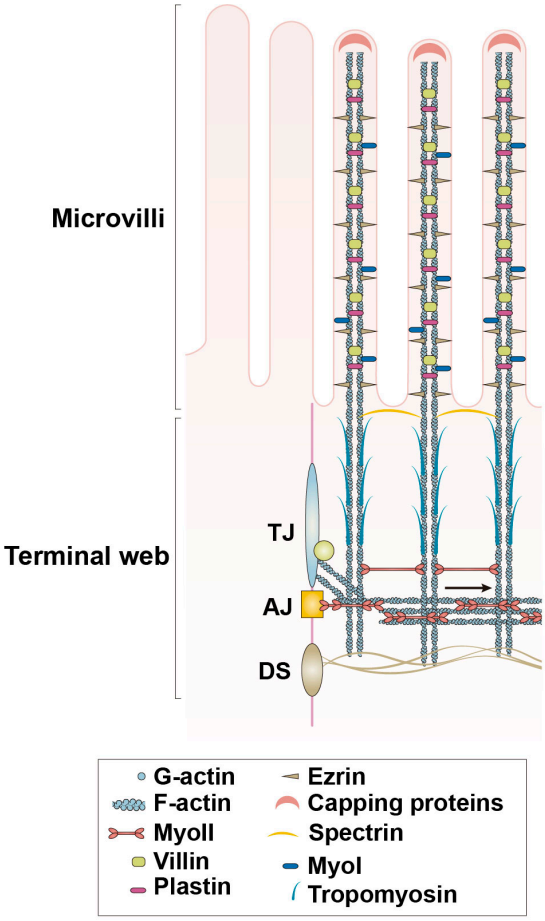

Figure I-9. Actin structures in the mature intestinal epithelium. The brush border is composed of two interconnected regions, the microvilli compartment and the terminal web. Microvilli are sustained by the role of actin bundling components such as villin, plastin and fimbrin. Actin filaments are anchored to the plasma membrane by myosin-Ia and ezrin, and capped by capping . At the base of the microvilli, the actin filaments are supported by the crosslinking effect of spectrin and the filament stabilizing role of tropomyosin. The terminal web is a more branched structure, connected to tight junctions (TJ), and adherens junctions (AJ). Contractile forces are generated by the actomyosin network and actively contribute to brush border contraction and shape modulation. (Adapted from Delacour et al. 2016)

the polymerization and bundling of actin microfilaments (Cameron et al., 2000; Delacour et al., 2016; Footer et al., 2007; Miyata et al., 1999; Parekh et al., 2005). Although a structural microvillus-anchoring function has been attributed to the actomyosin network, its organization and function in the brush border are still unclear. There are many congenital enteropathies involving brush border anomalies, such us congenital tufting enteropathy (CTE), microvillus inclusion disease (MID) and congenital sodium diarrhea, among others. These anomalies are frequently associated to pathological stresses such us infection and/or

inflammation resulting in microvilli structure disruption, compromising intestinal functions (Davidson et al., 1978). Due to the importance of the actomyosin contractile activity in the generation of tensile force for epithelial shape regulation, it is enticing to envisage that the cytoskeletal network might affect brush border organization and as consequence apical membrane maturation and function. Thus, studies of the mechanisms responsible for the apical maturation and morphogenesis in zebrafish could be critical for elucidating the molecular basis of uncharacterized congenital gut defects and potentially provide novel insight into intestinal oncogenic processes (Rubin, 2007; Zhong, 2005).

6. The actin cytoskeleton

Actin is a ubiquitously expressed ATPase that exists either in a monomeric state, known as globular or G-actin, or polymerized, forming filaments (F-actin). The actin polymer is polarized, with a positive end ("barbed" end) where new actin subunits are added, and a minus end ("pointed" end), where depolymerization occurs (Figure I-10). Actins are highly dynamic polymers and can polymerize or depolymerize in miliseconds, their net growth depending on free ATP-bound subunit concentrations. However, the rate-limiting step for spontaneous assembly of actin filaments from monomers is nucleation, that is, the formation of small oligomers, which can then rapidly elongate (Li and Gundersen, 2008). *De novo* actin nucleation is a biochemically unfavorable mechanism due to the

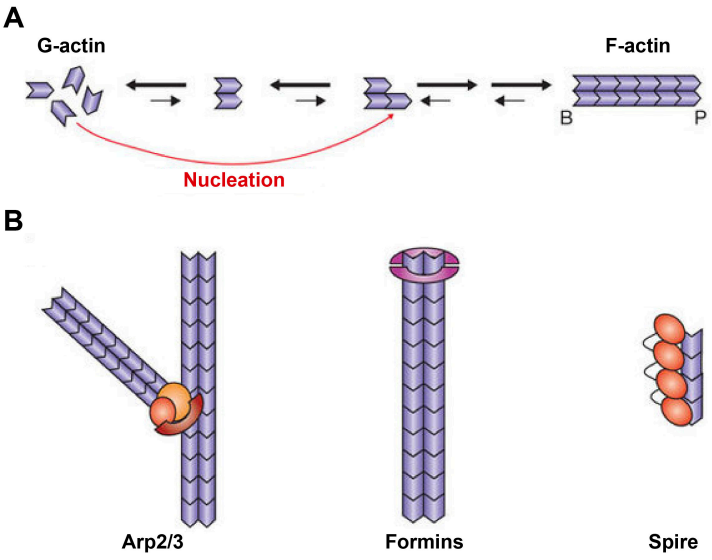

Figure I-10. Actin polymerization. A) Actin exists in either monomer (G, or globular) or polymer (F, or filamentous) form. Once nucleation of three actin monomers occurs, polymerization starts from the barbed (B, or positive) end to the pointed (P, or negative) end. **B)** Actin nucleation is promoted by the role of Arp2/3, formins or spire. (Adapted from Chhabra and Higgs 2007)

conformational instability of the initial actin dimer and trimer. This step is overcome by several actin-binding proteins and regulatory complexes, which support this process, thereby promoting actin polymerization to allow rapid cytoskeletal remodelling in response to cellular signals or during tissue homeostasis.

So far, three classes of protein have been identified to initiate new filament polymerization: the actin-related protein-2/3 (ARP2/3) complex, proteins of the formin superfamily and spire-family proteins. These factors are known as actin nucleators and each one promotes actin polymerization in different ways. The Arp2/3 complex is thought to mimic an actin dimer or trimer and function as a template for the initiation of a new actin filament, but can only assemble off of an existing filament, thus generating branched actin networks (Goley and Welch, 2006; Skau et al., 2015). On the other hand, formins are a superfamily of homodimeric proteins, which remain associated with the growing barbed ends and promote linear actin nucleation. Similarly, spire proteins favor actin polymerization into an unbranched filament, associating with the pointed end of the filament to prevent its depolymerization. The existence of multiple classes of nucleators provides the cell flexibility to assemble distinct populations of actin filaments with particular geometries and features in response to diverse signals (Goley and Welch, 2006).

6.1 Actin and apical junctions

In mature contacts of simple epithelia, F-actin concentrates at the apical region, where it forms a conspicuous circumferential ring, and at the lateral cortex, together with E-cadherins (Michael and Yap, 2013). There are a plethora of mechanisms that link E-cadherin to the actin cytoskeleton, but the major role is attributed to α-catenin, which can bind actin filaments directly and indirectly through several other scaffolding proteins (Kobielak and Fuchs, 2004; Lecuit and Yap, 2015; Roper, 2015). E-cadherin adhesions directly promote actin assembly at the junctional cortex by recruiting actin regulators and the signalling pathways that activate them. Assembly occurs at different stages, including actin nucleation at the membrane of junctions, both in nascent and mature cell–cell contacts, and

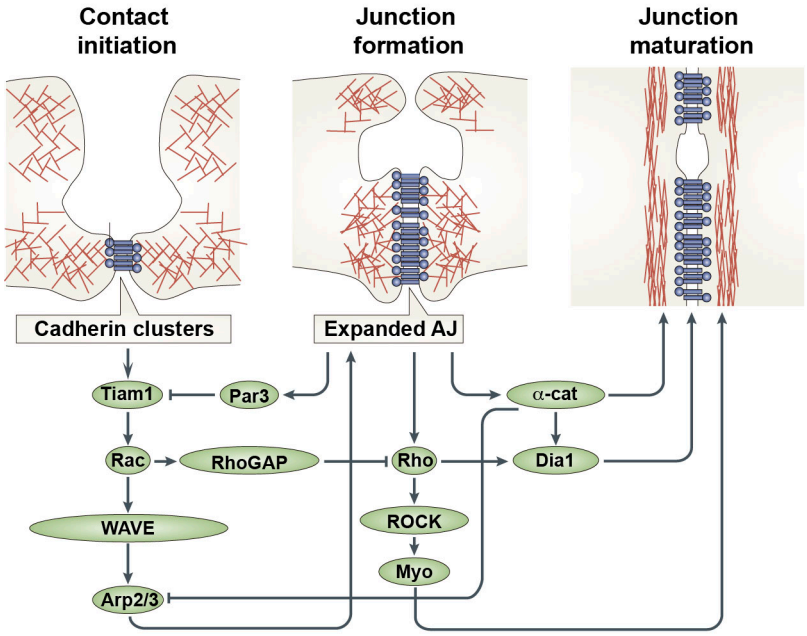

Figure I-11. Actin dynamics during junction formation. Branched F-actin is required for the initial cell-cell contact formation. Cadherin clusters recruit Tiam1, a Rac1 GEF, which activates Rac1, promoting the activity of WAVE, which in turn increases Arp2/3 mediated actin polymerization and junction expansion. Apical junctions recruit Par3, which inhibits Tiam1, and thus Rac activity, promoting RhoA/ROCK/Myosin mediated contractility together with mDia1 actin polymerization, required for junction maturation. (Adapted from Harris and Tepass 2010).

filament elongation followed by remodelling to form the contractile perijunctional rings (Figure I-11) (Verma et al., 2012). The actin rings observed among the apical-junctional boundaries appear to be highly dynamic. Fluorescence recovery after photo- bleaching (FRAP) experiments revealed a fast actin turnover at the cell–cell contacts with half-lives of around 10–50s and a high percentage of recovery, suggesting that the majority of junctional actin participates in a continuous cycle of polymerisation and disassembly (Kovacs et al., 2011; Michael and Yap, 2013; Yamada et al., 2005). Numerous studies have demonstrated that Arp2/3 complex is the major actin nucleator during junction biogenesis in simple epithelia (Kovacs et al., 2011; Tang and Brieher, 2012; Verma et al., 2012). The Arp2/3 complex itself presents a low intrinsic activity, which needs to be supplied by other proteins known as the nucleation promoting factors (NPF), which are recruited to cell-cell junctions to promote actin polymerization (Figure I-12). WASP/WAVE proteins compose the class I NPFs, which bind to G-actin in addition

to the Arp2/3 complex. WASP/WAVE proteins (N-WASP and WAVE1/2 in epithelia) form large protein complexes and are activated at cell-cell junctions through binding to PtdInsPs (PIP2 for WASP and PIP3 for WAVE) and RhoGTPases (Cdc42 for WASP and Rac1 for WAVE)(Takenawa and Suetsugu, 2007). In contrast, the class II NPFs, comprised by actin binding protein-1 (Abp1), Pan1, and cortactin, do not bind to G-actin directly and instead possess an F-actin binding domain that is required for Arp2/3 activation (Ohoka and Takai, 1998). Among class II NPFs, cortactin is the most studied and is expressed in a wide range of tissues. In polarized epithelia cells, cortactin is detected mostly in the apical surfaces associated to the terminal web and the microvilli, interacting and colocalizing with ZO-1, E-cadherin and F-actin (Croucher et al., 2010; Gonzalez-Mariscal et al., 2000; Helwani et al., 2004; Katsube et al., 1998; Lynch et al., 2003; Matter and Balda, 2003). Cortactin shows a weak ability to activate the Arp2/3 complex itself. Therefore, it usually binds and recruits other nucleating proteins, such us WASP/WAVE proteins, promoting Arp2/3 activation and actin polymerization in a synergistic fashion (Goley and Welch, 2006; Han et al., 2014; Weaver et al., 2002). Inhibition of cortactin activity in MDCK cells blocks Arp2/3-dependent actin assembly at cadherin adhesive contacts, resulting in a significantly reduction of cadherin contact zone extension, impairing both cell morphology and junctional accumulation of cadherins in polarized epithelial cells, indicating that actin polymerization and junction maturation form a feed-forward loop, reinforcing one another (Helwani et al., 2004).

Although branched filament formation by the Arp2/3 complex is well studied, the mechanisms for disassembling branched filament networks are less well understood. Most of the studies have been performed in spreading cells at the leading edge during lamelipodia formation. Gelsolin and ADF-cofilin are the best-studied proteins known to promote filament disassembly via severing F-actin and sequestering G-actin to favor depolymerization (Iwasa and Mullins, 2007; Stossel et al., 1982; Svitkina and Borisy, 1999; Wegner et al., 1994). Other disassembling factors affect polymerization indirectly, by inhibiting Arp2/3 function, such as Coronins. Coronins are a conserved family of actin-binding proteins that regulate cell motility in a variety of contexts (Uetrecht and Bear, 2006). Coronin-1B

remodels Arp2/3-containing actin branches and plays a significant role in directing actin dynamics within lamellipodia. Paradoxically, although Coronins inhibit Arp2/3 function *in vitro*, their *in vivo* expression results in an increase of cell motility in a variety of models. Interestingly, Coronin-1B seems to potentially antagonize cortactin activity *in vitro* and *in vivo*, exerting opposing activities on lamellipodia dynamics (Cai et al., 2007a; Cai et al., 2007b), suggesting that their concerted activity is required for cell migration. In epithelial polarized cells, coronins are localized along the apical junction domain, where they interact with the actomyosin cytoskeleton regulating cell-cell junction maturation (Michael et al., 2016). Moreover, exciting studies are emerging in polarized epithelial cells to decipher the role of these proteins in the context of epithelial morphogenesis.

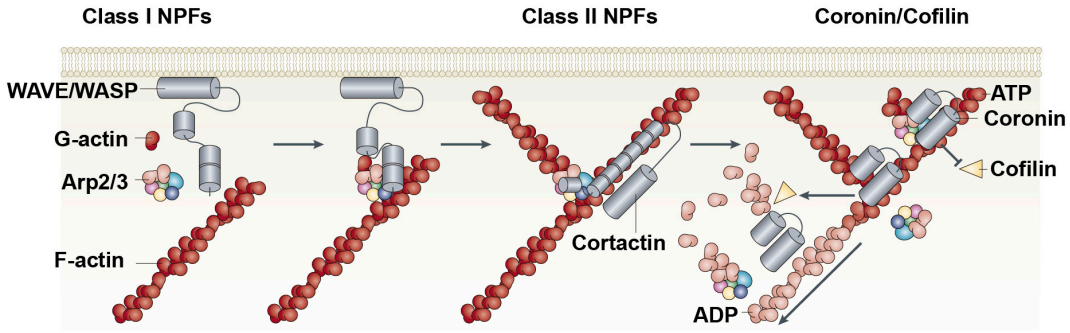

Figure I-12. Role of nucleation promoting factors and coronin/cofilin. Class I NPFs such as WAVE/WASP promote the binding of Arp2/3 to G-actin on an actin filament. Class II NPFs, such as Cortactin, stabilize Arp2/3 binding to the actin filament, enhancing Arp2/3-mediated polymerization. Coronin prevents Cofilin depolymerizing activity through binding of Arp2/3. Also, Coronin can displace Arp2/3, leading to actin debranching. (Adapted from Campellone and Welch 2010).

6.2 Actomyosin contractility in epithelial cells

Understanding the cellular basis of epithelial morphogenesis requires comprehending how contractility is generated at junctions and how it may be regulated. Actin microfilaments provide the "rails" along which myosin "motors" perform work in a variety of cellular functions (dos Remedios et al., 2003). Actin and myosin form an interconnected network at the cell cortex where continuous assemblies of myosin pull on anti-parallel actin filaments to generate contractile tension that can deform cell shape. The classic unit of contractile actomyosin

organization is the sarcomere, a structure that is well characterized in muscle cells and present in stress fibers of nonmuscle cells (Cramer et al., 1997). In epithelial cells, contractile actomyosin networks are coupled to adherens junctions, which mediate the transmission of forces between neighboring cells and integrate single cell behaviors to produce tissue-level changes during morphogenesis also to preserve tissue integrity and barrier function (Harris and Tepass, 2010; Kasza and Zallen, 2011). Epithelial cells express several classes of myosin family proteins, but contractile activity is traditionally attributed to the action of non-muscular myosin class II proteins (NMII). Just like muscular sarcomeric myosin, NMII is a complex formed by two heavy-chains (of either isoform NMIIA, B or C), two essential light chains (ELC2) and two regulatory light chains (RLC2), and can form bipolar filaments. In contrast to cardiac and muscle myosins, smooth muscle myosin and epithelial NMII activity is regulated by phosphorylation of the RLC2 subunits, mediated by a variety of kinases and phosphatases. In mature epithelial cells, cadherin adhesions are sites of RhoA signaling, which activates Rho-associated coiled-coiled containing kinase (ROCK), and Cdc42 signaling, which activates myotonic dystrophy kinase-related Cdc42-binding kinase (MRCK). ROCK and MRCK-mediated phosphorylation of RLC2 increases during junctional maturation, and results in the assembly of a sarcomeric-like structure of actin and myosin filaments that mediate epithelial compaction and rigidity. In addition to regulating epithelial maturation, the assembly of an apical actomyosin-rich cortex is also required for morphogenetic cell movements (Lecuit and Yap, 2015; Michael and Yap, 2013). One example is apical constriction, in which cells maintain contact with their neighbours but shrink the length of cell junctions through the apical activity of myosin II, regulated by the RhoA-ROCK-RLC2 module (Harris and Tepass, 2010; Skau and Waterman, 2015). Another example of morphogenetic contractility is the mechanism of cell extrusion. When a cell undergoes apoptosis in an epithelial sheet, a contractile ring forms in its neighbors that is thought to drive its extrusion and preserve the integrity of the epithelium (Rosenblatt et al., 2001). Non-muscle myosin II activity can also control several key aspects of junctional actin dynamics. For instance, myosin activity increases the F-actin turnover at the lateral junctions of epithelial cells. However, in the apical region F-actin content appears to be protected by the activities of proteins such as N-WASP, Arp2/3 and vinculin, which

stabilize and promote actin filament polymerization. Consistent with this, junctional tension is higher at the apical region than at the lateral junctions, due to local stabilization of cortical F-actin. The role for Arp2/3 in the junctional activity of myosin II is, however, somewhat paradoxical. Myosin II is generally thought to favor anti-parallel actin filament networks, rather than the branched networks that are nucleated by Arp2/3. However, one likely explanation is that filament reorganization, perhaps debranching, is necessary to allow Arp2/3-generated networks to be suitable for myosin II incorporation (Michael and Yap, 2013). How this may occur at the junctional cytoskeleton is not yet understood, and will be an essential question for investigation.

6.3 Blebs

Blebs are protrusions of the cell membrane resulting in actomyosin contractility in the cortex. Blebs are caused either by transient detachment of the cell membrane from the actin cortex or by a rupture in the actin cortex (Figure I-13). Blebs appear to be highly dynamic, emerging and dissolving on a timescale of minutes, and contractile, since the incubation with either Myosin class II inhibitor blebbistatin or ROCK inhibitor Y-27632 results in bleb suppression (Charras, 2008; Charras et al., 2006; Charras et al., 2005; Cheung et al., 2002). Blebbing is a common feature of normal cell physiology that happens during cell movement of embryonic cells, cytokinesis, cell spreading and apoptosis, and also in pathophysiological conditions, such as during tumour migration (Bereiter et al., 1990; Blaser et al., 2006; Boss, 1955; Boucrot and Kirchhausen, 2007; Burton and Taylor, 1997; Friedl and Wolf, 2003; Kubota, 1981; Pletjushkina et al., 2001; Sahai and Marshall, 2003; Sroka et al., 2002; Trinkaus, 1973). Blebs differ from other cellular protrusions, such as lamellipodia or filopodia, in that their growth is pressure-driven, rather than due to polymerizing actin filaments pushing against the membrane (as in lamellipodia or filopodia). Initially, the bleb membrane is not supported by an actin cytoskeleton, but an actin cortex subsequently reassembles before bleb retraction. The bleb life cycle can be simplified almost in three phases: bleb initiation (often referred to as nucleation), bleb expansion and bleb retraction. Two distinct mechanisms of bleb initiation have been observed

experimentally: a local dissociation of the membrane from the cortex or a local rupture of the actin cortex. Both mechanisms rely on the activation of the Rho-ROCK/MLCK-pMLC module, which drives the contractility of the actin cortex. Bleb expansion occurs due to the pressure that is generated after actomyosin contractility. In this scenario, flow of cytosol penetrates into the bleb, increasing both the volume and the surface area of the bleb. Finally, the last stage involves the reformation of an actomyosin cortex, followed by bleb retraction. The mechanisms that regulate actin nucleation in blebs remain unclear. For instance, the two best-

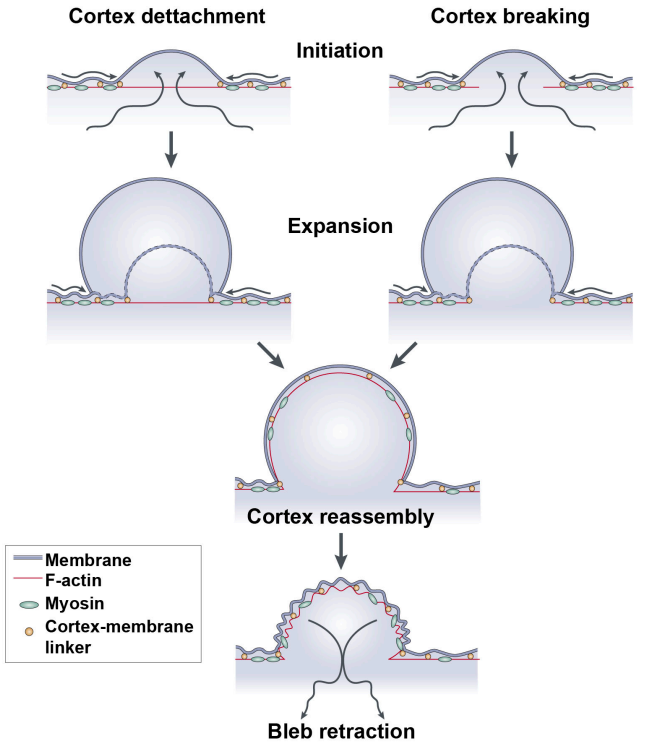

Figure I-13. Bleb formation dynamics. Blebs can be formed through two distinct initiating events. Cortex detachment is caused by the separation of the plasma membrane from the actin cortex. Cortex breaking requires the rupture of the actomyosin cortex. Both events, lead to membrane curving and expansion, due to the high intracellular pressure. Membrane curvature is followed by actin cortex reassembly and myosin recruitment, which results in bleb retraction. (Adapted from Charras and Paluch 2008)

characterized actin nucleators, the actin-related protein-2/3 (ARP2/3) complex and the mammalian formin diaphanous (mDia1), are not detected under the membrane of blebs. Some studies demonstrate a sequential recruitment to of F-actin, membrane-linker proteins, bundling proteins and finally contractile proteins, which will initiate retraction. In migrating cells, retraction does not always occur, but instead the cell body moves forward as a result of contraction at the rear. In addition to migrating cells, blebs have also been described in epithelial cells, but their function in this context has been elusive so far.

7. The Smoothelin protein family

The smoothelin and smoothelin-like family members represent a family of poorly understood muscle proteins that happen to act as structural components of the contractile apparatus. The protein family is characterized by the presence a single C-terminal type-2 calponin homology (CH) domain (Figure I-14). Smoothelin expression is often used as marker of differentiated contractile smooth muscle cells. Smoothelin A and Smootelin B are proteins of 59-kDa and 94-kDa respectively, which are both encoded by a single copy gene located on human chromosome 22q12.2 (Engelen et al., 1997; Rensen et al., 2000). Smoothelins influence the contractile potential of smooth muscle cells through their interaction with F-actin within the CH and the actin-binding domain (ABD) present in their structure. The more recently identified smoothelin-like proteins, SMTNL1 and SMTNL2, have more diverse functional implications. SMTNL1, originally termed the calponin homology-associated smooth muscle protein or CHASM, is the most studied and is linked to the regulation of smooth and skeletal muscle contractility and adaptations to hypertension, pregnancy, and exercise training. The SMTNL1 protein has been proposed to play multiple roles through functional interactions with contractile regulators such us calmodulin, tropomyosin, and myosin phosphatase as well as transcriptional control of the contractile phenotype and $Ca2^{+}$-sensitizing capacity. (Borman et al., 2009; Ishida et al., 2008; Lontay et al., 2015; Lontay et al., 2010; Ulke-Lemee et al., 2014; Wooldridge et al., 2008). Additional studies suggest a direct relationship between SMTNL1 levels and the expression levels of both progesterone receptor (PR)-B and estrogen receptor (ER)-α, which were regulated during pregnancy (Bodoor et al., 2011; Ulke-Lemee et al., 2011). Interestingly, despite possessing a Smoothelin-type CH domain, SMTNL1 does not mediate a direct interaction with F-actin *in vitro*.

In contrast to its protein siblings, SMTNL2 remains essentially uncharacterized. Two splice variants are predicted to be expressed in human and mouse tissues, resulting in a large variant of 50 kDa and a shorter variant of 35 kDa, lacking the first 144 amino acids. According to multiple databases, SMTNL2 is highly expressed in skeletal muscle and in the heart, but interestingly it is also

present in most epithelial tissues, including the kidney and intestine. Previous studies using *smtnl* morpholinos have shown that Smtnl (the SMTNL2 orthologue in zebrafish) is required for choroidal fissure closure during zebrafish eye development, suggesting a role in morphogenesis (Kurita et al., 2004). Previous work has identified Smntl2 as one of the strongest candidate regulators required for correct lumen formation in the 3D-MDCK model. As previously mentioned, SMTNL2 protein contains a Calponin-homology (CH) domain, which confers a putative actin-binding function. This feature renders SMTNL2 even more attractive to its study, implying that it could be playing a role similar to other smoothelins in regulating the actomyosin cytoskeleton during the process of epithelial morphogenesis. Finally, emerging opportunities exist to understand the significance of smoothelins as disease-associated markers and in some cases as specific modulators of pathophysiology.

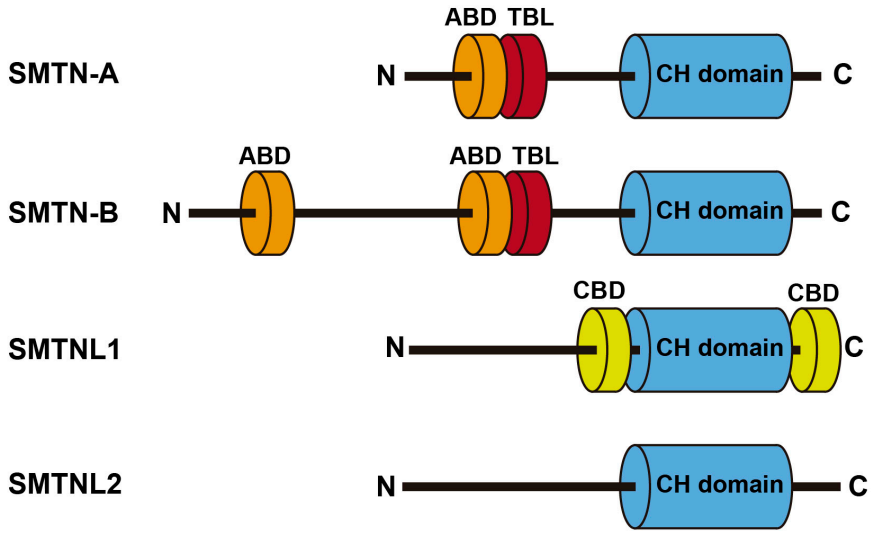

Figure I-14. The Smoothelin protein family. There are four vertebrate smoothelin family proteins, SMTN-A, SMTN-B, SMTNL1 and SMTNL2. They are characterized by a distinct calponin homology domain, placed in the C-terminus. In addition, SMTN-A and SMTN-B present actin binding domains (ABD) in the N terminus, and a TnT-binding like (TBL) domain. SMTNL1 presents two calmodulin binding domains (CBD). SMTNL2 is the least characterized member of the family.

OBJECTIVES

The present work has focused in the accomplishment of three main objectives:

I. Functional characterization of SMTNL2 in lumen formation in the 3D-MDCK model.

II. Functional characterization of SMTNL2 *in vivo* using the zebrafish model.

III. Analysis of the mechanism of action of SMTNL2.

MATERIALS AND METHODS

1. Cell culture

1.1 2D Culture

MDCKII cells were maintained in MEM supplemented with 5% Fetal Bovine Serum (FBS), 2 mM L-glutamine, 100 U/ml penicillin and 100 mg/ml streptomycin at 37°C in a humidified atmosphere containing 5% CO_2. All the above-mentioned cell lines were passaged approximately twice per week and subcultured at a 1:5 or 1:10 ratio. MDCK cells stably expressing SMTNL2-myc-myc-BirA*, SMTNL2-GFP, CTTN-GFP, CORO1B-GFP and TAGNL2-GFP were made by transfecting each plasmid (Lipofectamine 2000, Invitrogen) and selecting for 15 days using medium supplemented with 0.5 mg/ml G418. MDCK cells stably expressing double SMTNL2-Cherry together with CTTN-GFP, CORO1B-GFP or TAGNL2-GFP were made by co-transfection with the blasticidin-resistant gene (Invitrogen) and selected for 15 days using medium supplemented with 0.5 mg/ml blasticidin-HCl. Cells were cultured as single cell clones and positive colonies were trypsinised individually. Stable cell lines were further selected for 5 days using G418 or blasticidin (0.5 mg/ml) and then selected by fluorescence using fluorescence activated cell sorting (FACS). Mycoplasma testing was regularly performed to avoid contamination. HEK-293T cells were cultured in DMEM supplemented with 10% Fetal Bovine Serum, 2mM L-glutamine, non-essential aminoacids (Glycine, 7.5 mg/L, L-alanine, 8.9 mg/L; L-Asparagine, 13.2 mg/L; L-aspartic acid, 13.3 mg/L; L-glutamic acid, 14.7 mg/L; L-proline, 11.5 mg/L; L-serine, 10.5 mg/L), and Sodium pyruvate, 1mM. HEK-293T used for coimmunoprecipitation experiments were transiently transfected with Lipofectamine 2000.

1.2 3D Culture

To prepare MDCK cysts in Matrigel (BD Biosciences), cells were trypsinised to a single cell suspension of $2x10^4$cells/ml and mixed in cold 2% Matrigel in 5% FBS-supplemented MEM. Cells-Matrigel mixes were plated in 8-well coverglass chambers (250µl/well) (Ibidi) precoated with pure Matrigel (8-15µl/well). The medium was changed every 2 days and cysts were grown for 1–3 days or until lumens formed in the controls.

2. Transcriptomic analysis

For real-time quantitative PCR assays, MDCK II cells were grown in 60-mm dishes to form 2D monolayers or 3D cysts in Matrigel (at 10^5 cells/ml in a final volume of 4 ml). For 3D cultures 60-mm dishes were precoated with 100 µl of Matrigel before seeding the cells. Total RNA was isolated at 24h, 48h, 72h and 120h after cell seeding and purified using the RNeasy kit (Qiagen). All RNA samples were analyzed by Bioanalyzer (Agilent Technologies) to ensure RNA quality. Only RNA samples presenting a RIN value of 8 out of 10 or superior were used in the assay. Typically 1 µg of RNA per condition was used to retrotranscribe into cDNA using the High Capacity cDNA Reverse Transcription kit (Applied Biosystems). To perform the PCR, a set of primers was designed with the NCBI primer designing tool (**www.ncbi.nlm.nih.gov/tools/primer-blast**) (Supplementary Table 1, Apendix). All the amplicons were designed to spam an exon-to-exon junction whenever it was possible. Real-time PCR was performed in 386-well plates in an ABI 7900 HT system (Applied Biosysistems) using the Master Mix SYBR Green Kit (Agilent, Santa Clara, CA). Conditions of real-time quantitative PCR were as follows: 95ºC for 10min, then 40 cycles of 95ºC for 15s and 60ºC for 1min followed by a dissociation stage. Analysis of the melting fluorescence was used to validate a single melting peak, indicating target specificity. Every condition was tested by 3 experimental replicates per gene and assay. Experiments were typically conducted 4 to 6 times in independent conditions.

2.1 Mathematical and statistical analysis

To analyse the real-time quantitative PCR data, the HPRT gene was used as normalizer. Relative quantification analysis was used to determine the relative amount of RNA relative to 2D at 24h (condition 0). To test gene silencing, the amount of RNA was relative to the control siRNA sample. The Pfaffl model was used to calculate the N number (relative quantity of RNA relative to control) (Pfaffl, 2001):

$$N_{\text{gene A condition 1}} = \frac{E_{\text{gene A}}^{-\Delta CT\,(CT_{\text{condition1}} - CT_{\text{condition0}})}}{E_{\text{Normalizer gene}}^{-\Delta CT\,(CT_{\text{condition1}} - CT_{\text{condition0}})}}$$

E, represents the efficiency of the amplification (E ≤ 2) of the PCR. The efficiency was calculated for each gene by creating a standard curve with a gradient of concentrations of cDNA and calculating the slope of the straight line. CT is the cycle threshold, which is the cycle number at which the fluorescence generated within a reaction crosses the fluorescence threshold, a fluorescent signal significantly above the background fluorescence (typically between $1/10^{th}$ to $1/100^{th}$ of maximum signal). At the threshold cycle, a detectable amount of amplicon product has been generated during the early exponential phase of the reaction. ΔCT is the difference between the CT of the two conditions examined (Control vs KD). The three experimental replicates were used to calculate the standard error of the experiment. All the data with an SE > 50% was supressed and repeated.

3. Silencing by siRNA

RNAi oligo sequences are listed in Table 1. For each gene, 25 nucleotide stealth siRNA duplexes targeting specific mRNA sequences were designed and purchased from Invitrogen using the Stealth RNAi BLOCK-IT technology. Sequences were submitted to BLAST search to ensure targeting specificity. For siRNA transfection, MDCK cells were transfected by Lipofectamine 2000 with siRNA duplexes or scrambled siRNA. After a 24h incubation, cells were resuspended and plated in 12-well plates and/or in coverglass chambers coated with Matrigel to grow into cysts. Total cell lysates from 3D cultures were analyzed by quantitative real-time PCR (Q-PCR) to confirm siRNA efficiency. For rescue experiments, GFP-tagged human SMTNL2 was verified to be resistant to SMTNL2 siRNA by RT-qPCR.

Table 1: List of target silencing sequences

siRNA	Target sequence (5'-3')
SMTNL2.1	**CAGAAUACCCAGGGUUCCUUCCAUU**
SMTNL2.2	**GAGGUAACUGCAUCUGUACUGUUGA**
Coronin-1B.1	**GGCAGAGCAAAUUCCGGCAUGUGUU**

Coronin-1B.2	**CACCCUGACCUCAUCUACAACGUCA**
Cortactin.1	**GGACAGAGUUGAUCAGUCUGCUGUA**
Cortactin.2	**AAGCGUGAAGCAAGCAGAGAGUGAU**
Trangelin-2.1	**GCUGUGGCUGCAGGGACUUAAUUUA**
Transgelin-2.2	**UGUGGCUGCAGGGACUUAAUUUAUA**
Control	**GCUGGUCCGGAGGCAUUAAUUGUUA**

4. Antibodies

Table 2: The primary antibodies used in the present work.

Protein	Species	Reference	Dilution IF	Dilution WB
β-catenin	**Rabbit**	Santa Cruz Biotechnologies (sc7199)	**1/500**	**-**
Gp135	**Rabbit**	**Gift Dr. Ojakian (State University of New York Downstate Medical Center)**	**1/500**	**1/500**
ZO-1	**Rat**	**DSHB (R4076)**	**1/500**	**-**
Claudin2	**Rabbit**	**Zymed (51-6100)**	**1/500**	**1/500**
GFP	**Rabbit**	**Invitrogen (A-6455)**	**-**	**1/500**
RFP	**Rabbit**	**MBL International Corporation (PM005)**	**-**	**1/500**
p-MRLC	**Rabbit**	**Cell Signalling Technology (3671S)**	**1/250**	**1/200**
Caspase3	**Rabbit**	**Cell Signalling Technology (9661)**	**1/500**	**-**
Myc	**Mouse**	**Roche (9E10)**	**1/500**	**-**
Acetylated α-tubulin	**Mouse**	Sigma-Aldrich Clone 6-11B-1 (T7451)	**1/500**	
GAPDH	**Mouse**	**Santa Cruz Biotechnology (sc-32233)**	**-**	**1/1000**

Table 3: The secondary antibodies used in the present work.

Antibody	Species/Tracer	Reference	Dilution IF	Dilution WB
Anti-mouse IgG, HRP	**Goat**	Jackson Immunoresearch	**-**	**1/5000**
Anti-rabbit IgG, HRP	**Goat**	Jackson Immunoresearch	**-**	**1/5000**

WGA-FITC	**Lectins**	Sigma	**1/1000**	
Alexa Fluor 488 anti-Rabbit	**Donkey**	Invitrogen (A-21206)	**1/1000**	
Alexa Fluor 488 anti-Mouse	**Donkey**	Invitrogen (A-21202)	**1/1000**	
Alexa Fluor 555 anti-Rabbit	**Donkey**	Invitrogen (A-31572)	**1/1000**	
Alexa Fluor 555 anti-Mouse	**Donkey**	Invitrogen (A-31570)	**1/1000**	
Alexa Fluor 647 anti-Rabbit	**Donkey**	Invitrogen (A-31573)	**1/1000**	
Alexa Fluor 647anti-Mouse	**Donkey**	Invitrogen (A-31571)	**1/1000**	
Alexa Fluor 647anti-Rat	**Goat**	Invitrogen (A-21247)	**1/1000**	
DAPI	**Nuclei**	Merck(268298)	**1/1000**	
Phalloidin-488	**F-actin**	Invitrogen (A-12379)	**1/1000**	
Phalloidin-555	**F-actin**	Sigma (P-1951)	**1/5000**	
Phalloidin-647	**F-actin**	Invitrogen (A-22287)	**1/1000**	

5. Immunofluorescence

For Immunofluorescence (IF), MDCK cells in 2D monolayers (over boroslicate coverslips) and cysts (IBIDI chambers) were fixed with 4% PFA for 20min and then permeabilised with PBS + 0.2% Triton Tx-100 + 0.2% SDS for 10min at 4ºC. The only exception was for IF with the anti-myc antibody, in which the fixation was performed with ice-cold 100% methanol for 5 min at -20ºC. Cells were then blocked with PBS + 3% BSA at room temperature for 30min (monolayers) or 1 h (cysts), and then the primary antibodies were diluted in PBS +3% BSA and incubated for 1h at room temperature or overnight at 4ºC. After several washes in PBS +3% BSA, secondary antibodies, phalloidin or DAPI were incubated for 30min (monolayers) or 1h (cysts) in the dark and then washed with PBS. Cells cultured as 2D monolayers were mounted with Prolong Gold (Life-Technologies) over glass slides. Cells cultivated in cysts in chambers that did not need mounting medium were conserved with PBS 0.01% Azide at 4ºC for a maximum period of 2 weeks. Zebrafish embryos and larvae were fixed with 4% PFA for at least 2h at RT and then stored overnight at 4ºC. Embryos were stained either in whole mount or sectioned in slices. For sectioning, embryos where

embedded in 4% low-melting point agarose, and cut with a vibratome into 150 μm sections and placed in PBS-0.1% Tween 20 (PBST). The embryos or the sections were washed in PBST, and blocked in PBST with 3% BSA for 1h at room temperature. Primary antibodies and reagents were incubated overnight at 4ºC using the following concentrations: acetylated tubulin, 1/500; TRITC-Phalloidin, 1/1000; 488-Phalloidin; 1/500, DAPI, 100 μg/ml. The embryos were mounted with Prolong-gold (Life Technologies) for posterior microscopy analysis. For distal tubule and cloaca analysis, embryos were cut using a sharpened micro-knife just beneath the larger part of the yolk, mounting the posterior part laying on its side, in order to take images longitudinally to the anteroposterior axis.

6. Microscopy

Zeiss laser scanning confocal microscopes LSM510, LSM710, two-foton LSM710 and Nikon AR1+ used for laser scanning confocal imaging. Objectives used were usually 40×/0.95 oil-Plan Apochromat and 63×/1.4 oil-Plan Apochromat (Zeiss).

For electron microscopy, larvae were fixed in 2% (w/vol) PFA, 2% (w/vol) glutaraldehyde in 0.1 M phosphate buffer at pH 7.4 for 2h at room temperature and overnight at 4ºC. Subsequently, midgut sections were embedded in Epon resin, sectioned using a ultramicrotome (Ultracut E, Leica), and stained with uranyl acetate and lead citrate and imaged at 80 kV using a JEM1010 Jeol microscope.

The analysis and composition of images taken from the microscopy were done with ImageJ, Fiji or Zen (Zeiss) programs. For quantifications, more than three experiments were quantified per condition. Significance was calculated using a paired, two-tailed Student's t test, and significant p-values are indicated in each experiment.

7. Co-immunoprecipitation

HEK 293T (10^6 cells) transiently coexpressing SMTNL2–GFP/ CORO1B-GFP /CTTN-GFP or GFP alone were grown for 48h, washed once in cold PBS and lysed in 1 ml of lysis buffer (150 mM NaCl, 20 mM Tris–HCl, pH 8.0, 5% glycerol, 1% NP-40), containing protease inhibitor cocktail (Sigma-Aldrich). Each 1 ml of lysate was

incubated with 2 µg of purified monoclonal anti-GFP (Life Technologies) or 2 µg of monoclonal GAPDH as isotype IgG1 control (Santa Cruz). Monoclonal anti-GFP-coated magnetic beads were washed in lysis buffer 5 times and dried by aspiration. Bound proteins were eluted in 100 µl of 2x Laemmli protein-loading buffer (Sigma-Aldrich) and analysed by western blotting. We performed experiments at least three independent times to be confident in the experimental reproducibility.

8. Plasmids.

Human TAGNL2–GFP plasmids were kind gifts from Dr Chang Duk-Jun, from the Gwangju Institute of Science and Technology in South Korea. Human SMTNL2–GFP and SMTNL2–Cherry were constructed by PCR and cloned into pEGFP/mCherry vectors (Clontech). Human SMTNL2–myc/myc–birA* was constructed by PCR and cloned into mCherry vector (Clontech), substituting mCherry with birA* (+). The plasmids containing *smtnl* under SP6/gUAS promoter were generated by PCR and multi GATEWAY cloning throug the BP and LR reactions (Invitrogen), following the protocol provided. The backbone plasmids were kind gifts from Dr. Gilmour from the EMBL Heidelberg (Germany) and the gUAS plasmid was a gift from Dr. Michel Bagnat from Duke University (USA).

9. *In vivo* biotinylation of SMTNL2-proximal proteins

MDCK cells stably expressing the promiscuous mutant (R118G) of the humanized bacterial biotin-ligase (birA∗) or human SMTNL2–myc/myc–birA∗ constructs were incubated with 50 µM biotin for 16h and lysed using 4% SDS. After reducing the SDS concentration to 2%, biotinylated peptides were purified using streptavidin-coated magnetic beads (Genscript). The bioID technique was performed as previously described (Roux et al., 2012) and eluted peptides were analyzed by liquid chromatography tandem mass spectrometry and peptide-mass fingerprinting, considering up to 2 biotinylations per peptide, in collaboration with the Proteomics unit at Centro Nacional de Biotecnología (CSIC).

10. Cell proliferation

To perform cell proliferation assays, SMTNL2 siRNA-treated and control 2D MDCKII cells were seeded at 50,000 cells/well in 12-well plates, and incubated for different times. After incubation, the cells were trypsinized and stained with crystal violet and the mean fluorescent intensity was measured by flow cytometry. Cell proliferation assays were carried out in triplicates and averaged per experiment.

11. Bioinformatic analysis

To analyze the bioID results, the ranked gene list was processed using gene-set enrichment analysis (http://software.broadinstitute.org/gsea) and STRING (http://string-db.org/). From the resulting list of enriched gene pathways we selected the three top ranked genes by amount of detected peptides (TAGLN2, CORO1B and CTTN) that belonged to the top enriched pathway (actin regulation).

12. Measurements and quantifications

MDCK cysts with a single (or double) actin/Gp135 staining at the interior surface and β-catenin facing the ECM were identified as normal "single" lumens. We excluded cyst formation experiments that presented lower than 50% normal lumen formation (at 72 h), usually due to poor Matrigel gelification conditions. These experiments were repeated. To randomize cyst or cell counting, we randomly selected fields using low magnification, and then counted or took images at higher magnification for measurements. Immunofluorescence experiments in cell lines were performed at least three independent times and images shown are representative from samples that were used for quantification. For fluorescence intensity quantification in MDCK cysts, background was removed using Fiji, projections of single cells were obtained and fluorescence signal was quantified as integrated density per cell or per total cyst volume. To quantify actin signal polarization, the ratio of apical (actin staining facing the lumen) over total or over [total minus apical] signal was measured. At least 10 cysts (approximately 50 cells) were quantified per experiment, a minimum of three experiments per condition.

For bleb measurements, cysts containing 80% of the cells with basal blebs (apparent circular shaped breaks in the basolateral actin cortex) were considered

as positive and the percentage of cysts with blebs (over the total number of cysts in a field) was quantified.

For electron microscopy quantifications, larvae with apical blebs were considered abnormal (more than one cell presenting apical blebbing and lack of microvilli in a transversal slide was considered as positive). For the microvilli measurements, we quantified the number of microvilli in normal cells versus cells with apical blebs in the same experiment. For all the measurements, the number of independent experiments, the sample size and the statistical significance is specified in the figure legends.

13. Transepithelial resistance

For transepithelial resistance measurements, MDCKII cells were trypsinised until single cell suspensions were obtained and then plated onto 8-well ECIS plates (Applied BioPhysics) at 10^5 cells/well in 200 μl of culture medium). ECIS plates were connected to the ECIS array station. ECIS plates were placed in an incubator at 37ºC for 72h with a single change of medium at 48h post seeding. TER was continuously measured as resistance (Ω) and posteriorly represented as normalized resistance, assigning 1 to time 0 (~500Ω) resistance and referring the records to this initial resistance. Graphics represent the average of 2 experimental replicates. Three different independent experiments were conducted per condition.

14. Cell spreading

To analyze cell spreading, cells treated with SMTNL2 siRNA or control siRNA were grown in low confluence (20,000 cells/well) in a 24-well plate on crystal coverslips or fibronectin coated coverslips. Then cells were fixed at different time points and stained for DAPI, β–Catenin and phalloidin. Images of different zones were taken using a confocal 10X objective. Cell area measurements were calculated automatically after fluorescence intensity thresholding with Image-J.

15. Riboprobe synthesis

For *smtnl* probe production, total RNA from different stages embryos was isolated. RNA was retrotranscribed to cDNA with ThermoScript RT kit (Life technologies) using RT primers following the manufacturer protocol. To amplify the probes, PCR was performed using Taq Polymerase or Pfu Polymerase, with the primers specified in Table 5. The probes were designed to hybridize with different segments of the coding sequence on the mRNA of the gene, and the specificity was checked by alignment by BLAST (NCBI). The primer sequences and plasmids used for each probes are detailed in Table 5. Claudin-15a probe plasmid was kindly provided by Dr. Michel Bagnat. The digoxigenin RNA probes were synthesized with the SP6 or T7 RNA polymerase kit from New England Biolabs, using digoxigenin-labeled nucleotides from Roche and following the manufactures protocol.

Probe	Plasmid	Fw primer	Rv primer
zfSMTNL-P1	**pGEM3Z**	GGTCACTGGTGTCAAGACTTCTATA	GGAGGCCGAGCCGCTGGCGGAGCC
zfSMTNL-P2	**pGEM3Z**	CGAGCGCAGACTAGAAGAGG	CGTGCCACACACAAAGACTG
zfSMTNL-P3	**pGEM3Z**	TGGATCCAGCACCAATTCCC	AGTGCAGAGGCTGAGACCTA
zfSMTNL-P4	**pGEM3Z**	CCTGACCCGACAGGTAGAGA	CAGCCTATCACAGCCAGCTT
zfSMTNL-P5	**pGEM3Z**	CCAGCGATAACCAGCCTCAA	TGACTAAAATGCAACGGCGG
zfCLDN15a	**pCS2+**	**Gift from Dr. Michel Bagnat**	**-**

16. *In- situ* Hybridization (ISH)

Embryos of different stages were hand dechorionated, fixed for 24h in 4% PFA in PBS and dehydrated overnight in methanol at -20°C. Then the embryos were re- hydrated stepwise in methanol/PBS and saved on 100% PBST. Embryos older than 24h were treated 1 to 5 minutes with proteinase K (10 mg/ml in PBT). Embryos were post fixed in 4% paraformaldehyde for 20min and then rinsed in PBST 5 times for 5min each. The embryos were prehybridized at least 1h at 67ºC in hybridization buffer (50% formamide, 5xSSC, 50 mg/ml heparin, 500 μg/ml

Torula yeast RNA, 0.1% Tween 20 and 9 mM citric acid). Hybridization was done in the same buffer containing 50 ng to 100 ng of probe overnight at 67ºC. Then, embryos were washed at 67°C 2 times for 30min each in wash buffer (50% formamide, 25% 2x SSCT (SSC with 0.1% Tween-20)), 1 time 15 minutes in 2x SSCT and then 2 times for 30 minutes in 0.2x SSCT. Another 3 washes were performed at room temperature for 5 min in MABT (100mM maleic acid, pH7.5, 150 mM NaCl, 0.1% Tween), and then once in blocking buffer (MABT with 2% Boehringer ISH blocking buffer) prior to antibody incubation. After blocking, embryos were incubated overnight at 4°C with the alkaline phosphatase-coupled anti-digoxigenin antiserum (described in Boehringer instruction manual) at a 1/5000 dilution in blocking buffer. Finally, the embryos were washed 5 times for 30 minutes in MABT at room temperature. For detection, embryos were washed in staining buffer freshly prepared (100 mM Tris pH 9.5, 50 mM MgCl2, 100 mM NaCl, 0.1% Tween-20), and then incubated in BMPurple solution (Roche) at 37ºC in darkness. The reaction was stopped depending on the efficiency of the signal probe. Generally, the embryos were checked every 15 minutes under a bright field scope, performing overnight incubation at 4ºC if it was necessary. Reaction was stopped by washing with PBST and then fixing for 20 min with 4% PFA. Embryos were stored at 4ºC in PBST or at -20ºC after progressive dehydration with methanol as aforementioned prior to microscopy analysis.

17. Probe design for *In-situ* Hybridization

Five different probes tagging the coding sequence of *smtnl* gene were designed. All the probes presented the same localization. We chose probe number 4 as it resulted in a cleaner staining for our experiments. For *Claudin15la*, probes were topped with PBST and then fixed for 20 min.

18. CRISPR design

An allele consisting of a 17bp deletion in the *smtnl* **transcript** (NP_997970.1) was generated using CRISPR/Cas9 system targeting the second exon of *smtnl* gene. The Cas9 target site was designed using ZIFIT Targeter (a web-based online tool) together with the Genome Browser using the “CRISPRs” track of the “ZebrafishGenomics” data hub at http://genome.ucsc.edu/cgi-

bin/hgHubConnect. The targeting site sequences were as follows: GGCCGAGCCGCTGGCGGAGC.

18.1 sgRNA template assembly and preparation of sgRNA and Cas9 protein

To generate sgRNA templates, an oligo consisting of the T7 promoter, 18- to 20-nt target sequences, and 20-nt sequence (Oligo A) that overlapped to a generic sgRNA template (Oligo B) was designed as follows: (5'-3'):

Oligo A:

taatacgactcactataGGTGACTCAGAGCCAAGAGGgttttagagctagaa

OligoB:

aaaagcaccgactcggtgccacttttttcaagttgataacggactagccttattttaacttgctatttcta gctctaaaac

The targeting oligo was annealed with an 80-nt chimeric sgRNA core sequence. The annealed oligos were then filled in using KAPA polymerase (Roche) under the following conditions: 98°C for 30min; 60°C for 10 seg; 72°C for 5min.

The quality of the assembled oligos was checked on a 1.5% agarose gel. DNA purification was performed with the Min-elute gel extraction kit and gRNA were synthesized using Megashort T7 mRNA transcription synthesis kit (Thermofisher scientific). Cas9 protein was a purchased gift from Dr. Gilmour.

19. Embryo injections

A mix of Cas9 protein (150 ng/ul) and gRNA (30 ng/µL) together with 180mM of KCl was co-injected into one-cell stage WT embryos. To determine mutation efficiency, genomic DNA was extracted from approximately 30 24hpf embryos followed by mutation screening by sequencing.

The target gene region was amplified with forward primer 5'-tgtaaaacgacggccagtCACTCCACACACTCTAACAAATGTC-3' and reverse primer 5'-gtgtcttCTCCTCACTGGAGGGTCACAG-3'. Remainder embryos were raised to sexual maturity, and positive F0 adults were mated with WT to obtain the F1 generation. Germline transmission was tested using genomic DNA extracted from

approximately 30 24hpf embryos. F1 from positive germline-transmitting F0s were grown and analyzed by fin-clipping. Positive F1 zebrafish with identical mutations were then intercrossed to obtain F2 homozygous mutant offspring and WT offspring. Homozygous mutants (M1 and M2) were used for experiments and WT siblings were used as controls. The *smtnl-gfp* mRNA (200 pg) was injected into one-cell stage and then embryos were fixed at 36hpf for imaging. A gUAS-*smtnl-gfp* plasmid (100 ng) was coinjected together with the tol2 transposase mRNA (200 pg) into one-cell stage WT embryos and larvae were fixed at 6dpf for imaging.

20. Fluorescent PCR and Fragment analysis

PCR reactions used 1.5 µL of diluted DNA and 5 µL of PCR mix containing AmpliTaq Gold DNA polymerase (Life Technologies) with appropriate buffer, $MgCl_2$, dNTPs, and equimolar ratios of the following three primers at 5 pmol/µL: M13-F primer with fluorescent tag, amplicon-specific forward primer with M13 forward tail (5′-TGTAAAACGACGGCCAGT-3′) and 5′ PIG-tailed (5′ -GTGTCTT-3′) amplicon-specific reverse primer. PCR conditions were as follows: denaturation at 94°C for 12 min, followed by 35 cycles of amplification (94°C for 30 sec, 57°C for 30 sec, and 72°C for 30 sec), final extension at 72°C for 10 min, and infinite hold at 4°C. Denatured PCR products were analyzed to identify wild-type and mutant fragments generated by insertion or deletion on a Genetic Analyzer 3130xl using POP-7 polymer. Data were analyzed for allele sizes and corresponding peak heights using the local Southern algorithm available in the Genescan and Genotyper software of the GeneMapper software package (Life Technologies). The allele sizes were used to calculate the observed indel mutations. Mutations from two independent founders that were not in multiples of 3 bp and thus predicted to be frameshift truncations were selected for further confirmation by sequencing. Adult F1 progeny of these founder fish were genotyped similarly by fluorescent PCR using DNA extracted from fin clips

RESULTS

1. SMTNL2 mRNA expression is induced in 3D MDCK cells

To determine if SMTNL2 was induced in 3D MDCK cultures cells, we seeded MDCK cells in 2D and in 3D for up to 5 days, and then we performed a qPCR to analyze the mRNA levels of SMTNL2 using HPRT as a loading control. We observed an increase of 13.5±7.6 fold in SMTNL2 mRNA in 3D at 5 days in comparison with 2D. This result indicates that SMTNL2 is induced during lumen formation. This suggested a role for SMTNL2 during epithelial morphogenesis.

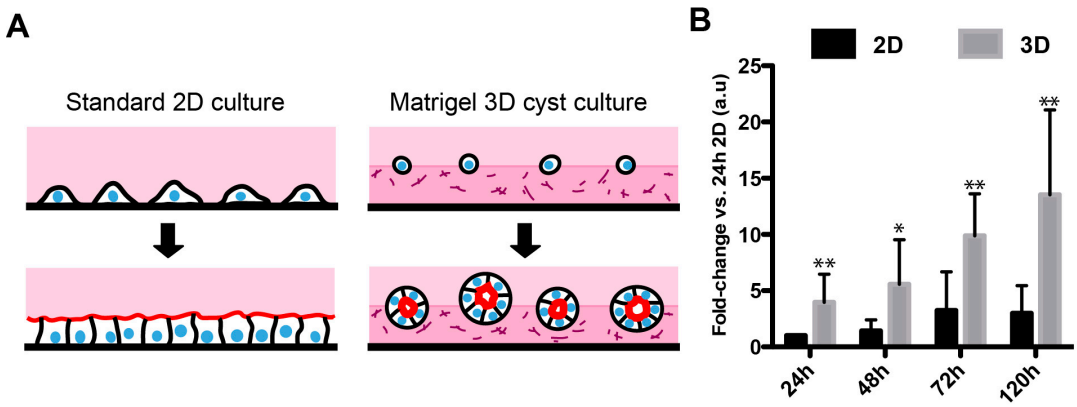

Figure R-1. SMTNL2 expression is induced in 3D cultures. A) Cartoon of 2D vs. 3D MDCK cell cultures. **B)** Analysis of SMTNL2 expression in 2D vs. 3D at different time points (from 24h to 120h) by RT-qPCR. Results are mean ± SD relative to 24h 2D and normalized with Hprt1. n=3; *, $P < 0.05$; ** $P < 0.01$ (Student´s t-test).

2. SMTNL2 is required for epithelial morphogenesis in 3D MDCK cells

To study the role of SMTNL2 during lumen formation, we used siRNA to silence the gene expression of SMTNL2 in MDCK cells. We designed two different siRNAs specific to canine SMTNL2 and tested their knock-down efficiency by RT-qPCR (si1: 43.3±7%, si2: 23.5±4.4% of control). Next, we transfected MDCK cells with these siRNAs, performed 3D cultures and fixed them after 72h. 3D cultures were stained with apical marker Gp135 to visualize the lumen and then analyzed with confocal microscopy to quantify lumen formation. We observed that the MDCK cysts that were treated with SMTNL2 siRNA presented a defect in lumen formation compared to the control (siControl: 60±7.9%, si1: 47±15.5%, si2: 34±3.9%), showing a stellar like shape and small multi lumen phenotype. This result indicates that SMTNL2 is required for correct lumen formation.

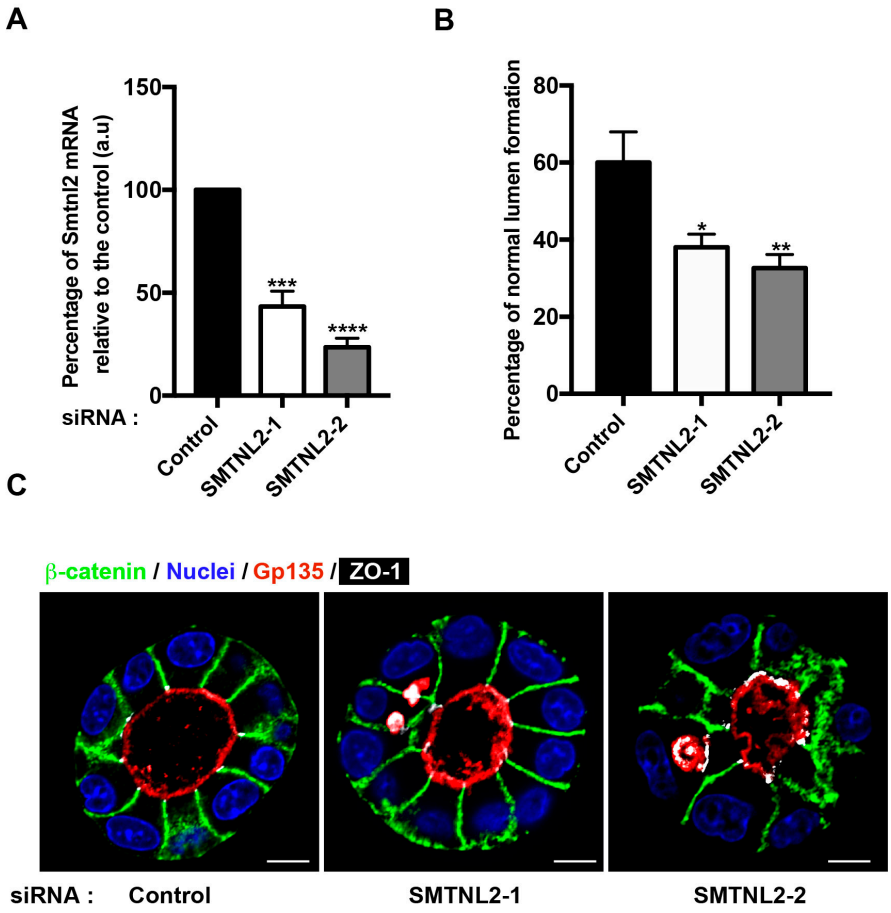

Figure R-2. SMTNL2 is required for correct lumen formation. A) MDCK cells were transfected with control or two different SMTNL2 siRNAs and grown in 3D cultures up to 72h. The siRNA mediated SMTNL2 decay was analyzed by RT-qPCR. Results are mean ± SD relative to the control and normalized with Hprt1. **B)** Quantification of cysts with normal lumens in cells silenced for SMTNL2 vs control cells. **C)** Effect of SMTNL2 silencing on lumen formation in 72h MDCK cysts. MDCK cysts were fixed and labelled with anti-Gp135 (red), anti-β-catenin (green), anti ZO-1 (grey) and DAPI (blue). Bars, 5µm. All values are mean ± SD from three different experiments. n ≥ 100 cysts/experiment; *, P < 0.05; **, P<0.01; ***, P<0.001; ****, P<0.0001 (Student´s t-test).

3. Human SMTNL2-GFP rescues the epithelial morphogenesis defect caused by SMTNL2 siRNA

To verify that this phenotype was specific for SMTNL2 knock–down, we generated stable MDCK clones expressing human SMTNL2-GFP resistant to canine SMTNL2 siRNA and we transfected them with control or SMTNL2 siRNA and performed 3D cultures. We observed that SMTNL2-GFP cysts generated single lumens at 72h, comparable to the MDCK control cysts (siControl: 64±5.3%, siSMTNL2: 37±0.5%, SMTNL2-GFP siControl: 63±5%, SMTNL2-GFP siSMTNL2: 69±4.3%).

All these data points that SMTNL2 is required for correct luminogenesis in 3D MDCK cells. Furthermore, it indicates that GFP-tagged SMTNL2 generates a functional protein, at least for the mechanism of lumen formation in this context.

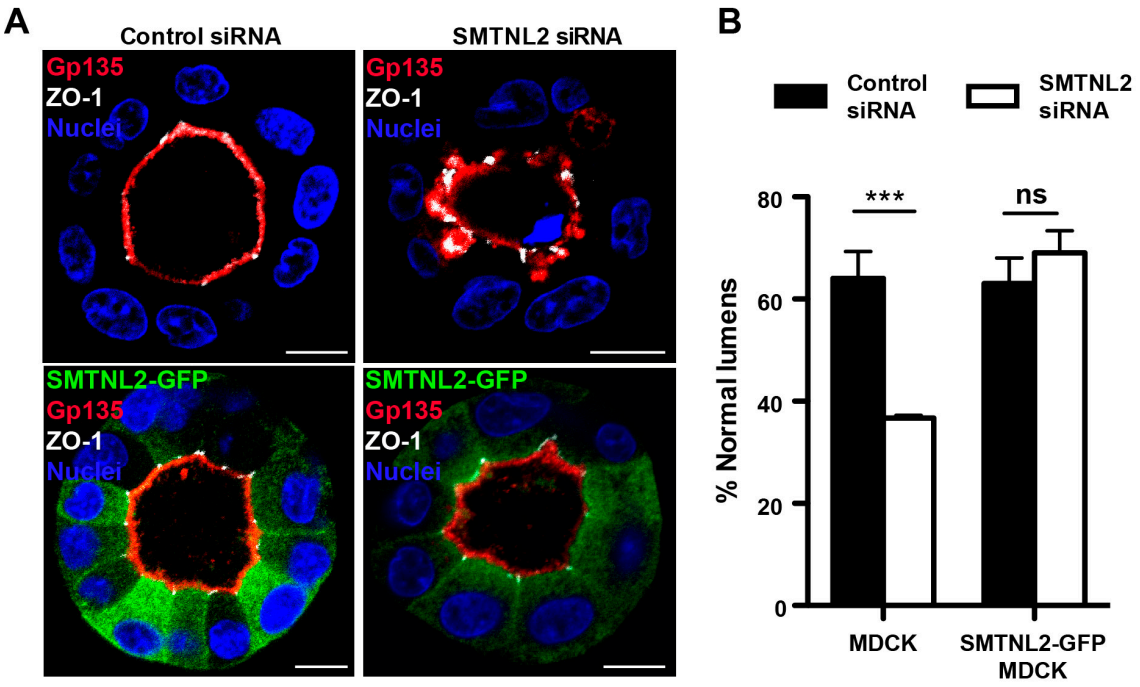

Figure R-3. Human SMTNL2 rescues to a normal phenotype. A) SMTNL2-KD phenotype in MDCK cysts, and phenotype rescue. WT MDCK cells or MDCK cells stably expressing siRNA-resistant SMTNL2–GFP protein were transfected with control or SMTNL2-specific siRNAs and grown to form cysts at 72h. MDCK cysts were fixed and labelled with anti-Gp135 (red), anti ZO-1 (grey), DAPI (blue) and analyzed by confocal microscopy. Scale bars, 5µm. **B)** Quantification of SMTNL2 KD phenotype and rescue. Measurements are expressed as mean ± SD percentage compared to control single- lumen-forming cysts. n = 3 independent transfection experiments; ***, P<0.001, ns, not significant (Student's *t*-test).

4. SMTNL2 is localized to the cytoplasm and clusters apically and in apical junctional boundaries in 3D and 2D MDCK cells

The endogenous localization of SMTNL2 could not be determined due to the lack of a specific antibody that worked in immunofluorescence. Therefore, to identify the subcellular localization of SMTNL2 in MDCK cells we used the stable cell line expressing human SMTNL2 tagged to GFP that was used for the rescue experiments. SMTNL2-GFP cells were cultured in 2D and in 3D for 72h and then they were fixed and stained. We observed that SMTNL2 is localized to the cytoplasm and to the plasma membrane in 2D MDCK cells and clusters apically and in junction boundaries in 3D MDCK cysts. To better define SMTNL2 localization, we

stained SMTNL2-GFP cysts at 72h for ZO-1, a tight junction protein, and F-actin (which is enriched in the apical domain of polarized epithelial cells). Immunofluorescence revealed that SMTNL2 colocalizes with tight junction protein ZO-1 and with F-actin apically. The apical and junctional localization of SMTNL2, together with its requirement for normal lumen shape further supports the role of SMTNL2 in the maturation of the apical domain of epithelial cells.

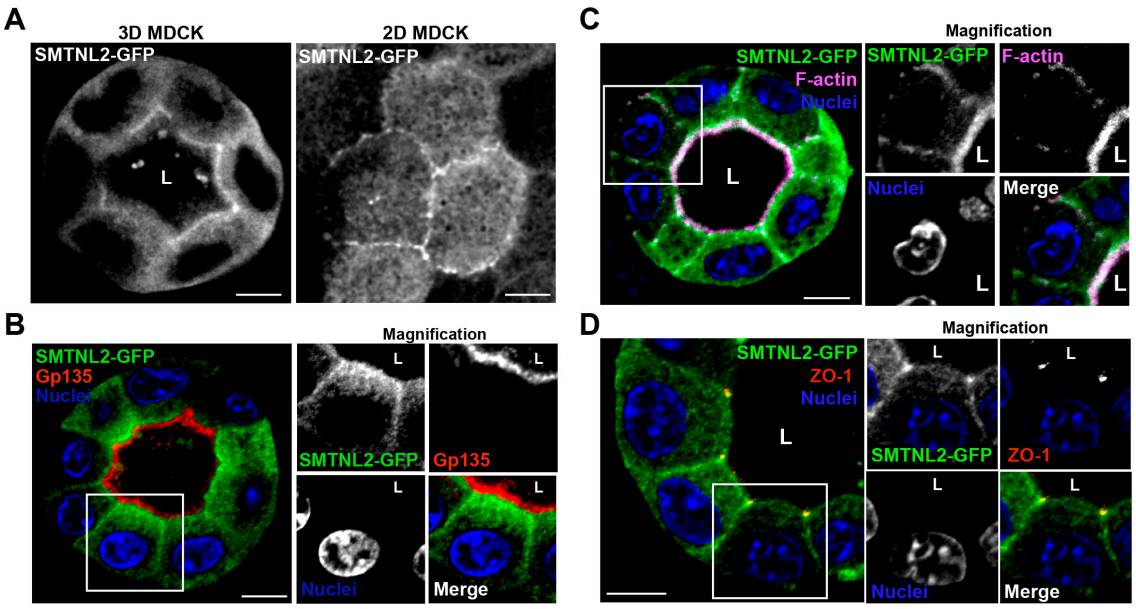

Figure R-4. SMTNL2-GFP colocalizes partially with apical F-actin and in tight junctions with ZO-1. A) Live imaging of stable cells expressing human SMTNL2-GFP. Left, MDCK 3D cultures at 72h. Right, apical middle-apical view of MDCK 2D cultures at 72h. **B)** SMTNL2–GFP stable cells were grown to form cysts at 72h. MDCK cysts were fixed and labelled with anti-Gp135 (red), DAPI (blue). **C)** SMTNL2–GFP stable cells were grown to form cysts at 72h. MDCK cysts were fixed and labelled with Phalloidin (magenta) and DAPI (blue). **D)** SMTNL2–GFP stable cells were grown to form cysts at 72h. MDCK cysts were fixed and labelled with ZO-1 (red) and DAPI (blue). All images were analyzed by confocal microscopy. Scale bars, 5µm. L, Lumen.

5. *smtnl* mRNA is expressed in tubular epithelia in the zebrafish

Next, we wanted to analyze the subcellular localization of SMTNL2 *in vivo*. We designed and synthesized riboprobes for Smtnl, the zebrafish homolog of Smtnl, to identify the tissue expression of this gene. Four probes were designed covering different regions of the *smtnl* mRNAs (see methods). The *in situ* hybridization (ISH) staining pattern revealed that *smtnl* was expressed mostly in the head, intestine, posterior lateral line primordium, cloaca and the skeletal

muscle early in development. Later during development *smtnl* expression was mostly restricted to the gut. To confirm *smtnl* expression in the intestine, we also performed an ISH of Claudin15la, a gene that is expressed only in the gut (used as marker). These results confirm that *smtnl* is expressed in tubular epithelia during development (24-144 hpf).

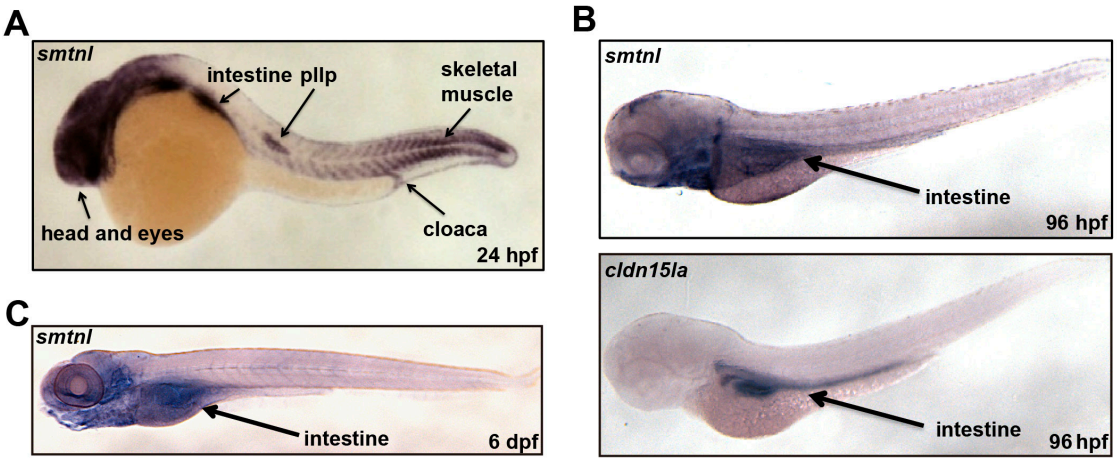

Figure R-5. *smtnl* is expressed in the gut. A) In situ hybridization (ISH) showing localization of *smtnl* mRNA at 24hpf (adapted from Thisse et al. 2007). **B)** In situ hybridization (ISH) showing localization of *smtnl* and gut marker *cldn15la* mRNA at 96hpf.**C)** In situ hybridization (ISH) showing localization of *smtnl* mRNA at 6dpf.

6. Smtnl is localized in the cytoplasm and in the apical membrane in epithelial tissues in the zebrafish.

To determine the subcellular localization of Smtnl *in vivo*, we cloned Smtnl fused to GFP under the T7 promoter, we performed *in vitro* transcription of mRNA and then injected the mRNA at the one-cell stage. Embryos were grown until 32hpf and we performed an immunofluorescence of the zebrafish pronephros (Figure R-6AB). We observed that Smtnl is localized to the cytoplasm and apically in this epithelial tissue. Next, we wanted to analyze Smtnl localization in the gut. Since very little mRNA expression is left at 72h when the gut lumen forms, we used the Tol2 transposase system to generate stable expression clones. To address this question we used tissue specific transgenic lines that expressed GAL4 specifically in the gut. To guide the expression in enterocytes we cloned Smtnl fused to GFP under the gUAS promoter. We performed single cell DNA injections together with Tol2 transposase mRNA and then embryos were grown until 6 days. Fixed

embryos were stained to detect F-actin (which is enriched in apical microvilli) and nuclei, and confocal images were taken on transversal gut sections. Smtnl localization in the gut was similar to the localization in the pronephros. In polarized enterocytes, Smtnl localized apically and in the cytoplasm. This localization confirms the subcellular localization that we observed in 3D MDCK cells, and further suggests a role of Smtnl in epithelial morphogenesis in tubular organs.

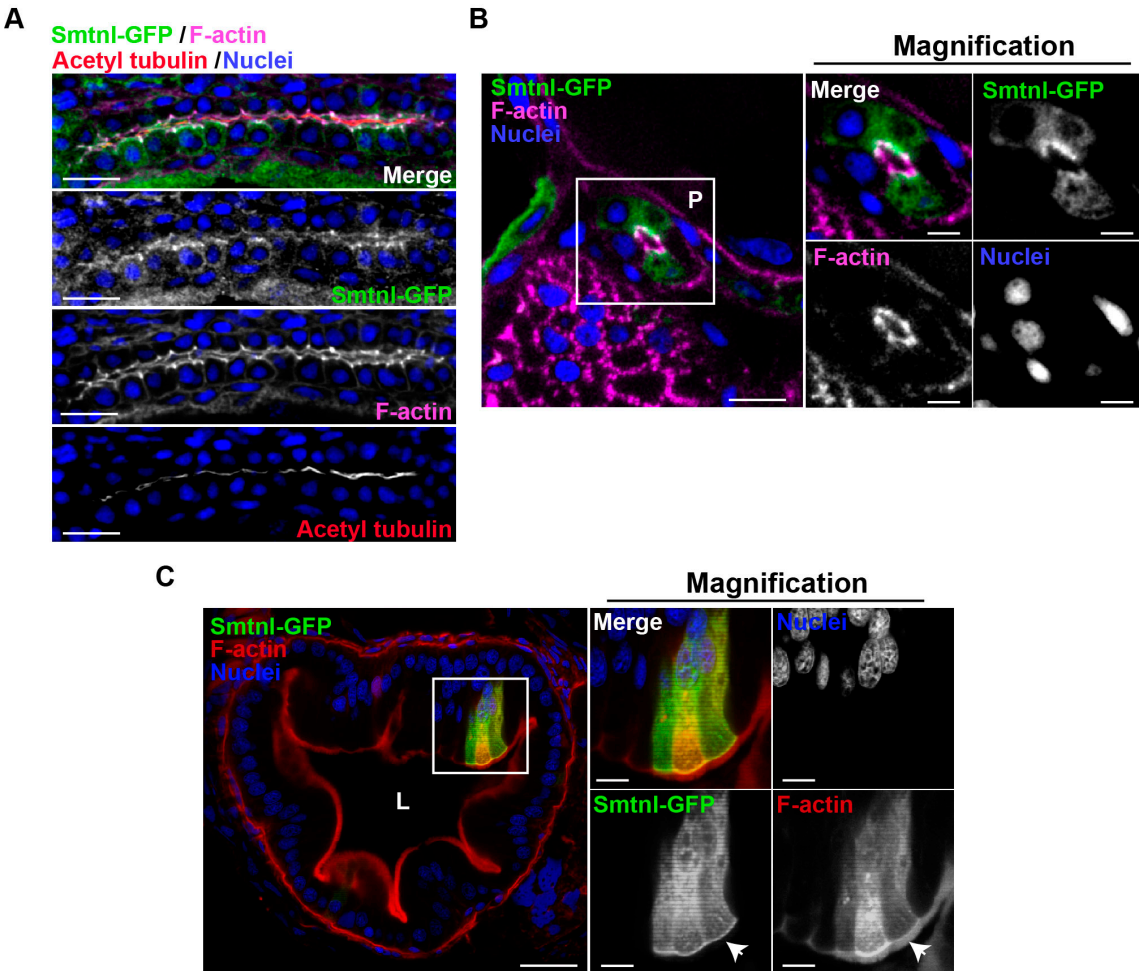

Figure R-6. Smtnl localizes apically in zebrafish epithelial tissues. A) *smtnl*–GFP mRNA was injected at the one cell stage. Embryos were grown up to 32hpf at 28ºC and then fixed and labelled with Phalloidin (magenta), anti-Acetylated tubulin (red) and DAPI (blue). Image is a longitudinal confocal section of the pronephros. **B)** Transversal section of whole embryo at 32hpf. P, pronephros. **C)** gUAS-Smtnl-GFP DNA was injected at the one cell stage of Cldn15la-Gal4 (gut-specific) transgenic lines. Embryos were grown up to 6 days at 28ºC. Larvae were sectioned and fixed and slides were labelled with Phalloidin (red) and DAPI (blue). All images were analyzed by confocal microscopy. Scale bars, 10µm, (magnification 5µm). L, lumen. Arrows indicate apical localization.

7. Generation of a zebrafish *smtnl* mutant using the CRISPR-Cas9 technology

To analyze if *smtnl* has a role in epithelial morphogenesis *in vivo*, we generated a zebrafish mutant using the CRISPR-Cas9 technology. We designed three single guide RNAs against different exons (see methods) of the *smtnl* gene. Both sgRNA and Cas9 protein were injected at the one-cell stage in wild type zebrafish. The efficiency of Cas9 and specificity of the sgRNA was validated by PCR using primers that flanked our region of interest. We isolated a mutant allele presenting a 17bp deletion in the Exon2 of the *smtnl* gene, which results in a non-sense mutation that generates a putative protein of 16 kDa. To ensure that we mutated specifically the gene of interest, we performed RT-qPCR and we analyzed gene expression of *smtnl* and their homologues (*smtna*, *smtnb* and *smtnl1*). RT-qPCR reveals that mutants present non-sense mediated mRNA decay only in the *smtnl* gene. This result indicates that we succesfully generated a null allele for *smtnl* in zebrafish.

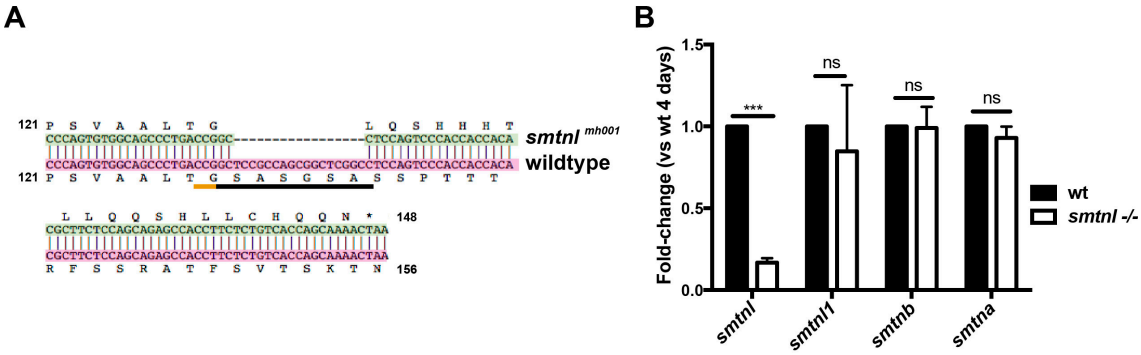

Figure R-7. Generation of *smtnl* zebrafish mutant using CRISPR-Cas9 technology. A) CRISPR-Cas9 generated *smtnl* mutant null allele. sgRNA were designed to target the second exon of zebrafish *smtnl* (black bar, PAM sequence in orange). Cas9-sgRNA complexes were injected at the one cell stage. After raising the founders, we cloned an allele, *smtnl*^{mh001} that harbors a null mutation. **B)** Analysis of RNA nonsense mediated decay of the *smtnl* mRNA in the homozygous mutant embryos by measuring *smtnl* mRNA levels and *smtnl* homologues (*smtnl1, smtnb, smtna*) in *smtnl* mutant and wild-type larvae at 4 days by RT-qPCR. Results are mean ± SD expression relative to control and normalized with Hprt expression. n=3; ***, P<0.001, ns, not significant (Student's *t*-test).

8. smtnl -/- zebrafish guts present apical membrane bulges into the lumen

To analyze if Smtnl has a role in epithelial morphogenesis *in vivo*, we decided to analyze the gut, a tubular epithelia that presented the main localization of *smtnl* expression. Overall morphology of *smtnl* mutants was not apparently

different from wild-type larvae, with normal formation of single lumens. Apart from the single lumen formation phenotype, SMTNL2-KD cysts presented defects in apical membrane shape (Figure R-2). To precisely determine the structure of the apical plasma membrane in *smtnl* mutant guts, fixed larvae were sectioned in slices and treated with wheat germ agglutinin (WGA) conjugated with Alexa 488 to stain lectins, which are enriched in the apical membrane of enterocytes, and then analyzed by confocal microscopy. Inspection of *smtnl* mutants revealed the presence of apical plasma membrane blebs of enterocytes facing the lumen in the middle-posterior gut region at 6dpf. (wild-type: 7.3±12.7%, *smtnl* mutant: 81.3±9.8%). This result suggests a clear role of Smtnl in maintaining the apical membrane structure in epithelial tubes. To visualize in higher detail the nature of

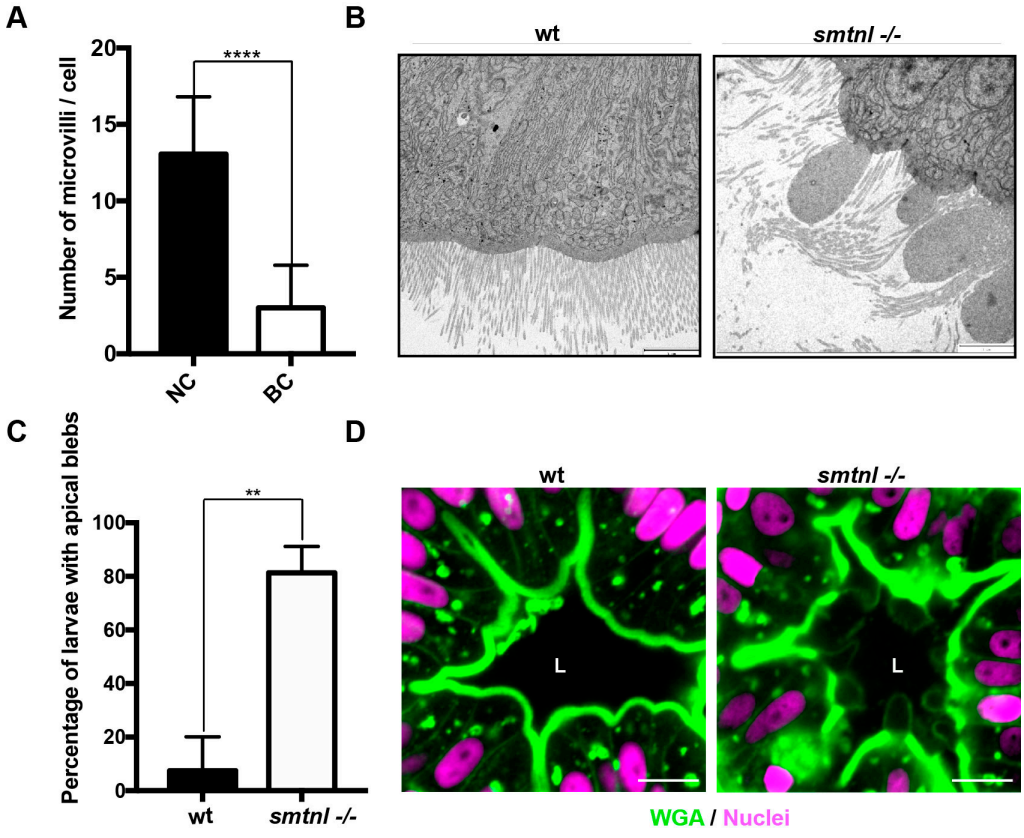

Figure R-8. *smtnl* mutant present apical membrane blebs and microvilli defects. A) Quantification of microvilli numbers per cell, in normal enterocyte cells (NC) vs. blebbing cells (BC) from electron microscopy transversal sections. Values are mean ± SD; n=17 cells; ****, P<0.001 (Student's *t*-test). **B)** Apical blebs were observed in *smtnl* mutant by transmission electron microscopy of transversal sections of larvae at 6dpf. **C)** Quantification of apical blebs in *smtnl* mutant vs wild-type larvae at 6dpf, from electron microscopy images. Values are mean ± SD; n=3 independent experiments; **, P<0.01 (Student's *t*-test). **D)** Apical membrane is disrupted in *smtnl* mutant. Larvae were fixed at 6dpf, sectioned and labelled with WGA (green) and DAPI (magenta). L, lumen. Scale bars, 10µm

these structures we decided to perform transmission electron microscopy (TEM) on *smtnl* mutant and wild-type larval guts. TEM imaging revealed the presence of bulging apical membranes of enterocytes in transversal *smtnl* gut sections.

The cells that present these blebs also show a defect in microvilli organization/formation resulting in a decrease on number of microvilli per cell compared with normal cells (NC: 13±3.7, BC: 3±2.3). The content of these apical blebs in *smtnl* mutants resembled the microvilli or cytoplasm. This phenotype suggested a role for SMTNL2 in the maintenance of apical membrane tension.

Previous studies done in chick intestines observed that enterocytes develop apical bulges into the luminal space upon treatment with Cytochalasin B, a drug that reduces actin polymerization and formation of contractile microfilaments. Taking all these results together, we attribute a function for Smtnl in controlling apical contractility in epithelial cells *in vivo*. To unravel the molecular mechanism behind Smtnl function, we went back to our *in vitro* model of 3D MDCK cells.

9. SMTNL2 silencing causes reduced levels of cortical F-actin in mature cysts

The phenotype that we observed in the zebrafish gut led us to hypothesize that SMTNL2 regulates apical tension. Since other Smoothelin family proteins have been shown to directly regulate the actomyosin cytoskeleton (for instance, Smtnl1 controls Myosin Light Chain 2 phosphorylation through inhibition of Myosin Light Chain Phosphatase 1)(Lontay et al., 2010), we asked whether SMTNL2 phenotypes were associated to a decrease in apical actomyosin contractility. To test this hypothesis, we first measured the intensity of cortical F-actin in SMTNL2 siRNA-treated cysts compared to controls. We fixed and stained 3D-MDCK cells with Phalloidin, a compound that binds and stabilizes filamentous actin (F-actin) and prevents actin fiber depolymerization. Cysts that were silenced for SMTNL2 presented a reduced intensity of apical F-actin compared to control cysts (siControl: 0.32±0.2, siSMTNL2: 0.20±0.07). This result suggests a role for SMTNL2 in apical actin microfilament regulation. A defect in apical actin belt organization could be associated to the failure of Myosin-II activity, which disturbs actin polymerization. Thus, we examined the phosphorylation level of Myosin Light

Chain-2 (p-MLC), as a proxy for contractility. We performed a western-blot analysis of SMTNL2 siRNA-treated and control cysts and observed a significant decrease of MLC phosphorylation in the SMTNL2-depleted cysts compared to controls (siSMTNL2: 0.66±0.18) Moreover, we observed an increase in p-MLC levels in cysts overexpressing SMTNL2-GFP compared to control (SMTNL2-GFP: 1.17±0.1) These results support our previous hypothesis of SMTNL2 requirement for apical actomyosin contractility in epithelial cells.

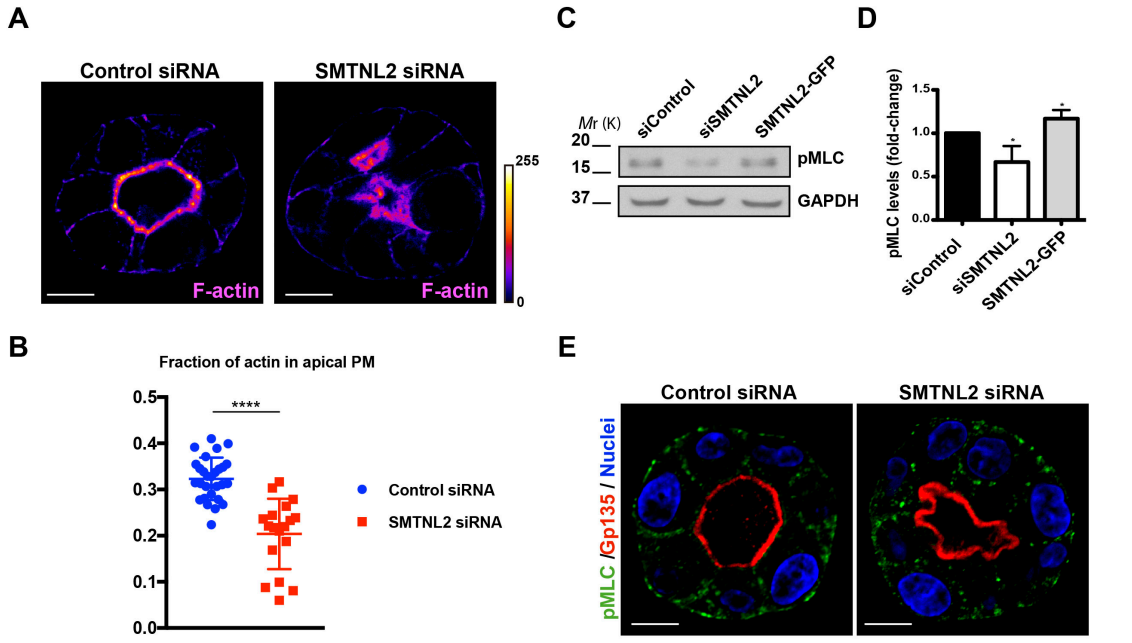

Figure R-9. SMTNL2 is required for the maintenance of the apical actomyosin structure organization in 3D MDCK cells. A) Representative images showing abnormal lumen phenotype in SMTNL2-KD cysts. Control and SMTNL2-KD cysts were grown up to 72h and labeled with Phalloidin to stain F-actin. **B)** Measurement of fraction of apical/total F-actin in PM. **C)** Western blot showing pMLC expression of total lysates from control, SMTNL2-KD cysts and cysts stably expressing SMTNL2-GFP (grown up to 72h). **D)** Protein levels quantified by densitometry and normalized to the control siRNA-treated cysts. GAPDH was used as loading control. **E)** MDCK cysts transfected with control or SMTNL2 siRNAs were grown up to 72h and stained for pMLC, (green), Gp135 (red) and DAPI (blue). Scale bars, 5 µm. Measurements in **B** and **D** are expressed as mean ± SD from 3 independent transfection experiments; *, P < 0.05, ****, P<0.0001 (Student's *t*-test).

10. SMTNL2 silencing results in reduced levels of Gp135 and Claudin2 in 3D MDCK cells.

Apical actomyosin is required for stabilization of apical membrane proteins and receptors implicated in polarization and morphogenesis of epithelial cells (Klingner et al., 2014; Miyoshi and Takai, 2008). Thus, to explain the effect of

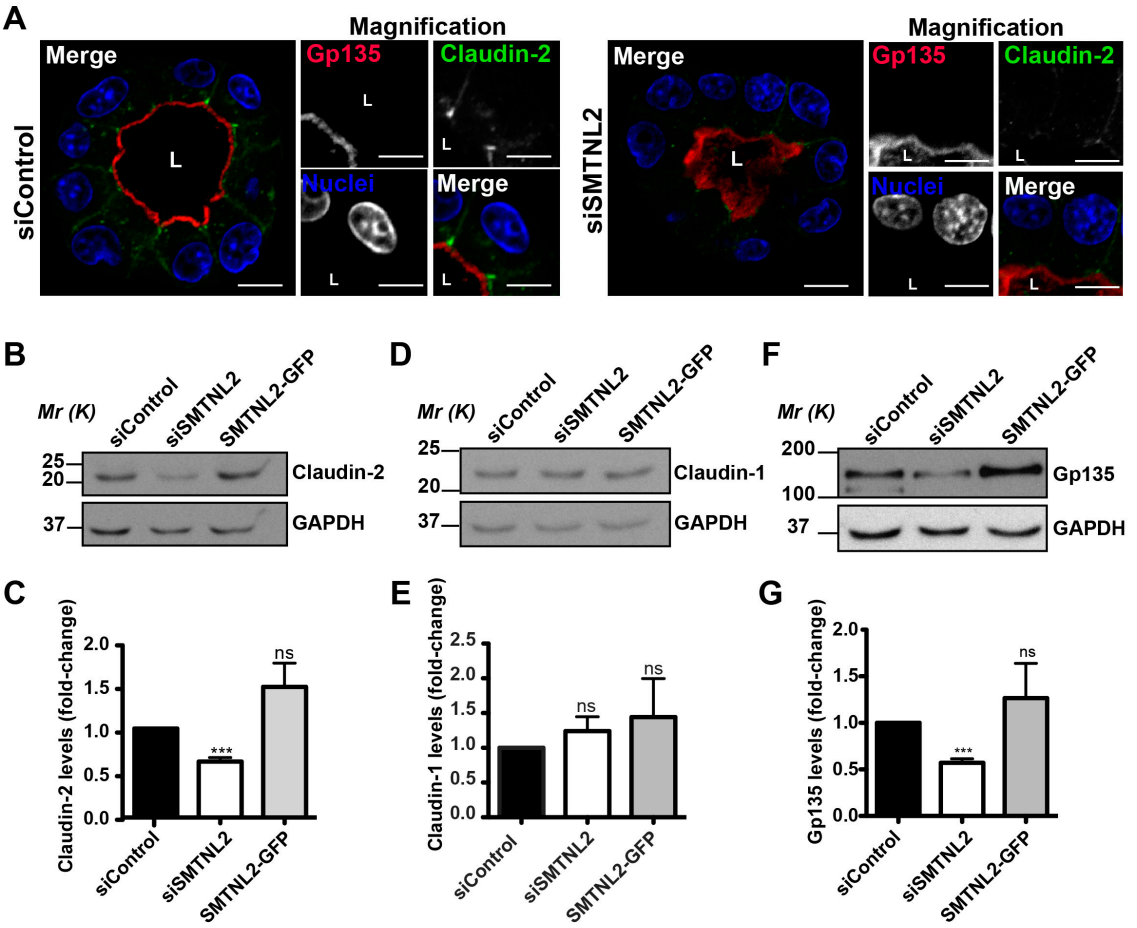

Figure R-10. SMTNL2 is required for apical membrane maturation in 3D MDCK cells. SMTNL2-KD induced abnormal lumen morphologies with a decrease in apical protein Gp135 and Claudin2. **A)** Immunofluorescence of Claudin2 and Gp135 in SMTNL2-KD MDCK cysts. Control and SMTNL2-KD cysts were grown up to 72h and stained for Gp135 (red), Claudin2 (green) and DAPI (blue). **B)** Western blot showing Claudin2 expression in MDCK cysts transfected with siControl or siSMTNL2 and cysts stably expressing SMTNL2-GFP (72h). **C)** Protein levels of Claudin2 quantified by densitometry and normalized to the control. GAPDH was used as loading control. **D)** Western blot showing Claudin1 expression in MDCK cysts transfected with siControl or siSMTNL2 and cysts stably expressing SMTNL2-GFP (72h). **E)** Protein levels of Claudin1 quantified by densitometry and normalized to the control. GAPDH was used as loading control. **F)** Western blot showing Gp135 expression in MDCK cysts transfected with siControl or siSMTNL2 and cysts stably expressing SMTNL2-GFP (72h). **G)** Protein levels of Gp135 quantified by densitometry and normalized to the control. GAPDH was used as loading control. Measurements are expressed as mean ± SD n = 4 independent transfection experiments. ***, P<0.001, ns, not significant (Student's *t*-test). Scale bars, 10µm

SMTNL2 in lumen formation we analyzed the protein levels of two apical markers required for correct 3D cyst maturation. First we examined the levels of Gp135 (also known as Podocalyxin), which has been characterized to bind the actin cytoskeleton in the apical plasma membrane (Meder et al., 2005; Takeda et al., 2001). We performed a western-blot analysis of SMTNL2 siRNA-treated and control cysts and observed a significant decrease in Gp135 total protein levels in

the SMTNL2-depleted cysts compared to controls (siSMTNL2: 0.57±0.1). This suggests that SMTNL2 is required for Gp135 delivery or stability in the apical domain, possibly through its interaction with apical actin.

Previous studies had shown that "leaky" Claudins such as Claudin-2 play an important role during the process of lumen formation (Galvez-Santisteban et al., 2012) and are required for correct lumen expansion (Bagnat et al., 2007). Thus, we analyzed the levels of Claudin-2 in the SMTNL2 siRNA-treated cysts. We observed a significant reduction in protein levels of Claudin-2 but not Claudin-1 in cysts silenced for SMTNL2 compared to control cysts (siSMTNL2: 0.62±0.1; SMTNL2-GFP: 1.47±0.6). Supporting these results, MDCK cysts silenced for SMTNL2 also showed lower levels of Claudin-2 protein by immunofluorescence. All these data suggest that SMTNL2 deficiency causes a defect in actin belt organization, which results in a failure of apical membrane maturation (exemplified by the reduction in Claudin-2 and Gp135 levels) and, as a consequence, a defect of lumen expansion.

11. SMTNL2 is required for the formation of an epithelial monolayer by regulating cell spreading

Previous studies demonstrated the role of apical actomyosin contractility in the establishment of barrier integrity (Acharya et al., 2017). Therefor, we interrogated the role of SMTNL2 in the establishment of the epithelial barrier function. To address this question we cultured SMTNL2 siRNA-treated, control siRNA-treated and SMTNL2-GFP overexpressing and wild-type MDCK cells in a monolayer and analyzed the Trans-Epithelial Resistance (TER) using the ECIS device (see methods), which measures the resistance of a monolayer to the current of ions.

We observed a decrease in TER in SMTNL2-depleted cells compared to controls. Moreover, cells that overexpress SMTNL2-GFP present a faster increase in TER compared to controls, indicating a role for SMTNL2 during the early steps of junction formation. Defects in TER could also be associated to a decrease in cell proliferation, cell death or due to a defect in cell spreading. To investigate which of these biological processes were perturbed, we first decided to measure cell proliferation in 2D. Cells were silenced for SMTNL2 and marked with crystal violet

and then seeded in 2D and analyzed by FACS at different time points (Figure R-11B). SMTNL2-depleted cells did not present any difference in cell proliferation compared to controls. This indicates that SMTNL2 does not control cell proliferation. Next, we decided to measure the ability of SMTNL2-depleted cells to spread in 2D. We observed a significant decrease in cell area SMTNL2 siRNA-treated cells compared to controls. These results show that SMTNL2 regulates cell spreading, and is required for the correct initiation of cell- cell contacts contributes to junction maturation *in vitro*. Since, all these results point that SMTNL2 may act directing the actomyosin cytoskeleton together with the apical epithelial cell architecture, we decided to perform gain of function experiments to evaluate the sufficiency of SMTNL2 for actomyosin contractility and actin polymerization.

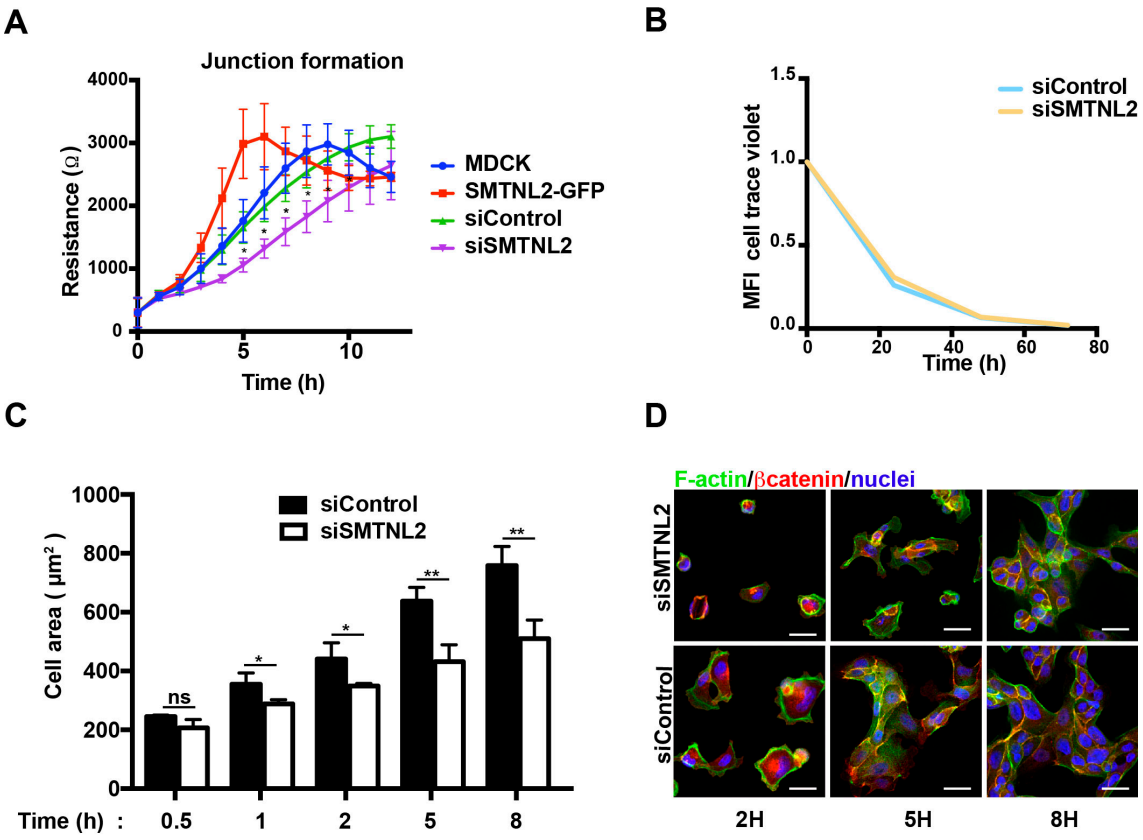

Figure R-11. SMTNL2-KD cells increase TER by decreasing cell-spreading area in 3D MDCK cells. **A)** Plot of measurement of TER showing the initial polarization stage of siControl (green), siSMTNL2 (magenta), MDCK (blue) and SMTNL2-GFP (red) cells. **B)** Analysis of cell proliferation by measurement of cell trace violet mean intensity in Control and SMTNL2-KD cells. **C)** Measurement of cell area in cells silenced for SMTNL2 vs control cells (from 0.5h to 8h). **D)** 2D representative image of control cells and SMTNL2-KD cells at 2h, 5h and 8h. MDCK cells were fixed and labelled with F-actin (green), anti-β- catenin (red) and DAPI (blue). Measurements are expressed as mean ± SD; n = 3 independent transfection experiments; *, P < 0.05; **, P<0.01; ns, not significant (Student's *t*-test). Scale bars, 5µm.

12. SMTNL2 overexpression induced contractile non-apoptotic basal blebs

Blebs are spherical membrane protrusions, which are initiated by rupture of the plasma membrane from the underlying cytoskeleton and are frequently observed during apoptosis, cytokinesis and also during cancer cell migration in both 3D cultures and *in vivo* (Charras et al., 2005; Sahai and Marshall, 2003). In addition bleb contractility is driven by myosin activation through i) RhoA and its effector ROCK and/or ii) myosin light chain kinase (Charras et al., 2005).

Overexpression experiments revealed that MDCK cysts expressing high levels of SMTNL2-GFP induced basal bleb formation (Figure R-12A). Whereas only 30%±0.13 of MDCK cysts normally show basal blebs (as defined by the spherical structure of F-actin and pMLC staining in the basal plasma membrane), 85%±0.04 of MDCK cysts expressing SMTNL2-GFP presented basal bleb formation (Figure R-12B). In addition, since pMLC was shown to localize at the base of these the blebs (Figure R-12AC) we wanted to characterize the blebbing process by incubating cysts expressing SMTNL2-GFP with drugs targeting known actomyosin regulators. Blebbistatin, which inhibits myosin II in an actin-detached state (Kovács et al., 2004), and the Y27632 compound, which inhibits MLCK-kinases ROCKI/II (Takeichi et al., 2014) caused a reduction of 26.6%±8.3 and 32%±7.2 in bleb formation, respectively, indicating that SMTNL2-GFP expression induces canonical actomyosin-mediated membrane blebbing (Figure R-12A). Finally, we wanted to determine if blebs were formed because of an apoptotic response to SMTNL2 overexpression. For this purpose, cysts expressing SMTNL2-GFP were stained for activated (cleaved) Caspase-3 (Casp3). We did not observe positive Casp3 staining in cells presenting membrane blebbing (Figure R-12G).

Since actin polymerization also plays a role in polarized bleb formation and maintenance (Charras et al., 2006; Oyama et al., 2015), we measured F-actin intensity in SMTNL2-GFP overexpressing cysts. We observed a significant increase in basolateral, but not apical, F-actin in SMTNL-GFP cysts compared to controls (MDCK: 10.5±1.4; SMTNL2-GFP: 16±1.8). Indeed, this result supports that SMTNL2 overexpression induces cortical contractility revealed by basal membrane blebbing. Together, these results indicate that SMTNL2 overexpression induces

formation of non-apoptotic basal contractile blebs in MDCK cysts, where Myosin-II activation is driven by ROCK-mediated phosphorylation. All these data prove the role of SMTNL2 in the regulation of cell contractility and modulation of actomyosin dynamics, which is required for correct lumen formation in epithelial morphogenesis.

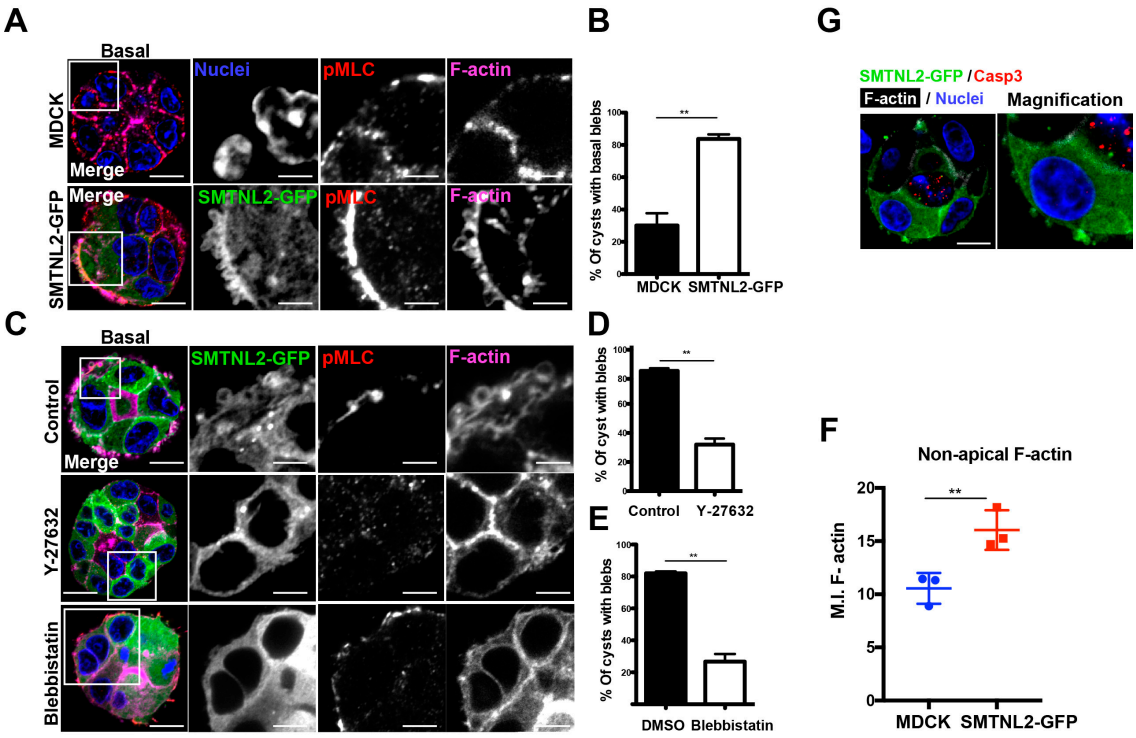

Figure R-12. SMTNL2 overexpression induces non apoptotic basal blebs. **A)** MDCK and SMTNL2-GFP cysts were grown up to 72h and stained for anti-pMLC (red), Phalloidin (magenta) and DAPI (blue). **B)** Quantification of cysts with basal blebs. **C)** SMTNL2-GFP cysts were grown up to 72h. At this time point, cysts were treated with DMSO (control), Blebbistatin (25 mM) or Y27632 (10µM) for 5h. **D)** Quantification of the number of cysts with blebs after Y27632 treatment. **E)** Quantification of the number of cysts with blebs after Blebbistatin treatment. **F)** Mean intensity measurement of non-apical F-actin in control vs. SMTNL2-KD cysts. **G)** SMTNL2-GFP cysts were grown up to 72h and stained for anti-Caspase-3 (red), Phalloidin (grey) and DAPI (blue). Measurements are expressed as mean ± SD percentage of total cysts compared to control; n = 3 independent experiments; *, P < 0.05; **, P<0.01; ns, not significant (Student's *t*-test). Scale bars, 5µm.

13. *In vivo* BioID assay to identify SMTNL2 interacting proteins

To characterize the molecular mechanism associated with SMTNL2 function, we devised an *in vivo* biotinylation assay (bioID) of SMTNL2 proximal proteins.

BioID (for proximity-dependent biotin identification) is based on the fusion of the promiscuous mutant of *Escherichia coli* biotin ligase (birA*) to a targeting protein of interest. This enzyme is highly active in the presence of biotin and is able to biotinylate proteins that are near-neighbors of the fusion protein. Biotinylated proximal proteins can then be isolated by pulldown assay, due to the high affinity of biotin to streptavidin. Finally, we can identify interacting and neighboring proteins in their native cellular environment by mass spectrometry.

To perform the experiment, we cloned human SMTNL2 followed by a double myc tag fused to birA* (SMTNL2-myc-myc-birA*). Next, we generated stable cell lines expressing this construct and tested its subcellular localization. SMTNL2-myc-myc-BirA* presented a similar localization compared to SMTNL2-GFP in MDCK 3D cysts. This result indicates that neither birA* or the myc tag

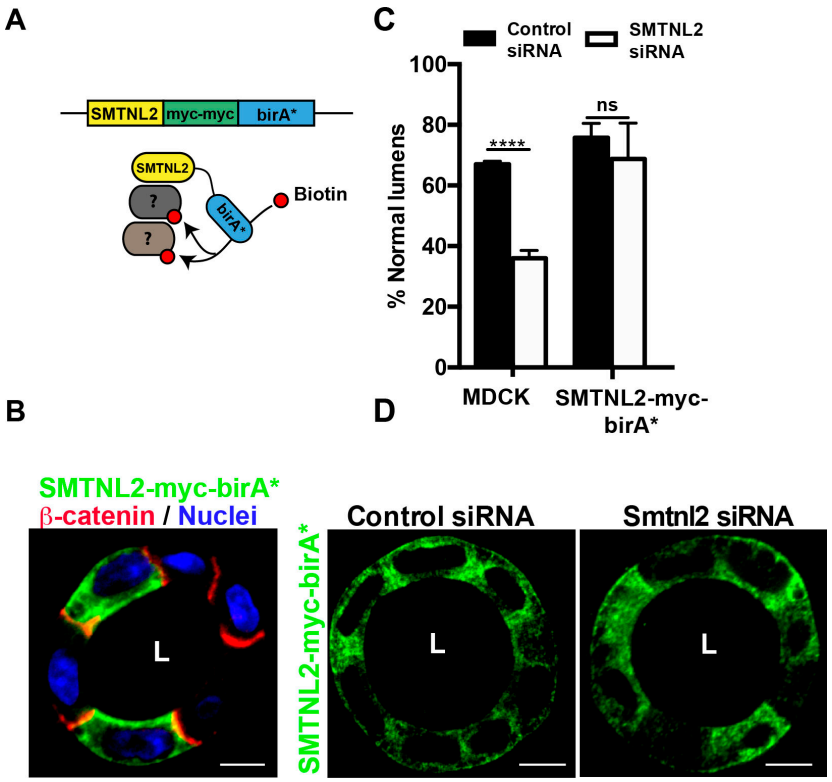

Figure R-13a. SMTNL2-myc-birA*stable cells rescues SMTNL2 deficiency.
A) Cartoon of the SMTNL2 bioID assay. **B)** SMTNL2-myc-birA*stable cells were grown to form cysts at 72h. MDCK cysts were fixed and labelled with anti-β-catenin (red), anti-Myc (green) and DAPI (blue). **C)** Quantification of SMTNL2 KD phenotype and rescue. Measurements are expressed as mean ± SD percentage compared to control single lumen-forming cysts; n = 3 independent transfection experiments; ****, P<0.0001, ns, not significant (Student's *t*-test). **D)** Phenotype rescue of SMTNL2-myc-birA*. WT MDCK cells or MDCK cells stably expressing siRNA-resistant SMTNL2-myc-birA* protein were transfected with control or SMTNL2-specific siRNAs and grown to form cysts at 72h. MDCK cysts were fixed and labelled with anti-Myc (green), and analyzed by confocal microscopy. Scale bars, 5µm. L, lumen.

affects SMTNL2 localization. To determine if SMTNL2-myc-myc-BirA* protein was functional we performed a rescue experiment. For this purpose we generated stable MDCK clones expressing human SMTNL2-myc-myc-BirA* resistant to canine SMTNL2 siRNA and we transfected them with control or SMTNL2 siRNA and performed 3D cultures. We observed that SMTNL2-myc-myc-BirA* cysts generated single lumens at 72h at similar levels compared to the control cysts (siControl: 67±1%, siSMTNL2: 36±2.6%, SMTNL2- birA* siControl: 76±4.7%, SMTNL2- birA* siSMTNL2: 69±11.8%). This result suggests that this construct is functional and can be used for the BioID assay, since its functional interactome must resemble that of endogenous SMTNL2.

To perform the bioID experiment, SMTNL2-myc-myc-birA* stable MDCK cells were grown in biotin free medium in 3D for 72-96h and then lysates were processed in a pull down assay. Two different time points were tested for biotin

A

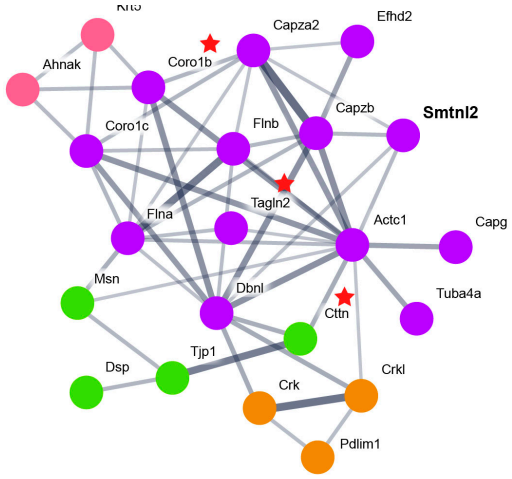

B

Enriched GO terms	p-value	key components
Cadherin (cell adhesion molecule) binding	0.002	CTTN, CAPG, DSP, AHNAK, FLNB, MSN, PDLIM1, CORO1C, CORO1B, FLNA, TJP1, CCT8, CRKL, TAGLN2, ERC1, VAPB, SWAP70
Actin filament (cytoskeletal protein) binding	0.004	CTTN, CAPG, CAPZB, CORO1B, DBNL, CORO1C, FLNA, FLNB, MSN, TAGLN2
Cell-cell contact zone (cell junction)	0.009	CTTN, CAPZB, AHNAK, FLNB, MSN, PDLIM1, CORO1C, CORO1B, FLNA, TJP1, ACTC1, TAGLN2
Actin filament (cytoskeleton)	0.001	CTTN, CAPG, CAPZB, AHNAK, CORO1B, DBNL, CORO1C, FLNA, FLNB, ACTC1, CRKL, MSN, TAGLN2
Intermediate filament (cytoskeleton)	0.001	DSP, KRT5, KRT74, KRT79, PRPH, NEFH
Lamellipodium	0.013	CTTN, CAPZB, CORO1B, FLNA, ACTC1
Focal adhesions (cell-substrate junction)	$6x10^{-05}$	CTTN, CAPZB, AHNAK, FLNB, MSN, PDLIM1, CORO1C, CORO1B, FLNA, ACTC1
Extracellular exosome (vesicle)	$5x10^{-10}$	STOM, CLU, CRKL, VCP, KRT5, FETUB, FLNA, AHNAK, CCT8, ...
Negative regulation of actin depolymerization	0.015	CAPZB, CAPG, CAPZA2, TAGLN2, SWAP70
Regulation of actin filament polymerization	0.014	CTTN, CORO1B, CORO1C, CAPG, CAPZB, CAPZA2, FCHSD1, SWAP70, TAGLN2
Cytoskeleton organization	0.003	CTTN, FLNA, FLNB, DSP, ACTC1, CORO1B, TUBA4A, KRT74, NEFH, CORO1C, CAPZB, SWAP70

molecular function biological process cellular component

Figure R-13b. SMTNL2 interactome. A) STRING plot of SMTNL2 interactome identified in the bioID assay. Thicker connecting lines represent a lower False Discovery Rate (FDR) in STRING analysis (higher confidence). Red stars indicate the proteins with the highest specific peptide counts. Green nodes represent components enriched in cell junctions. Purple nodes represent components enriched in actin cytoskeleton. Pink nodes represent components enriched in intermediate filaments. Orange nodes represent kinases/signaling components. Only interconnected components (nodes with connections) are shown. **B)** Gene ontology (GO) analysis of SMTNL2 interactors. The full list of interacting proteins ranked by their enrichment score (vs. control) was analyzed with GOrilla to visualize enriched GO terms.

exposure (4h and an 12h). Western blot analysis with Streptavidin-peroxidase revealed that the lysates expressing SMTNL2-myc-myc-birA* present several protein bands compared with controls. We did not find any apparent difference between the 4h and 12h biotin exposure times. We then performed mass spectrometry analysis to identify pulled-down proteins. The SMTNL2-specific proximal proteome was then analyzed with STRING (www.string-db.org) including SMTNL2 as a node, to visualize the connected components. Gene ontology analysis revealed that the SMTNL2 proximal proteome was enriched in actin cytoskeleton regulators, cell-cell junctional components and other cytoskeletal components. After ranking the bioID interactome list by peptide abundance, the top three proteins were known actin cytoskeletal regulators: Cortactin, Coronin-1B and Transgelin-2. Since all of our previous results indicated a role for SMTNL2 in actomyosin regulation, we proceeded to better characterize the interaction of SMTNL2 with Cortactin, Coronin-1B and Transgelin-2.

14. Cortactin, Coronin-1B and Transgelin-2 are not induced in MDCK 3D cells

To determine if Cortactin (CTTN), Coronin-1B (CORO1B) and Transgelin-2 (TAGLN2) were induced in 3D, we seeded MDCK cells in 2D and in 3D for up to 5 days, and then we performed a qPCR to analyze the mRNA levels of each gene

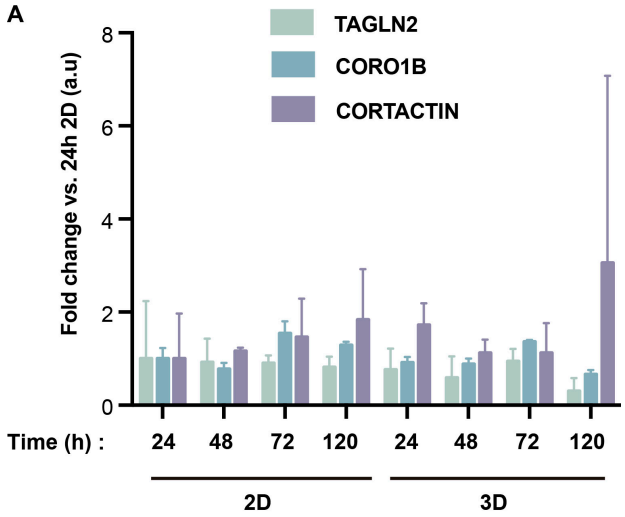

Figure R-14. SMTNL2 biointeractos are not induced in 3D MDCK cells. A) Analysis of TAGLN2, CORO1B and CTTN expression in 2D vs. 3D at different time points (from 24h to 120h) by RT-qPCR. Results are mean ± SD relative to 24h 2D and normalized with HPRT1 (n=3). Student´s t-test.

using HPRT as a loading control. We did not observe a significant increase in mRNA expression in 3D during the process of lumen formation in comparison with 2D cultures. This result indicates that SMTNL2 is the only protein from this network of interacting components that is induced during lumen formation. This further suggested that SMTNL2 is a key regulatjory component within this network, which implies its induced expression during morphogenesis may control the assembly or function of the Cortactin/Coronin-1B/Transgelin-2 protein network. Next, we decided to analyze if either of these components are required for epithelial morphogenesis, and if they phenocopied the silencing of SMTNL2 in MDCK 3D cysts.

15. Cortactin, Coronin-1B and Transgelin-2 are required for epithelial morphogenesis in 3D MDCK cells

To study the role of Cortactin, Coronin-1B and Transgelin-2 during lumen formation, we used siRNA to silence the gene expression of each protein in MDCK cells. We designed two different siRNAs specific to canine Cortactin, Coronin-1B and Transgelin-2 and tested their knock-down efficiency by RT-qPCR (si1CTTN: 47.25±7.96%, si2CTTN: 55.4±8.7% si1CORO1B: 28±11.8%, si2CORO1B: 38.8±9.3% si1TAGNL2: 26.2±6.8%, si2TAGNL2: 24.6±7.9% of control). Next, we transfected MDCK cells with these siRNAs, performed 3D cultures and fixed them after 72h. 3D cultures were stained with apical marker Gp135 to visualize the lumen and then analyzed with confocal microscopy to quantify lumen formation. We observed that MDCK cysts that were treated with Cortactin, Coronin-1B and Transgelin-2 targeting siRNAs presented defects in lumen formation compared to the control (siContol: 72.2±9%, si1CTTN: 17.8±10.8%, si2CTTN: 26±11.5% si1CORO1B: 46.2±19.6%, si2 CORO1B: 23.5±8.3% si1TAGNL2: 65.6±8.3%, si2TAGNL2: 54.2±9.9%). This result indicates that Cortactin, Coronin-1B and Transgelin-2 are required for correct lumen formation. Interestingly, we obtained different phenotypes upon the silencing of each protein in 3D MDCK cells. The more severe phenotype was obtained with the silencing of Cortactin. MDCK cells silenced for Cortactin were no longer able to form lumens, and presented apical marker Gp135 localization facing the basal extracellular matrix, a phenotype

resembling inverted polarity, which is rarely present in control cysts (siControl:

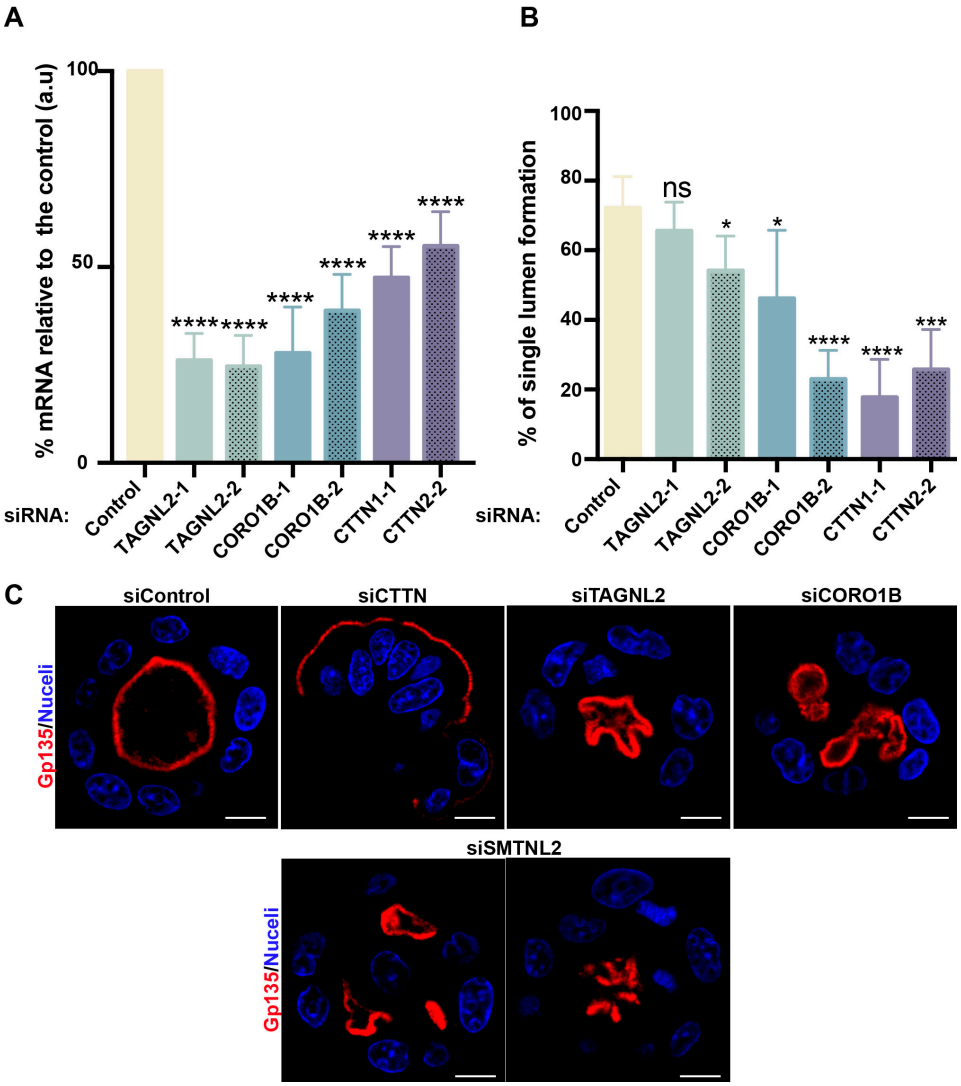

Figure R-15. Trangelin2, Coronin1B and Cortactin are required for normal lumen formation. A) MDCK cells were transfected with control or two different TAGNL2, CORO1B and CTTN siRNAs and grown in 3D cultures up to 72h. The siRNA mediated TAGNL2, CORO1B and CTTN decay was analyzed by RT-qPCR. Results are mean ± SD relative to the control and normalized with HPRT (n=3). **B)** Quantification of cysts with normal lumens in cells silenced for TAGNL2, CORO1B and CTTN vs control cells. **C)** Effect of SMTNL2,TAGNL2, CORO1B and CTTN silencing on lumen formation in 72h MDCK cysts. MDCK cysts were fixed and labelled with anti-Gp135 (red), and DAPI(blue). Bars, 5µm. All values are mean ± SD from three different experiments (n ≥ 100 cysts (or cells)/experiment; (*, P < 0.05; ***; P<0.001; ****, P<0.0001). Student´s t-test

14.6±3.3%, si1CTTN: 72±8.6%, si2CTTN: 55±10.5%). Inverted polarity in MDCK cysts was first described to result upon blocking integrin signaling (Bryant et al., 2014; O'Brien et al., 2001). Integrin binding to laminin is required to trigger Rac1-GTPase activation, which is a known regulator of branched actin polymerization, suggesting that Cortactin is also implicated in this process during initial

polarization events. In contrast, the phenotype observed through the silencing of Coronin-1B was similar to the one obtained with SMTNL2 knock-down (Figure R-15C). Finally, the silencing of Trangelin-2 presents a mild phenotype that was observed only with one siRNA, suggesting a minor role in this process. All these results, suggest that Cortactin, Coronin-1B and Transgelin-2 are required for correct lumen formation, and may act in different steps during epithelial morphogenesis in 3D MDCK cells.

16. Cortactin, Coronin-1B and Transgelin-2 colocalize apically with SMTNL2 .

We wanted to determine the subcellular localization of Cortactin, Coronin-1B and Transgelin-2 in 3D MDCK cells at 72h. To do this experiment we generated

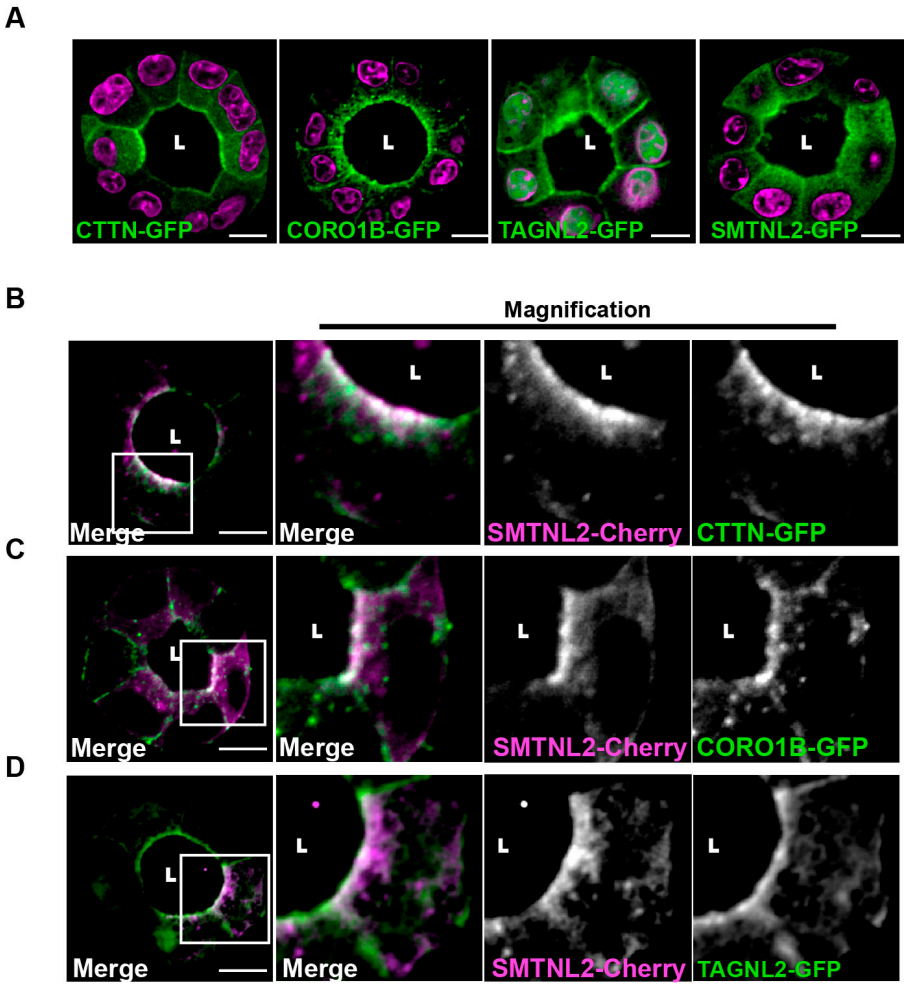

Figure R-16. CTTN-GFP, CORO1B-GFP and TAGNL2-GFP localize apically with SMTNL2-Cherry. A) MDCK stable cell lines expressing CTTN-GFP, CORO1B-GFP, TAGNL2-GFP or SMTNL2-GFP were grown to form cysts at 72h. MDCK cysts were fixed and labelled with DAPI (magenta). **B)** MDCK double stable cell lines expressing CTTN-GFP, CORO1B-GFP or TAGNL2-GFP together with SMTNL2-Cherry**,** were grown to form cysts at 72h. MDCK cysts were fixed and analyzed by confocal microscopy. Scale bars, 5µm.L, Lumen.

stable cell lines expressing CTTN-GFP, CORO1B-GFP and TAGLN2-GFP. Next, we performed 3D cultures and stained to visualize F-actin and nuclei and analyzed the subcellular localization by confocal microscopy. We observed, that the three proteins (Cortactin, Coronin-1B and Transgelin-2) localized apically and at the cell-cell junctions. TAGLN2-GFP cysts also presented a nuclear localization (Figure R-16A). This result suggests that this entire network of actin regulators (SMTNL2, Transgelin-2, Coronin-1B and Cortactin) presents apical and junction localization in 3D-MDCK cells. As a complementary approach, we studied the colocalization of Transgelin-2, Coronin-1B or Cortactin with SMTNL2. For that purpose, we first cloned SMTNL2 tagged to mCherry (SMTNL2-Cherry) and then generated double stable cell lines, performed 3D cultures and analyzed them by confocal microscopy. We confirmed that Transgelin-2, Coronin-1B and Cortactin partially colocalized with SMTNL2-Cherry in the apical domain.

17. Cortactin and Coronin-1B interact with SMTNL2

Since the bioID experiment only provides information about protein proximity, we wanted to determine the physical interaction between SMTNL2 and the two components that presented the strongest phenotype, Coronin-1B and

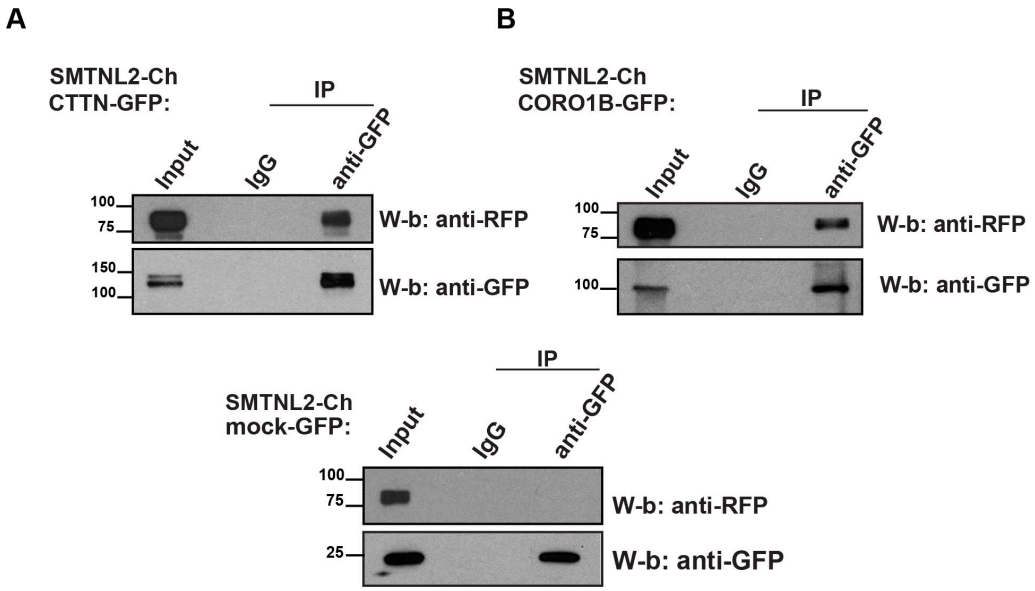

Figure R-17. SMTNL2-Cherry interacts with CORO1B-GFP and with CTTN-GFP in 293 HEK cells. A) Immunoprecipitation of exogeneous Coronin-1B with SMTNL2-Cherry. **B)** Immunoprecipitation of exogeneous Cortactin with SMTNL2-Cherry.

Cortactin. To address this question, we performed a Coimmunoprecipitation (CoIP) experiment. HEK293 cells were cotransfected with CTTN-GFP or CORO1B-GFP together with SMTNL2-Cherry and cultured for 48h. Lysates were incubated with anti-GFP or unspecific IgG antibodies. Western blot analysis using anti-RFP (to detect mCherry) revealed a clear interaction of Cortactin and Coronin-1B with SMTNL2. This result confirms our previous results obtained by immunofluorescence and the bioID assay, and suggests that SMTNL2 interaction with Coronin-1B and Cortactin might directly regulate their function.

18. Exogenous expression of SMTNL2 partially rescues Cortactin and Coronin-1B deficiency

We observed that cysts silenced for Cortactin were not able to form lumens, as they develop inverted polarity. Since SMTNL2 interacts with Cortactin directly, we wondered about the possibility of rescuing the Cortactin-deficient phenotype by inducing the exogenous expression of SMTNL2-GFP.

To perform this experiment, SMTNL2-GFP expressing cells were silenced for Cortactin and analyzed to quantify lumen formation at 72h. We observed that SMTNL2-GFP cells depleted for Cortactin were still unable to form single lumens. However, we observed cysts with multilumens and a significant decrease in inverted polarity (si1CTTN-MDCK: 72±8.6%, si1CTTN-SMTNL2-GFP: 28.6±18.5%, si2CTTN-MDCK: 55±10.6%, si2CTTN-SMTNL2-GFP: 7.8±5%). This result indicates, that exogenous expression of SMTNL2 is able to rescue the inverted polarity phenotype observed by silencing Cortactin in MDCK cells.

Next, we decided to analyze if a similar effect could be detected in SMTNL2-GFP cells depleted for Coronin-1B. We observed that SMTNL2-GFP cells silenced for Coronin-1B were able to form cysts with single lumens at 72h similar to controls (siControl-MDCK: 67±9%, siCORO1B-SMTNL2-GFP: 23±8.3%, siControl-MDCK: 76.7±5%, siCORO1B-SMTNL2-GFP: 56.3±5%). Together, these results demonstrate that exogenous SMTNL2 expression is able to rescue lumen formation defects caused by either Cortactin or Coronin-1B deficiency. This further supports a role for SMTNL2 in controlling this network of actin regulators.

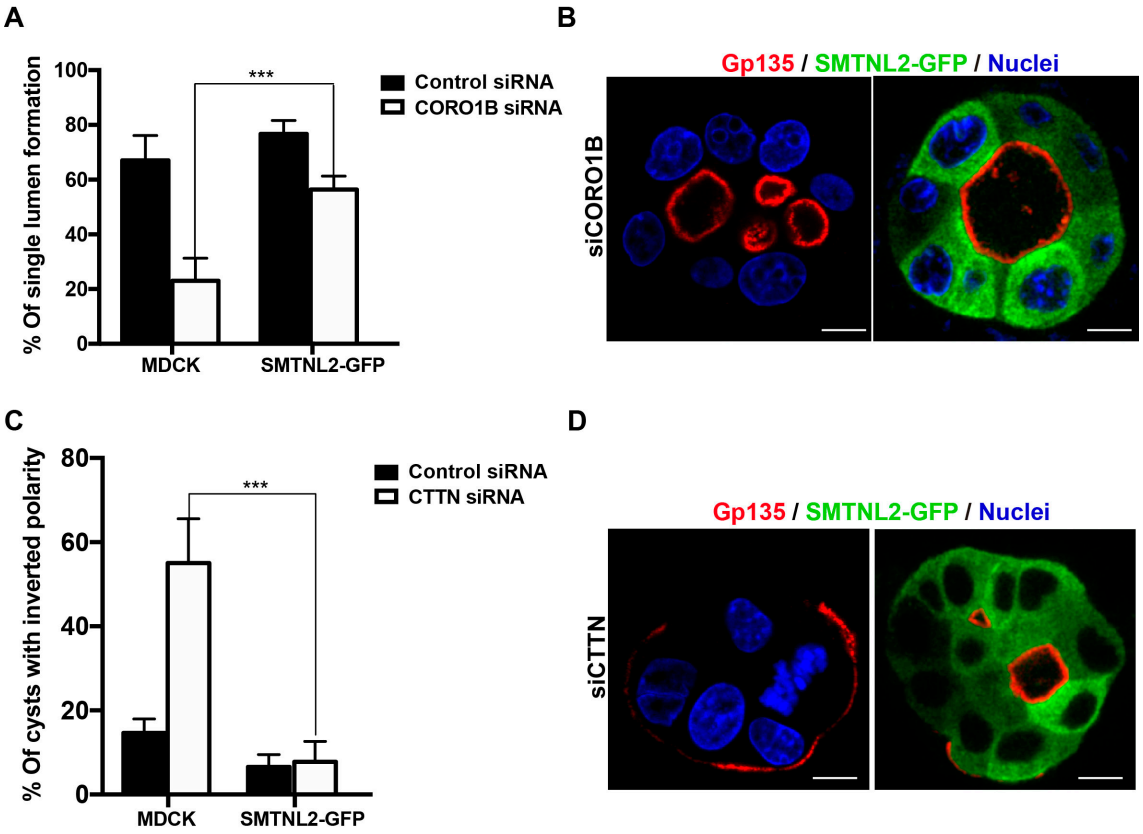

Figure R-18. SMTNL2-GFP rescues Coronin-1B and Cortactin deficiency in 3D MDCK cells. **A)** Quantification of CORO1B-KD phenotype and rescue. Measurements are expressed as mean ± SD percentage compared to control single lumen-forming cysts **B)** CORO1B-KD phenotype in MDCK cysts, and phenotype rescue. WT MDCK cells or MDCK cells stably expressing SMTNL2–GFP protein were transfected with control or CORO1B-specific siRNAs and grown to form cysts at 72h. MDCK cysts were fixed and labelled with anti-Gp135 (red), DAPI (blue) and analyzed by confocal microscopy. Scale bars, 5µm. **C)** Quantification of CTTN-KD phenotype and partial rescue. Measurements are expressed as mean ± SD percentage compared to control inverted polarity forming cysts. **D)** CTTN-KD phenotype in MDCK cysts, and phenotype rescue. WT MDCK cells or MDCK cells stably expressing SMTNL2–GFP protein were transfected with control or CORO1B-specific siRNAs and grown to form cysts at 72h. MDCK cysts were fixed and labelled with anti-Gp135 (red), DAPI (blue) and analyzed by confocal microscopy. Scale bars, 5µm. n = 3 (n ≥ 100 cysts (or cells)/experiment; (***, P<0.001). Student´s t-test

19. Exogenous expression of Cortactin rescues SMTNL2 deficiency in 3D MDCK

Previous results indicated that SMTNL2-GFP is controlling the function of Cortactin during lumen formation. We decided to do the reverse experiment and analyze whether exogenous Cortactin expression rescued SMTNL2 deficiency during lumen formation. We observed that the CTTN-GFP cysts that were treated with SMTNL2 siRNA were able to form single lumens compared to MDCK cyst

treated with SMTNL2 siRNA (siControl CTTN-GFP: 58±21.8%, siSMTNL2 CTTN-GFP: 63.7±5%). This experiment indicates that exogenous expression of Cortactin is sufficient to rescue a normal lumen formation phenotype upon silencing of SMTNL2.

20. Coronin-1B overexpression disrupts epithelial morphogenesis

Coronin-1B and Cortactin have been described to interact in a negative feedback loop, where Cortactin promotes Arp2/3 actin polymerization and Coronin-1B antagonizes this process(Cai et al., 2007b). Since Cortactin was required for single lumen formation, we hypothesized that Coronin-1B overexpression might negatively impact this process. To investigate that, we cultured CORO1B-GFP and CTTN-GFP cells in 3D cultures and analyzed single lumen formation at 72h. Cells that overexpress Cortactin formed open lumens similar to control or SMTNL2-GFP cells in 3D. However, Coronin-1B-overexpressing cells presented a dramatic lumen formation defect, with small multiple lumens (MDCK: 64±5.3%, SMTNL2-GFP: 63±5%, Cortactin-GFP: 65.6±8.7% Coronin1B-GFP: 8±1.5%). This result indicates that Coronin-1B overexpression disturbs single lumen formation and epithelial morphogenesis in

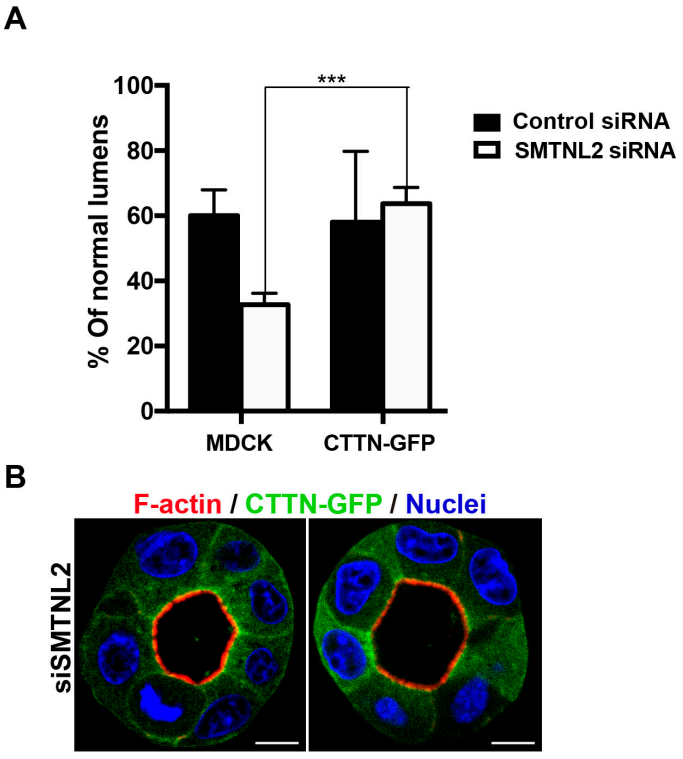

Figure R-19. CTTN-GFP rescues SMTNL2 deficiency in 3D MDCK cells. A) Quantification of SMTNL2 KD phenotype and rescue. Measurements are expressed as mean ± SD percentage compared to control single-lumen-forming cysts **B)** Smntl2-KD phenotype in MDCK cysts, and phenotype rescue. MDCK cells stably expressing CTTN–GFP protein were transfected with control or CORO1B-specific siRNAs and grown to form cysts at 72h. MDCK cysts were fixed and labelled with anti-Gp135 (red), DAPI (blue) and analyzed by confocal microscopy. Scale bars, 5µm. n = 3 (n ≥ 100 cysts/experiment; ***, P<0.001).

3D MDCK cells. These results suggested us to perform epispastic experiments, to identify the pathway required for correct lumen formation in our MDCK 3D model.

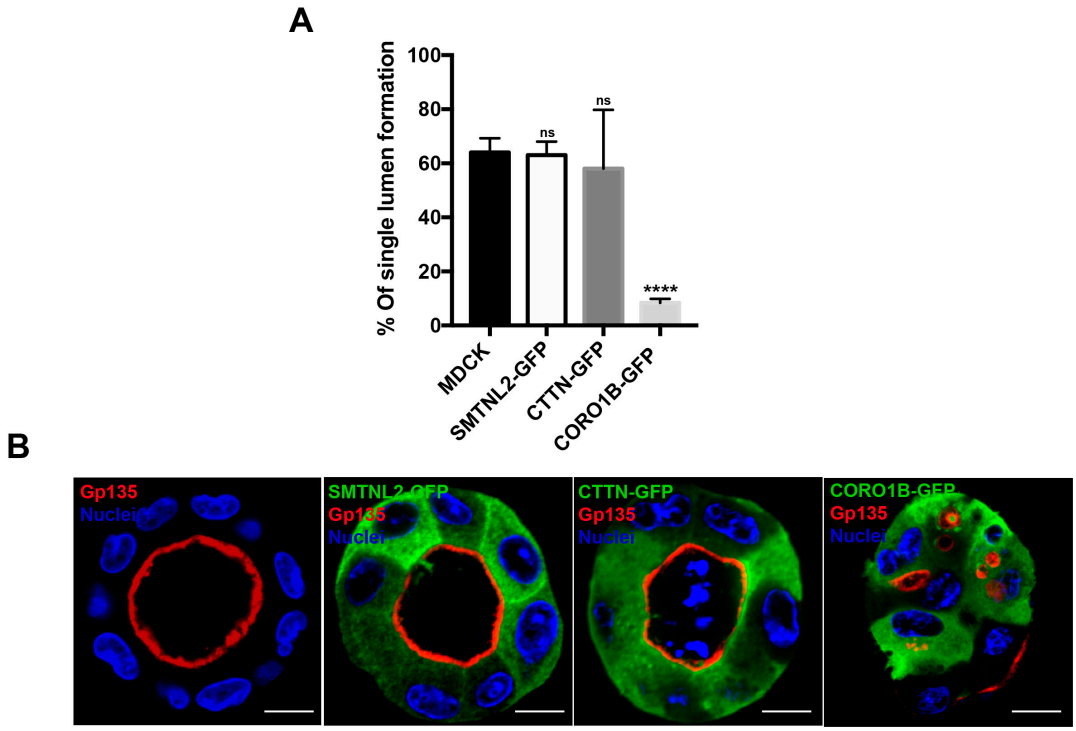

Figure R-20. CORO1B-GFP induce multilumen phenotype. A) Quantification of cysts with normal lumens in cells stably expressing SMTNL2-GFP, CORO1B-GFP and CTTN-GFP vs control cells. **C)** Effect of expressing SMTNL2-GFP, CORO1B-GFP and CTTN-GFP on lumen formation in 72h MDCK cysts. MDCK cysts were fixed and labelled with anti-Gp135 (red), and DAPI(blue). Bars, 5µm. All values are mean ± SD from three different experiments (n ≥ 100 cysts (or cells)/experiment; (****, P<0.0001, ns, not significant). Student´s t-test

DISCUSSION

1. SMTNL2-mediated actomyosin contractility is a novel component of the genetic program that regulates lumen formation

In this present work, we identify the novel function of a cytoskeletal protein in epithelial tissues. SMTNL2 is required for the correct lumen formation in 3D MDCK as well as for the apical membrane maturation in the enterocytes during zebrafish gut development. SMTNL2 forms part of the genetic program that is induced in 3D cultures compared to 2D (Galvez-Santisteban et al., 2012). We have previously identified the function of two other components of this genetic network, Synaptotagmin-like proteins and Plasmolipin, which regulates apical trafficking in different pathways to ensure the formation of a single apical surface in MDCK cysts (Galvez-Santisteban et al., 2012; Rodriguez-Fraticelli et al., 2015). However, at least in our hands, SMTNL2 does not appear to contribute to the apical trafficking mechanism. A number of experiments provided clues to the contribution of SMTNL2 to actomysosin contractility during the process of lumen formation. First, SMTNL2 forms part of the Smtnl family, which all control contractility in different contexts (Lontay et al., 2010; Murali and MacDonald, 2018; Turner and MacDonald, 2014; Ulke-Lemee et al., 2014). Second, SMTNL2 overexpression resulted in very apparent formation of contractile non-apoptotic basal blebs, which is a hallmark of high Rho and myosin activity.

Our experiments suggest that SMTNL2 upregulation in 3D is sufficient to induce actomyosin contractility, based on an increase of MLC phosphorylation, which is catalyzed by ROCK. It is not known whether RhoA activity levels change during 3D morphogenesis, but RhoA has a prominent role in epithelial morphogenesis in flies, where it commands the function of ROCK to stabilize cell-cell junctions and promote apical contractility. *In vivo* studies using the zebrafish posterior lateral line primordium (pllp) have shown that the process of apical constriction, which results in rosette formation with a small central lumen, depends on ROCK activity and RLC2 phosphorylation (Harding and Nechiporuk, 2012). In addition, experiments performed in *Xenopus* observed that ROCK inhibition disrupts gut morphogenesis, resulting in defects in tube elongation, rotation and lumen formation (Reed et al., 2009). In this context, it is likely that contractility is required to partially disassemble junctions and drive junction remodeling, which is necessary for lumen coalescence. Another example of

actomyosin requirement is during lumen formation in the vascular aorta. In this scenario, lumen formation is triggered by extracellular signals where VEGF-A interacts with its receptor VEGFR2 to activate Rho-dependent kinases (ROCK-1, ROCK-2 or both). ROCK subsequently increases the phosphorylation of the RLC2, thus driving the recruitment of NMII to form contractile fibers (Strilic et al., 2009; Sun et al., 2006).

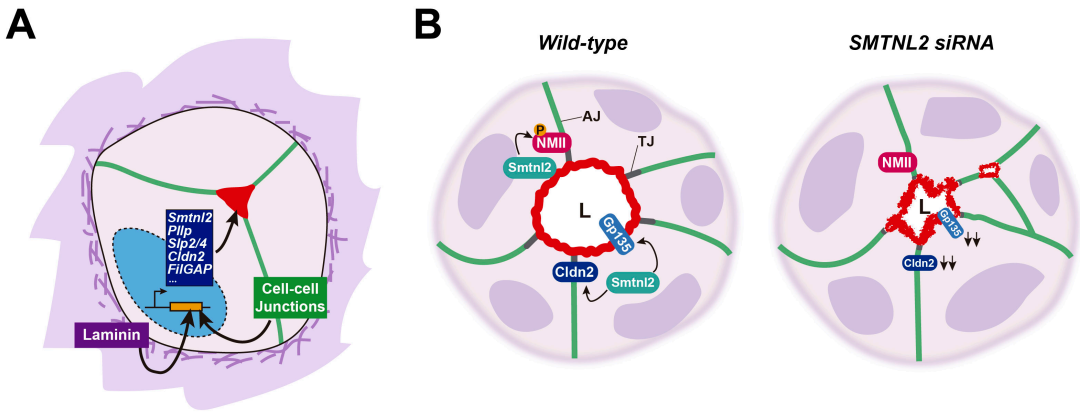

Figure D-1. SMTNL2 forms part of the 3D epithelial polarity program. A) SMTNL2 is induced during 3D epithelial morphogenesis. Mechanical and chemical cues derived from laminin-rich extracellular matrix and cell-cell junctions induce a set of genes involved in the proper polarization and differentiation of epithelial cells. **B)** SMTNL2 depletion causes loss of Myosin Regulatory Light Chain 2 phosphorylation and downregulation of Claudin-2 and Gp135, leading to a defect in single lumen formation and apical membrane expansion.

Interestingly, most experiments evaluating the requirement of ROCK and Rho in mammalian epithelial morphogenesis have shown the opposite effect. Long-term inhibition of ROCK or Myosin results in increased junction formation in epithelial monolayers, and stimulated single lumen formation in 3D-MDCK cysts, whereas overexpression of RhoA constitutive active mutant impairs these processes (Sahai and Marshall, 2002). Interestingly, *in vitro* MDCK tubes treated with ROCK inhibitor result in a multilumen phenotype (Kim et al., 2015), indicating the existence of additional pathways regulating lumen coalescence in tubes that differs from simple 3D cysts.

The lack of a multilumen phenotype in the Y27632 or Blebbistatin-treated cysts is paradoxyal with our interpretation of a role for SMTNL2 in the control of actomyosin contractility. However, most experiments using Y27632 or Blebbistatin were performed during initial steps of lumen formation (Ferrari et al.,

2008; Taniguchi et al., 2015). One explanation is that contractility antagonizes epithelial polarity during the first steps of luminogenesis, but once the lumen and the apical membrane are formed it is necessary to sustain the actomyosin dynamics specifically at the apical domain. An additional possibility is that SMTNL2 would be regulating contractility indirectly, through other myosins (such as Myosin-VI), which depend on Calmodulin rather than in RLC2 for activation, or through organization of the F-actin meshwork, which would then result in a failure of NMII incorporation and activation. The later hypothesis is further supported by our bioID results, which suggest that SMTNL2 is proximal to a variety of actin binding and regulatory proteins, but not Myosins. It is also likely that the RLC2 phosphorylation defect that we observed by western blot analysis and immunofluorescence is happening only in concrete domain within the cells, mostly at the apical pole, according to SMTNL2 localization. In contrast, myosin-inhibitor experiments affect the entire contractility of the cell/cysts, which may also affect the natural physiological process of luminogenesis, resulting in a non-physiological, enhanced process of lumen formation. It will be interesting to check the phosphorylation levels of other Myosins that depend on Calmodulin, such us Myosin-I, V and VI, or inhibit contractility in localized domains, such us at the adherens junctions, through the use of photoactivatable blebbistatin.

The fact that SMTNL2 mRNA is further increased in later steps of lumen formation also suggests that SMTNL2 may have a larger role in lumen maintenance and apical membrane differentiation, in addition to single lumen formation. In this sense, inhibition of actomyosin contractility is known to disrupt junction stability, which would result in abnormal morphologies, including apical domain maturation. It is possible that actomyosin contractility is required for apical membrane maturation and correct microvilli function in epithelial cells. In agreement with this possibility, our *smtnl* -/- mutant did not present a multiple lumen phenotype in the gut, in contrast to the SMTNL2 siRNA phenotype observed in 3D cysts. One hypothesis is that zebrafish may express alternative pathways or mechanisms that overcome the *smtnl* defect and enable the zebrafish gut to develop single lumen. Another explanation is that *smtnl1*, which is also expressed in the gut, partially compensates *smtnl* deficiency. To test these hypotheses, future studies will benefit from double null mutants of *smtnl* and *smtnl1*, perhaps using

the Claudin-15la promoter to drive CRISPR-Cas9 expression and mutagenesis specifically in the gut.

Another important limitation of our study is that we only used the *in vitro* model of 3D-MDCK to dissect the mechanism of SMTNL2. Although SMTNL2 expression is induced and required for lumen formation in this model, these cells are derived from kidney tubules. Several alternative gut-derived models have also been shown to grow into spheric cysts, including Caco2 or primary gut organoids. Analyses of the SMTNL2 mechanism in these systems would greatly complement our observations.

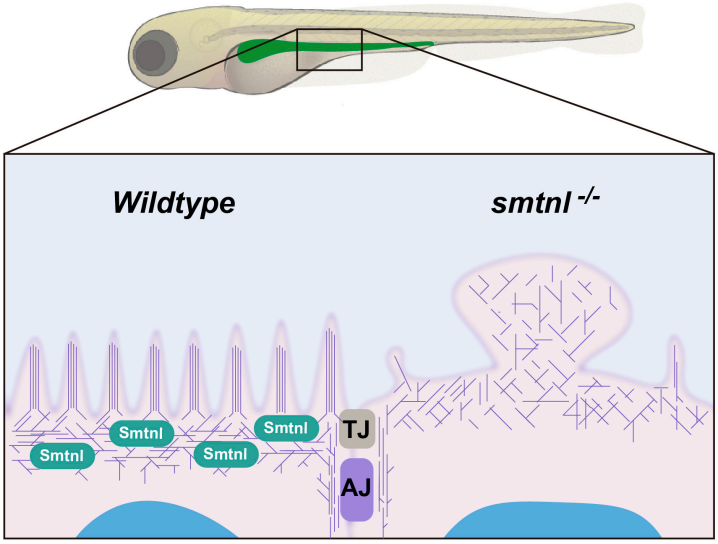

Figure D-2. Smtnl, the zebrafish orthologue of Smnl2, is required for apical maturation in the gut. Smtnl is localized at the apical plasma membrane in the zebrafish gut. Smtnl expression is required for the integrity of the apical cortex. Loss of Smtnl leads to the formation of large apical protrusions and loss of microvilli.

Although we definitely did not detect a defect in gut lumen formation in the *smtnl -/-* mutant, these enterocytes presented a conspicuous defect in apical membrane structure and microvilli integrity resulting in bulges that break inside the luminal cavity. Interestingly, brush border motility has been shown to rely on actomyosin ring contractility (Burgess, 1982; Burgess and Prum, 1982; Stossel et al., 1982). Additionally, a study that treated chick intestine explants with Cytochalasin-B, a drug that blocks the formation of contractile microfilaments, observed similar formation of apical membrane bulges (Burgess and Grey, 1974). Similar alterations are also observed in either genetic or acquired enteropathologies (Delacour et al., 2016; Wallace et al., 2005). It will be interesting to treat zebrafish guts with Cytochalasin, Blebbistatin or Y27632, and perform the same experiments in the zebrafish gut and observe if the enterocytes develop apical microvilli defects and

protrusions. Complementary experiments should also attempt to inhibit different actin nucleating factors, such as Arp2/3 or Formins, once the lumens are formed to observe their cooperation with SMTNL2 in MDCK cysts and the zebrafish gut.

2. Actomyosin control of cell-cell junctions and apical maturation

The actomyosin cytoskeleton is responsible for many changes in cell and tissue shape. For a long time, the actomyosin cytoskeleton has been known to display dynamic contractile behavior, in which F-actin and NMII first assemble in a subcellular structure and then disassemble, on a short timescale. An understanding of this process is recently emerging and is called the 'actomyosin pulsing'. In epithelia, evidence suggests that actomyosin pulsing, also known as actomyosin turnover, is required to maintain tissue integrity during contractile processes (Coravos et al., 2017). The functions of actomyosin pulsing *in vivo* are not fully elucidated. However, evidence suggests that it plays an essential role in maintaining intercellular mechanical connections in tissues that undergo morphogenesis. Pulsing was observed in the Drosophila embryo in several contexts, such us in the apical constriction of epithelial cells of the ventral furrow or during the process of constriction of the amnioserosa cells upon dorsal closure, among others (Blanchard et al., 2010; Martin et al., 2010; Martin et al., 2009; Solon et al., 2009). In those contexts, pulses correlate with contracting apical area (Martin et al., 2009), shrinking pre-existing cell contacts (Rauzi et al., 2010), or elongating junctions (Collinet et al., 2015), which leads to tissue extension. Since in our SMTNL2-knock down cysts and in *smtnl -/-* mutants we observed a specific defect in the apical membrane shape associated to the actomyosin network, it is not surprising to think that SMTNL2 could play a role in regulating actomyosin pulses in a concrete space and time at the apical/junctional boundaries in epithelia.

One way of testing this hypothesis would be to inhibit the expression of SMTNL2 orthologues in *Drosophila* (either with CRIPSR or siRNA), or, conversely, overexpress SMTNL2, and analyze the process of dorsal closure and ventral furrow formation during gastrulation. Another method to measure junctional tension in SMTNL2-knock down and overexpressing cells would be to perform laser ablation

experiments to measure the velocity recoil of the ablated junctions, giving us a cue about how SMTNL2 regulates epithelial cortical tension and junction maturation.

An interesting observation supporting the role of SMTNL2 in junctional maturation is the defect in Claudin-2 levels observed upon SMTNL2 silencing. It is known that leaky Claudins, including Claudin-2 paralogue Claudin-15, form paracelullar channels for small cations and water, which is required for fluid accumulation and lumen coalescence in the zebrafish gut. Interestingly, Claudin-2 expression is required for the proper sorting of Gp135 to the apical domain in 2D MDCK cultures (Yasuda et al., 2012). Since we observed a reduction in the protein levels of Claudin-2 and Gp135 in the SMTNL2 siRNA-treated cysts, one explanation to the observed multilumen phenotype would be that SMTNL2 controls Claudin-2 and Gp135 apical targeting, which are essential for lumen formation, expansion and resolution. An alternative hypothesis is that the decrease in apical marker Gp135 and tight junction Claudin-2 simply indicate an overall defect in epithelial maturation, especially since both genes are induced during 3D morphogenesis (Galvez-Santisteban et al., 2012; Lim et al., 2017; Meder et al., 2005). In agreement with this line of thought, we detected a partial downregulation of Claudin-2 mRNA in SMTNL2 siRNA-treated cysts (not shown). A simple experiment to solve this question will be to overexpress Claudin-2 in cysts knocked down for SMTNL2 to analyze if exogenous Claudin-2 expression is capable to rescue a normal single lumen phenotype.

Leaky claudins such as Claudin-2 are responsible to maintain a low Trans Epithelial Resistance (TER) in a monolayer of epithelial cells. Since the silencing of Claudin-2 is associated with an increase in the TER, our observed reduction in Claudin-2 levels is paradoxical with the TER measurements that we obtained upon SMTNL2 silencing. In our hands, SMTNL2 siRNA-treated cells displayed a delay in junction initiation but the final TER was comparable to control cells after 10h. Interestingly, the reduction in Claudin-2 mRNA and protein levels could only be observed in 3D but not in 2D cultures, further suggesting that Claudin-2 downregulation results from overall loss of epithelial polarity resulting from a lack of proper apical cytoskeleton organization. Previous studies have shown that Slp2 proteins are able to regulate Claudin-2 expression through the MAP Kinase pathway and ERM protein phosphorylation (Yasuda et al., 2012). As a follow-up to

our studies, it will be interesting to analyze ERM and MAP Kinase activity in SMTNL2 siRNA-treated cysts.

Our TER measurements also prompted us to evaluate how SMTNL2 was regulating junction initiation and expansion. Our observation that SMTNL2 siRNA-treated cells presented a significative decrease in cell spreading explains the delay in TER, as cells plated onto artificial adhesive surfaces first flatten and then deform extensively as they spread. Cell spreading is mostly driven by actin polymerization and promoted by the Rho-family GTPases Cdc42 and Rac1. These two molecules initiate actin polymerization by different pathways that drive extension of the leading cell edge (Worthylake et al., 2001). Subsequently, RhoA GTPase regulates myosin dependent contractile forces, which are required for formation of adhesive contacts and stress fibers. These results agree with the decrease in pMLC levels observed upon SMTNL2 knockdown and the formation of basal contractile blebs, which can be a consequence of local activation of RhoA. It will be highly informative to analyze the levels of Rac1 or Cdc42 activity in the absence or presence of SMTNL2 to further explain our TER results.

Another interesting angle of experimentation will be to measure junction permeability in 3D, when SMTNL2 is induced. Since it is very difficult to measure junction permeability in mature 3D MDCK cysts, one way to address this question is using the zebrafish *smtnl -/-* mutant. Microgavaging of zebrafish larvae with fluorescent 10kD dextran has been used previously to evaluate monolayer permeability (Marjoram et al., 2015). In a normal epithelial monolayer, the dextran is not able to cross the epithelial barrier. If SMTNL2 loss leads to a defect in junctional integrity or permeability, then gavaging of dextran would result in fluorescence accumulation in the circulatory system, which can be measured by microscopy. Together, these experiments should clarify the role of SMTNL2 in junction integrity and maturation, and the mechanisms that are related to its role in epithelial polarization.

3. An apical network of actin regulatory proteins coordinates actomyosin dynamics during epithelial morphogenesis

Decades of work have shown that epithelial actin remodeling is triggered by junction formation and maturation. However, dynamic actin remodeling in

epithelia has rarely been explained by changes in gene expression. Our works confirms that SMTNL2 is induced during lumen formation in MDCK cysts. Our study offers a new understanding of a possible actin binding protein network, which is required for apical membrane formation and maturation. SMTNL2 forms an apical junctional network together with Coronin-1B and Cortactin to control the actomyosin meshwork required for lumen formation and apical maturation. Although we could detect an interaction between SMTNL2 and Coronin-1B and Cortactin by coimmunoprecipitation, we do not have evidence of a direct or indirect interaction yet. Probing these interactions with *in vitro* purified proteins will shed further light onto the molecular mechanism of this network. Additionally, it will be essential to identify which domain of SMTNL2 is required for the interaction with either Cortactin or Coronin-1B, as well as for its apical/junctional localization. Likewise, it will be exciting to unravel if this interaction is exclusive of SMTNL2 or if it is also possible for other Smtnl family proteins.

The interaction of SMTNL2 with Cortactin, a class II NPF, suggests that it may regulate epithelial morphogenesis through the regulation of actin polymerization, which is indeed necessary for various aspects of lumen formation, including apical membrane initiation and lumen expansion. Previous works have demonstrated that the Arp2/3 complex is required for AMIS formation in human pluripotent stem cells and that inhibition of this complex reduces AMIS formation (Taniguchi et al., 2015). In addition, another study determined that Arp2/3 is required for junction initiation as well as for junction maturation in epithelial cells (Bernadskaya et al., 2011). There is a plethora of reports demonstrating the role of Cortactin in promoting actin polymerization through its interaction with the Arp2/3 complex, which would further suggest that SMTNL2 is a positive regulator of branched actin polymerization. Additionally, actin branching is antagonized by Coronin-1B, which was also forming part of the SMTNL2 proximal proteome (Cai et al., 2007a; Cai et al., 2007b), indicating that SMTNL2 might recruit proteins with opposing roles on actin fiber nucleation. Since SMTNL2 and Cortactin exogenous expression is compatible with single open lumens, and SMTNL2 depletion can be rescued by Cortactin exogenous expression, we suggest that SMTNL2 and Cortactin act in the same pathway. Further experiments must be addressed to determine if SMTNL2 is regulating this function by direct binding to Cortactin

promoting its nucleation activity through the binding to the Arp2/3 complex or indirectly, through the binding to Coronin-1B inhibiting its antagonist activity on actin polymerization through the Arp2/3 complex. In this sense, an essential experiment will be to analyze if SMTNL2 or Cortactin overexpression rescues the defects on lumen formation caused by Coronin-1B overexpression.

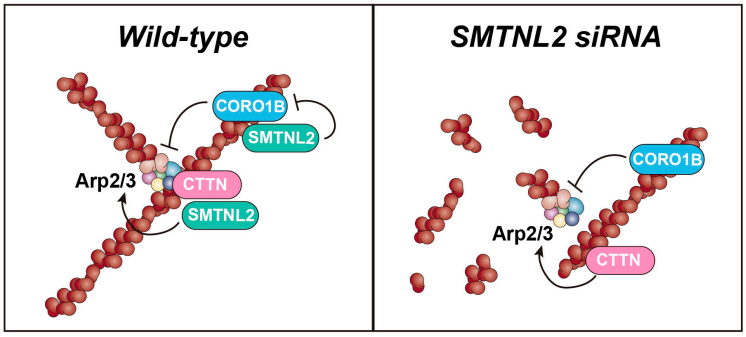

Figure D-3. SMTNL2 forms an apical network of actin regulators with CTTN and CORO1B. SMTNL2 stimulates CTTN nucleator promoting function, inducing polymerization of actin. In contrast, SMTNL2 prevents CORO1B-mediated debranching and filament depolymerization. Upon loss of SMTNL2, CORO1B function overcomes CTTN, leading to debranching and compromising the apical actin cortex.

Thus far, we are explaining our defects on lumen formation and apical membrane maturation with a failure on branched actin polymerization, based on the large list of Arp2/3 regulators that appear on the SMTNL2 bioID proteome. However, polymerization of unbranched filaments by Formins also plays an important role during lumen formation. In fact FMNL2 and INF2 are required for epithelial morphogenesis and their silencing impairs lumen formation in 3D organotypic cultures (Grikscheit et al., 2015; Madrid et al., 2010). It is enticing to quantify the distribution and determine the contribution of both branched and unbranched actin during lumen formation and maintenance. Several works demonstrate that the Arp2/3 complex is necessary for lumen initiation but whether the inhibition of branched actin polymerization disrupts apical membrane organization and function in mature cysts is still unknown. Treating cysts with Arp2/3 inhibitors after the lumen is formed (at 48h to 72h) would reveal its requirement for apical/junctional maintenance.

Further *in vitro* experiments must also be performed to validate the role of SMTNL2 on Cortactin or Coronin-1B, such as measuring the elongation of actin fibers in the presence of SMTNL2 alone or in presence of purified Cortactin, and/or Coronin-1B, together with Arp2/3 complex and VCA peptides to stimulate actin nucleation. Another alternative is to evaluate the contribution of SMTNL2 in the

process of lamellae formation in spreading cells, with or without concomitant expression or suppression of Cortactin and/or Coronin-1B. One simple experiment would be to add Arp2/3 inhibitor in SMTNL2-depleted cells and wash out and further imaging of lamellae recovery. This experiment will inform us if SMTNL2 is regulating actin nucleation through the Arp2/3 complex (Cai et al., 2007a; Cai et al., 2008; Cai et al., 2007b; Uetrecht and Bear, 2006).

One caveat of our proposed SMTNL2-Cortactin-Arp2/3 mechanism is that the silencing of Cortactin and SMTNL2 present completely different phenotypes in 3D MDCK cells. The phenotype observed upon Cortactin silencing leads us think that Cortactin may play a more significant role during the early steps of epithelial morphogenesis, due to the strong amount of cysts presenting inverted polarity. This suggests that branched actin is required for the establishment of the initial axis cues that orient epithelial cell polarity. It is highly likely that the mechanism forms part of the laminin-β1-integrin-Rac1 module that is present in 3D MDCK cells (Yu et al., 2005). Further suggesting this, Cortactin deficiency in endothelial cells and *in vivo* colon epithelial cells is associated with an increase in RhoA-ROCK activity. This part of our work opens up numerous interesting questions, such as why is SMTNL2 able to partially rescue the inverted polarity phenotype caused by Cortactin deficiency, and what is the role for SMTNL2 during polarity acquisition?

Again *in vivo*, however, it remains apparent that the SMTNL2-Cortactin pathway is not necessary for polarity orientation or lumen formation. Instead, Cortactin KO mice present a defect in the epithelial barrier integrity in the intestinal epithelium, further suggesting that this apical actin binding protein network is controlling apical maturation and epithelial integrity in this context. The same study reports that patients suffering from Inflammatory Bowel diseases (IBD) present a reduction in Cortactin mRNA and protein levels (Citalan-Madrid et al., 2017; Garcia Ponce et al., 2016). It will be interesting to analyze the levels of SMTNL2 mRNA in patients presenting with these symptoms.

4. SMTNL2 in tumor migration of epithelial cells

SMTNL2 mRNA is downregulated in several studies comparing epithelial primary tumors with normal tissues of origin, such us in kidney tumors and breast

cancer (Oncomine). Interestingly, 2 out of 10 studies comparing colorectal tumors with normal colon found a moderate yet significant upregulation of SMTNL2 expression, and 1 out of 10 studies found a strong downregulation. This suggests that loss of SMTNL2 might be implicated in the mechanism of carcinogenesis, but upregulation of SMTNL2 can also contribute to tumor survival or invasion. Along these lines, we observed bleb formation upon SMTNL2 overexpression, which are non-apoptotic and seems to appear only in soft matrix. It is known that tumor cells can develop additional ways of migration alternative to Rac1-mediated lamellipodia and metalloprotease-based ECM degradation, which is mediated by membrane blebbing (Sahai and Marshall, 2003; Tozluoglu et al., 2013). This blebbing-type migration mode requires RhoA/ROCK module activation. Therefore, it would be interesting to measure SMTNL2 levels during invasion or migration of tumor cells, and determine if SMTNL2 is required for progression of colon carcinoma.

5. Other SMTNL2 binding proteins

One of the most biotinylated proteins in our BioID assay was Desmoplakin. This protein is located and forms the desmosomes that constitute the junctional component below the AJs. Desmosomes associate with the intermediate filaments, formed by cytokeratins, which are abundant in epithelial cells and necessary for epithelial integrity. However, little is known about the role of cytokeratins and desmosomes in epithelial morphogenesis or lumen formation. Thus, it is a relatively new and exciting possibility to explore together with the contribution of SMTNL2 to the actin-cytokeratin dynamics in polarized epithelial cells.

CONCLUSIONS

1. SMTNL2 forms part of the genetic program that is induced during the process of lumen formation in epithelial morphogenesis and is required for single lumen formation and the maintenance of the correct 3D epithelial architecture.

2. SMTNL2 controls the epithelial architecture through the regulation of the apical actomyosin cytoskeleton by controlling both the F-actin polymerization and myosin regulatory light chain-II phosphorylation and function in 3D MDCK cells. This mechanism is further supported by the failure of cells to spread upon SMTNL2 silencing and the evidence that SMTNL2 overexpression results in formation of contractile basal blebs, processes that rely on actomyosin-mediated contractility.

3. Loss of SMTNL2 function compromises apical membrane structure, shape, integrity and functionality, as reflected by a reduction in the apical transmembrane marker Gp135 and junctional tight junction protein Claudin-2. The later is also induced and required for the process of lumenogenesis, thus suggesting a possible indirect mechanism explaining the phenotypes observed upon SMTNL2 silencing in 3D MDCK cells.

4. SMTNL2 regulates the apical membrane tension in the enterocytes of the zebrafish gut, as evidenced by the appearance of apical membrane bulges facing the central lumen in *smtnl* mutants. Loss of SMTNL2 also leads to a disorganization of the apical microvilli and thus affects brush border integrity, further supporting a role for SMTNL2 in regulating cortical actin dynamics.

5. SMTNL2 forms part of an apical junctional network composed by Cortactin, Coronin-1B and Trangelin-2, which are previously known modulators of the actin cytoskeleton in different systems. We have demonstrated that Cortactin, Coronin-1B and Trangelin-2 are required for single lumen formation in 3D MDCK and thus are novel regulators of epithelial morphogenesis, suggesting a prominent role of the actin cytoskeleton dynamics at different steps during luminogenesis.

6. SMTNL2 and Cortactin may act in the same pathway regulating actin branching/polymerization formation, which is essential for the apical membrane formation and maintenance in 3D MDCK. In contrast, Coronin-1B acts in an opposing manner, antagonizing this process possibly through its known role as an inducer of actin debranching.

1. SMTNL2 forma parte de un programa genético que está inducido durante el proceso de formación de lúmenes durante la morfogénesis epitelial y es necesaria para la formación de un único lumen y el mantenimiento de la arquitectura epitelial en 3D.

2. SMTNL2 controla la arquitectura epitelial a través de la regulación del citoesqueleto de la actomiosina apical controlando por un lado la polimerización de la F-actina y por otro lado la fosforilación y la función de la cadena reguladora ligera de la miosina-II. Este mecanismo está a su vez apoyado debido a que el silenciamiento de SMTNL2 afecta a la extensión celular y debido a que la sobreexpresión de SMTNL2 genera la formación de *blebs* basales contráctiles.

3. La pérdida de la función de SMTNL2 conlleva a la alteración de la estructura, forma, integridad y funcionalidad de la membrana apical, como se ve reflejada con la bajada de la proteína transmembrana Gp135 y la proteína de uniones estrechas Claudina-2. Ésta última está a su vez inducida y es necesaria para el proceso de formación de lúmenes, lo que sugiere un posible mecanismo indirecto que pueda explicar el fenotipo de multilumen observado tras el silenciamiento de SMTNL2 en células MDCK en 3D.

4. SMTNL2 regula la tensión de la membrana apical en los enterocitos del intestino del pez cebra, debido a que en el mutante de *smtnl* se observan bultos en la membrana apical proyectando hacia el interior del lumen. La pérdida de SMTNL2 conlleva a su vez a la desorganización de las microvellosidades, afectando a la integridad del borde en cepillo, lo cual sugiere una función de SMTNL2 en la regulación de la dinámica de la actina cortical.

5. SMTNL2 forma parte de una red apical compuesta por Cortactina, Corinina-1B y Transgelina-2, las cuales se conocen previamente sus funciones reguladoras de la actina en diferentes sistemas. Hemos demostrado que Cortactina, Corinina-1B y Transgelina-2 son necesarias para la formación de un único lumen células MDCK en 3D y por lo tanto son nuevas reguladoras de la morfogénesis epitelial. Sugiriendo una función prominente de la dinámica del citoesqueleto de actina en diferentes pasos durante la formación del lumen.

6. SMTNL2 y Cortactina podrían actuar sinérgicamente en la misma vía regulando la ramificación/ polimerización de actina, la cual es necesaria para la formación y el mantenimiento de la membrana apical en MDCK en 3D. Por el contrario Coronina-1B podría actuar de manera opuesta, antagonizando este proceso, posiblemente ejerciendo su función de desramificación de la actina.

BIBLIOGRAPHY

- Acharya, B.R., Wu, S.K., Lieu, Z.Z., Parton, R.G., Grill, S.W., Bershadsky, A.D., Gomez, G.A., and Yap, A.S. (2017). Mammalian Diaphanous 1 Mediates a Pathway for E-cadherin to Stabilize Epithelial Barriers through Junctional Contractility. Cell reports *18*, 2854-2867.

- Akhtar, N., and Streuli, C.H. (2013). An integrin-ILK-microtubule network orients cell polarity and lumen formation in glandular epithelium. Nature cell biology *15*, 17-27.

- Alvers, A.L., Ryan, S., Scherz, P.J., Huisken, J., and Bagnat, M. (2014). Single continuous lumen formation in the zebrafish gut is mediated by smoothened-dependent tissue remodeling. Development *141*, 1110-1119.

- Apodaca, G., Gallo, L.I., and Bryant, D.M. (2012). Role of membrane traffic in the generation of epithelial cell asymmetry. Nature cell biology *14*, 1235-1243.

- Atilgan, E., Wirtz, D., and Sun, S.X. (2006). Mechanics and dynamics of actin-driven thin membrane protrusions. Biophysical journal *90*, 65-76.

- Bagnat, M., Cheung, I.D., Mostov, K.E., and Stainier, D.Y. (2007). Genetic control of single lumen formation in the zebrafish gut. Nature cell biology *9*, 954-960.

- Bagnat, M., Navis, A., Herbstreith, S., Brand-Arzamendi, K., Curado, S., Gabriel, S., Mostov, K., Huisken, J., and Stainier, D.Y. (2010). Cse1l is a negative regulator of CFTR-dependent fluid secretion. Current biology : CB *20*, 1840-1845.

- Banon-Rodriguez, I., Galvez-Santisteban, M., Vergarajauregui, S., Bosch, M., Borreguero-Pascual, A., and Martin-Belmonte, F. (2014). EGFR controls IQGAP basolateral membrane localization and mitotic spindle orientation during epithelial morphogenesis. The EMBO journal *33*, 129-145.

- Bereiter, H., Gautier, E., and Huggler, A.H. (1990). [Infected prosthesis of large joints]. Therapeutische Umschau Revue therapeutique *47*, 606-611.

- Bernadskaya, Y.Y., Patel, F.B., Hsu, H.T., and Soto, M.C. (2011). Arp2/3 promotes junction formation and maintenance in the Caenorhabditis elegans intestine by regulating membrane association of apical proteins. Molecular biology of the cell *22*, 2886-2899.

- Bernascone, I., Hachimi, M., and Martin-Belmonte, F. (2017). Signaling Networks in Epithelial Tube Formation. Cold Spring Harbor perspectives in biology *9*.

- Blanchard, G.B., Murugesu, S., Adams, R.J., Martinez-Arias, A., and Gorfinkiel, N. (2010). Cytoskeletal dynamics and supracellular organisation of cell shape fluctuations during dorsal closure. Development *137*, 2743-2752.

- Blaser, H., Reichman-Fried, M., Castanon, I., Dumstrei, K., Marlow, F.L., Kawakami, K., Solnica-Krezel, L., Heisenberg, C.P., and Raz, E. (2006). Migration of zebrafish primordial germ cells: a role for myosin contraction and cytoplasmic flow. Developmental cell *11*, 613-627.

- Blumer, J.B., Kuriyama, R., Gettys, T.W., and Lanier, S.M. (2006). The G-protein regulatory (GPR) motif-containing Leu-Gly-Asn-enriched protein (LGN) and Gialpha3 influence cortical positioning of the mitotic spindle poles at metaphase in

symmetrically dividing mammalian cells. European journal of cell biology *85*, 1233-1240.

- Bodoor, K., Lontay, B., Safi, R., Weitzel, D.H., Loiselle, D., Wei, Z., Lengyel, S., McDonnell, D.P., and Haystead, T.A. (2011). Smoothelin-like 1 protein is a bifunctional regulator of the progesterone receptor during pregnancy. The Journal of biological chemistry *286*, 31839-31851.

- Borman, M.A., Freed, T.A., Haystead, T.A., and Macdonald, J.A. (2009). The role of the calponin homology domain of smoothelin-like 1 (SMTNL1) in myosin phosphatase inhibition and smooth muscle contraction. Molecular and cellular biochemistry *327*, 93-100.

- Bornens, M. (2008). Organelle positioning and cell polarity. Nature reviews Molecular cell biology *9*, 874-886.

- Boss, J. (1955). Mitosis in cultures of newt tissues. IV. The cell surface in late anaphase and the movements of ribonucleoprotein. Experimental cell research *8*, 181-187.

- Boucrot, E., and Kirchhausen, T. (2007). Endosomal recycling controls plasma membrane area during mitosis. Proceedings of the National Academy of Sciences of the United States of America *104*, 7939-7944.

- Brugman, S. (2016). The zebrafish as a model to study intestinal inflammation. Developmental and comparative immunology *64*, 82-92.

- Bryant, D.M., Datta, A., Rodriguez-Fraticelli, A.E., Peranen, J., Martin-Belmonte, F., and Mostov, K.E. (2010). A molecular network for de novo generation of the apical surface and lumen. Nature cell biology *12*, 1035-1045.

- Bryant, D.M., and Mostov, K.E. (2008). From cells to organs: building polarized tissue. Nature reviews Molecular cell biology *9*, 887-901.

- Bryant, D.M., Roignot, J., Datta, A., Overeem, A.W., Kim, M., Yu, W., Peng, X., Eastburn, D.J., Ewald, A.J., Werb, Z.*, et al.* (2014). A molecular switch for the orientation of epithelial cell polarization. Developmental cell *31*, 171-187.

- Bulgakova, N.A., and Knust, E. (2009). The Crumbs complex: from epithelial-cell polarity to retinal degeneration. Journal of cell science *122*, 2587-2596.

- Burgess, D.R. (1982). Reactivation of intestinal epithelial cell brush border motility: ATP-dependent contraction via a terminal web contractile ring. The Journal of cell biology *95*, 853-863.

- Burgess, D.R., and Grey, R.D. (1974). Alterations in morphology of developing microvilli elicited by cytochalasin B. Studies of embryonic chick intestine in organ culture. The Journal of cell biology *62*, 566-574.

- Burgess, D.R., and Prum, B.E. (1982). Reevaluation of brush border motility: calcium induces core filament solution and microvillar vesiculation. The Journal of cell biology *94*, 97-107.

- Burton, K., and Taylor, D.L. (1997). Traction forces of cytokinesis measured with optically modified elastic substrata. Nature *385*, 450-454.

- Cai, L., Makhov, A.M., and Bear, J.E. (2007a). F-actin binding is essential for coronin 1B function in vivo. Journal of cell science *120*, 1779-1790.

- Cai, L., Makhov, A.M., Schafer, D.A., and Bear, J.E. (2008). Coronin 1B antagonizes cortactin and remodels Arp2/3-containing actin branches in lamellipodia. Cell *134*, 828-842.

- Cai, L., Marshall, T.W., Uetrecht, A.C., Schafer, D.A., and Bear, J.E. (2007b). Coronin 1B coordinates Arp2/3 complex and cofilin activities at the leading edge. Cell *128*, 915-929.

- Cai, Y., Yu, F., Lin, S., Chia, W., and Yang, X. (2003). Apical complex genes control mitotic spindle geometry and relative size of daughter cells in Drosophila neuroblast and pI asymmetric divisions. Cell *112*, 51-62.

- Cameron, L.A., Giardini, P.A., Soo, F.S., and Theriot, J.A. (2000). Secrets of actin-based motility revealed by a bacterial pathogen. Nature reviews Molecular cell biology *1*, 110-119.

- Carracedo, A., and Pandolfi, P.P. (2008). The PTEN-PI3K pathway: of feedbacks and cross-talks. Oncogene *27*, 5527-5541.

- Charras, G.T. (2008). A short history of blebbing. Journal of microscopy *231*, 466-478.

- Charras, G.T., Hu, C.K., Coughlin, M., and Mitchison, T.J. (2006). Reassembly of contractile actin cortex in cell blebs. The Journal of cell biology *175*, 477-490.

- Charras, G.T., Yarrow, J.C., Horton, M.A., Mahadevan, L., and Mitchison, T.J. (2005). Non-equilibration of hydrostatic pressure in blebbing cells. Nature *435*, 365-369.

- Cheung, A., Dantzig, J.A., Hollingworth, S., Baylor, S.M., Goldman, Y.E., Mitchison, T.J., and Straight, A.F. (2002). A small-molecule inhibitor of skeletal muscle myosin II. Nature cell biology *4*, 83-88.

- Cheung, I.D., Bagnat, M., Ma, T.P., Datta, A., Evason, K., Moore, J.C., Lawson, N.D., Mostov, K.E., Moens, C.B., and Stainier, D.Y. (2012). Regulation of intrahepatic biliary duct morphogenesis by Claudin 15-like b. Developmental biology *361*, 68-78.

- Chifflet, S., and Hernandez, J.A. (2012). The plasma membrane potential and the organization of the actin cytoskeleton of epithelial cells. International journal of cell biology *2012*, 121424.

- Citalan-Madrid, A.F., Vargas-Robles, H., Garcia-Ponce, A., Shibayama, M., Betanzos, A., Nava, P., Salinas-Lara, C., Rottner, K., Mennigen, R., and Schnoor, M. (2017). Cortactin deficiency causes increased RhoA/ROCK1-dependent actomyosin contractility, intestinal epithelial barrier dysfunction, and disproportionately severe DSS-induced colitis. Mucosal immunology *10*, 1237-1247.

- Clarke, J. (2009). Role of polarized cell divisions in zebrafish neural tube formation. Current opinion in neurobiology *19*, 134-138.

- Coch, R.A., and Leube, R.E. (2016). Intermediate Filaments and Polarization in the Intestinal Epithelium. Cells *5*.

- Collinet, C., Rauzi, M., Lenne, P.F., and Lecuit, T. (2015). Local and tissue-scale forces drive oriented junction growth during tissue extension. Nature cell biology *17*, 1247-1258.

- Coravos, J.S., Mason, F.M., and Martin, A.C. (2017). Actomyosin Pulsing in Tissue Integrity Maintenance during Morphogenesis. Trends in cell biology *27*, 276-283.

- Cramer, L.P., Siebert, M., and Mitchison, T.J. (1997). Identification of novel graded polarity actin filament bundles in locomoting heart fibroblasts: implications for the generation of motile force. The Journal of cell biology *136*, 1287-1305.

- Croucher, D.R., Rickwood, D., Tactacan, C.M., Musgrove, E.A., and Daly, R.J. (2010). Cortactin modulates RhoA activation and expression of Cip/Kip cyclin-dependent kinase inhibitors to promote cell cycle progression in 11q13-amplified head and neck squamous cell carcinoma cells. Molecular and cellular biology *30*, 5057-5070.

- Datta, A., Bryant, D.M., and Mostov, K.E. (2011). Molecular regulation of lumen morphogenesis. Current biology : CB *21*, R126-136.

- Davidson, G.P., Cutz, E., Hamilton, J.R., and Gall, D.G. (1978). Familial enteropathy: a syndrome of protracted diarrhea from birth, failure to thrive, and hypoplastic villus atrophy. Gastroenterology *75*, 783-790.

- Debnath, J., Mills, K.R., Collins, N.L., Reginato, M.J., Muthuswamy, S.K., and Brugge, J.S. (2002). The role of apoptosis in creating and maintaining luminal space within normal and oncogene-expressing mammary acini. Cell *111*, 29-40.

- Delacour, D., Salomon, J., Robine, S., and Louvard, D. (2016). Plasticity of the brush border - the yin and yang of intestinal homeostasis. Nature reviews Gastroenterology & hepatology *13*, 161-174.

- Desclozeaux, M., Venturato, J., Wylie, F.G., Kay, J.G., Joseph, S.R., Le, H.T., and Stow, J.L. (2008). Active Rab11 and functional recycling endosome are required for E-cadherin trafficking and lumen formation during epithelial morphogenesis. American journal of physiology Cell physiology *295*, C545-556.

- Dessaud, E., McMahon, A.P., and Briscoe, J. (2008). Pattern formation in the vertebrate neural tube: a sonic hedgehog morphogen-regulated transcriptional network. Development *135*, 2489-2503.

- dos Remedios, C.G., Chhabra, D., Kekic, M., Dedova, I.V., Tsubakihara, M., Berry, D.A., and Nosworthy, N.J. (2003). Actin binding proteins: regulation of cytoskeletal microfilaments. Physiological reviews *83*, 433-473.

- Du, Q., Stukenberg, P.T., and Macara, I.G. (2001). A mammalian Partner of inscuteable binds NuMA and regulates mitotic spindle organization. Nature cell biology *3*, 1069-1075.

- Eaton, S., and Martin-Belmonte, F. (2014). Cargo sorting in the endocytic pathway: a key regulator of cell polarity and tissue dynamics. Cold Spring Harbor perspectives in biology *6*, a016899.

- Eiraku, M., Takata, N., Ishibashi, H., Kawada, M., Sakakura, E., Okuda, S., Sekiguchi, K., Adachi, T., and Sasai, Y. (2011). Self-organizing optic-cup morphogenesis in three-dimensional culture. Nature *472*, 51-56.

- Engelen, J.J., Esterling, L.E., Albrechts, J.C., Detera-Wadleigh, S.D., and van Eys, G.J. (1997). Assignment of the human gene for smoothelin (SMTN) to chromosome 22q12 by fluorescence in situ hybridization and radiation hybrid mapping. Genomics *43*, 245-247.

- Fath, K.R., Mamajiwalla, S.N., and Burgess, D.R. (1993). The cytoskeleton in development of epithelial cell polarity. Journal of cell science Supplement *17*, 65-73.

- Ferrari, A., Veligodskiy, A., Berge, U., Lucas, M.S., and Kroschewski, R. (2008). ROCK-mediated contractility, tight junctions and channels contribute to the conversion of a preapical patch into apical surface during isochoric lumen initiation. Journal of cell science *121*, 3649-3663.

- Folsch, H. (2008). Regulation of membrane trafficking in polarized epithelial cells. Current opinion in cell biology *20*, 208-213.

- Footer, M.J., Kerssemakers, J.W., Theriot, J.A., and Dogterom, M. (2007). Direct measurement of force generation by actin filament polymerization using an optical trap. Proceedings of the National Academy of Sciences of the United States of America *104*, 2181-2186.

- Friedl, P., and Wolf, K. (2003). Tumour-cell invasion and migration: diversity and escape mechanisms. Nature reviews Cancer *3*, 362-374.

- Galvez-Santisteban, M., Rodriguez-Fraticelli, A.E., Bryant, D.M., Vergarajauregui, S., Yasuda, T., Banon-Rodriguez, I., Bernascone, I., Datta, A., Spivak, N., Young, K.*, et al.* (2012). Synaptotagmin-like proteins control the formation of a single apical membrane domain in epithelial cells. Nature cell biology *14*, 838-849.

- Garcia Ponce, A., Citalan Madrid, A.F., Vargas Robles, H., Chanez Paredes, S., Nava, P., Betanzos, A., Zarbock, A., Rottner, K., Vestweber, D., and Schnoor, M. (2016). Loss of cortactin causes endothelial barrier dysfunction via disturbed adrenomedullin secretion and actomyosin contractility. Scientific reports *6*, 29003.

- Gassama-Diagne, A., Yu, W., ter Beest, M., Martin-Belmonte, F., Kierbel, A., Engel, J., and Mostov, K. (2006). Phosphatidylinositol-3,4,5-trisphosphate regulates the formation of the basolateral plasma membrane in epithelial cells. Nature cell biology *8*, 963-970.

- Gidon, A., Bardin, S., Cinquin, B., Boulanger, J., Waharte, F., Heliot, L., de la Salle, H., Hanau, D., Kervrann, C., Goud, B.*, et al.* (2012). A Rab11A/myosin Vb/Rab11-FIP2 complex frames two late recycling steps of langerin from the ERC to the plasma membrane. Traffic *13*, 815-833.

- Gilmour, D., Rembold, M., and Leptin, M. (2017). From morphogen to morphogenesis and back. Nature *541*, 311-320.

- Goldstein, B., and Macara, I.G. (2007). The PAR proteins: fundamental players in animal cell polarization. Developmental cell *13*, 609-622.

- Goley, E.D., and Welch, M.D. (2006). The ARP2/3 complex: an actin nucleator comes of age. Nature reviews Molecular cell biology *7*, 713-726.

- Gonzalez-Mariscal, L., Namorado, M.C., Martin, D., Luna, J., Alarcon, L., Islas, S., Valencia, L., Muriel, P., Ponce, L., and Reyes, J.L. (2000). Tight junction proteins ZO-1, ZO-2, and occludin along isolated renal tubules. Kidney international *57*, 2386-2402.

- Gottlieb, T.A., Ivanov, I.E., Adesnik, M., and Sabatini, D.D. (1993). Actin microfilaments play a critical role in endocytosis at the apical but not the basolateral surface of polarized epithelial cells. The Journal of cell biology *120*, 695-710.

- Grikscheit, K., Frank, T., Wang, Y., and Grosse, R. (2015). Junctional actin assembly is mediated by Formin-like 2 downstream of Rac1. The Journal of cell biology *209*, 367-376.

- Gumbiner, B.M. (2000). Regulation of cadherin adhesive activity. The Journal of cell biology *148*, 399-404.

- Han, S.P., Gambin, Y., Gomez, G.A., Verma, S., Giles, N., Michael, M., Wu, S.K., Guo, Z., Johnston, W., Sierecki, E.*, et al.* (2014). Cortactin scaffolds Arp2/3 and WAVE2 at the epithelial zonula adherens. The Journal of biological chemistry *289*, 7764-7775.

- Hao, Y., Du, Q., Chen, X., Zheng, Z., Balsbaugh, J.L., Maitra, S., Shabanowitz, J., Hunt, D.F., and Macara, I.G. (2010). Par3 controls epithelial spindle orientation by aPKC-mediated phosphorylation of apical Pins. Current biology : CB *20*, 1809-1818.

- Harding, M.J., and Nechiporuk, A.V. (2012). Fgfr-Ras-MAPK signaling is required for apical constriction via apical positioning of Rho-associated kinase during mechanosensory organ formation. Development *139*, 3130-3135.

- Harris, T.J., and Tepass, U. (2010). Adherens junctions: from molecules to morphogenesis. Nature reviews Molecular cell biology *11*, 502-514.

- Helwani, F.M., Kovacs, E.M., Paterson, A.D., Verma, S., Ali, R.G., Fanning, A.S., Weed, S.A., and Yap, A.S. (2004). Cortactin is necessary for E-cadherin-mediated contact formation and actin reorganization. The Journal of cell biology *164*, 899-910.

- Herwig, L., Blum, Y., Krudewig, A., Ellertsdottir, E., Lenard, A., Belting, H.G., and Affolter, M. (2011). Distinct cellular mechanisms of blood vessel fusion in the zebrafish embryo. Current biology : CB *21*, 1942-1948.

- Hogan, B.L., and Kolodziej, P.A. (2002). Organogenesis: molecular mechanisms of tubulogenesis. Nature reviews Genetics *3*, 513-523.

- Horne-Badovinac, S., Lin, D., Waldron, S., Schwarz, M., Mbamalu, G., Pawson, T., Jan, Y., Stainier, D.Y., and Abdelilah-Seyfried, S. (2001). Positional cloning of heart and soul reveals multiple roles for PKC lambda in zebrafish organogenesis. Current biology : CB *11*, 1492-1502.

- Iruela-Arispe, M.L., and Beitel, G.J. (2013). Tubulogenesis. Development *140*, 2851-2855.

- Ishida, H., Borman, M.A., Ostrander, J., Vogel, H.J., and MacDonald, J.A. (2008). Solution structure of the calponin homology (CH) domain from the smoothelin-like 1 protein: a unique apocalmodulin-binding mode and the possible role of the C-terminal type-2 CH-domain in smooth muscle relaxation. The Journal of biological chemistry *283*, 20569-20578.

- Ivanov, A.I., Hopkins, A.M., Brown, G.T., Gerner-Smidt, K., Babbin, B.A., Parkos, C.A., and Nusrat, A. (2008). Myosin II regulates the shape of three-dimensional intestinal epithelial cysts. Journal of cell science *121*, 1803-1814.

- Iwasa, J.H., and Mullins, R.D. (2007). Spatial and temporal relationships between actin-filament nucleation, capping, and disassembly. Current biology : CB *17*, 395-406.

- Jaffe, A.B., Kaji, N., Durgan, J., and Hall, A. (2008). Cdc42 controls spindle orientation to position the apical surface during epithelial morphogenesis. The Journal of cell biology *183*, 625-633.

- Johnson, M.D., and Mueller, S.C. (2013). Three dimensional multiphoton imaging of fresh and whole mount developing mouse mammary glands. BMC cancer *13*, 373.

- Kasza, K.E., and Zallen, J.A. (2011). Dynamics and regulation of contractile actin-myosin networks in morphogenesis. Current opinion in cell biology *23*, 30-38.

- Katsube, T., Takahisa, M., Ueda, R., Hashimoto, N., Kobayashi, M., and Togashi, S. (1998). Cortactin associates with the cell-cell junction protein ZO-1 in both Drosophila and mouse. The Journal of biological chemistry *273*, 29672-29677.

- Kerman, B.E., Cheshire, A.M., and Andrew, D.J. (2006). From fate to function: the Drosophila trachea and salivary gland as models for tubulogenesis. Differentiation; research in biological diversity *74*, 326-348.

- Kieserman, E.K., and Wallingford, J.B. (2009). In vivo imaging reveals a role for Cdc42 in spindle positioning and planar orientation of cell divisions during vertebrate neural tube closure. Journal of cell science *122*, 2481-2490.

- Kim, M., A, M.S., Ewald, A.J., Werb, Z., and Mostov, K.E. (2015). p114RhoGEF governs cell motility and lumen formation during tubulogenesis through a ROCK-myosin-II pathway. Journal of cell science *128*, 4317-4327.

- Klingner, C., Cherian, A.V., Fels, J., Diesinger, P.M., Aufschnaiter, R., Maghelli, N., Keil, T., Beck, G., Tolic-Norrelykke, I.M., Bathe, M., *et al.* (2014). Isotropic actomyosin dynamics promote organization of the apical cell cortex in epithelial cells. The Journal of cell biology *207*, 107-121.

- Kobielak, A., and Fuchs, E. (2004). Alpha-catenin: at the junction of intercellular adhesion and actin dynamics. Nature reviews Molecular cell biology *5*, 614-625.

- Kovacs, E.M., Verma, S., Ali, R.G., Ratheesh, A., Hamilton, N.A., Akhmanova, A., and Yap, A.S. (2011). N-WASP regulates the epithelial junctional actin cytoskeleton through a non-canonical post-nucleation pathway. Nature cell biology *13*, 934-943.

- Krupinski, T., and Beitel, G.J. (2009). Unexpected roles of the Na-K-ATPase and other ion transporters in cell junctions and tubulogenesis. Physiology *24*, 192-201.

- Kubota, H.Y. (1981). Creeping locomotion of the endodermal cells dissociated from gastrulae of the Japanese newt, Cynops pyrrhogaster. Experimental cell research *133*, 137-148.

- Kurita, R., Tabata, Y., Sagara, H., Arai, K., and Watanabe, S. (2004). A novel smoothelin-like, actin-binding protein required for choroidal fissure closure in zebrafish. Biochemical and biophysical research communications *313*, 1092-1100.

- Lammert, E., and Axnick, J. (2012). Vascular lumen formation. Cold Spring Harbor perspectives in medicine *2*, a006619.

- Landy, J., Ronde, E., English, N., Clark, S.K., Hart, A.L., Knight, S.C., Ciclitira, P.J., and Al-Hassi, H.O. (2016). Tight junctions in inflammatory bowel diseases and inflammatory bowel disease associated colorectal cancer. World journal of gastroenterology *22*, 3117-3126.

- Langevin, J., Morgan, M.J., Sibarita, J.B., Aresta, S., Murthy, M., Schwarz, T., Camonis, J., and Bellaiche, Y. (2005). Drosophila exocyst components Sec5, Sec6, and Sec15 regulate DE-Cadherin trafficking from recycling endosomes to the plasma membrane. Developmental cell *9*, 365-376.

- Lecuit, T., and Yap, A.S. (2015). E-cadherin junctions as active mechanical integrators in tissue dynamics. Nature cell biology *17*, 533-539.

- Leptin, M. (2005). Gastrulation movements: the logic and the nuts and bolts. Developmental cell *8*, 305-320.

- Li, R., and Gundersen, G.G. (2008). Beyond polymer polarity: how the cytoskeleton builds a polarized cell. Nature reviews Molecular cell biology *9*, 860-873.

- Lim, H., Yu, C.Y., and Jou, T.S. (2017). Galectin-8 regulates targeting of Gp135/podocalyxin and lumen formation at the apical surface of renal epithelial cells. FASEB journal : official publication of the Federation of American Societies for Experimental Biology *31*, 4917-4927.

- Lo, A.T., Mori, H., Mott, J., and Bissell, M.J. (2012). Constructing three-dimensional models to study mammary gland branching morphogenesis and functional differentiation. Journal of mammary gland biology and neoplasia *17*, 103-110.

- Lontay, B., Bodoor, K., Sipos, A., Weitzel, D.H., Loiselle, D., Safi, R., Zheng, D., Devente, J., Hickner, R.C., McDonnell, D.P.*, et al.* (2015). Pregnancy and Smoothelin-like Protein 1 (SMTNL1) Deletion Promote the Switching of Skeletal Muscle to a Glycolytic Phenotype in Human and Mice. The Journal of biological chemistry *290*, 17985-17998.

- Lontay, B., Bodoor, K., Weitzel, D.H., Loiselle, D., Fortner, C., Lengyel, S., Zheng, D., Devente, J., Hickner, R., and Haystead, T.A. (2010). Smoothelin-like 1 protein regulates myosin phosphatase-targeting subunit 1 expression during sexual development and pregnancy. The Journal of biological chemistry *285*, 29357-29366.

- Lubarsky, B., and Krasnow, M.A. (2003). Tube morphogenesis: making and shaping biological tubes. Cell *112*, 19-28.

- Lynch, D.K., Winata, S.C., Lyons, R.J., Hughes, W.E., Lehrbach, G.M., Wasinger, V., Corthals, G., Cordwell, S., and Daly, R.J. (2003). A Cortactin-CD2-associated protein (CD2AP) complex provides a novel link between epidermal growth factor receptor endocytosis and the actin cytoskeleton. The Journal of biological chemistry *278*, 21805-21813.

- Madrid, R., Aranda, J.F., Rodriguez-Fraticelli, A.E., Ventimiglia, L., Andres-Delgado, L., Shehata, M., Fanayan, S., Shahheydari, H., Gomez, S., Jimenez, A.*, et al.* (2010). The formin INF2 regulates basolateral-to-apical transcytosis and lumen formation in association with Cdc42 and MAL2. Developmental cell *18*, 814-827.

- Madsen, C.D., Hooper, S., Tozluoglu, M., Bruckbauer, A., Fletcher, G., Erler, J.T., Bates, P.A., Thompson, B., and Sahai, E. (2015). STRIPAK components determine mode of cancer cell migration and metastasis. Nature cell biology *17*, 68-80.

- Marjoram, L., Alvers, A., Deerhake, M.E., Bagwell, J., Mankiewicz, J., Cocchiaro, J.L., Beerman, R.W., Willer, J., Sumigray, K.D., Katsanis, N.*, et al.* (2015). Epigenetic control of intestinal barrier function and inflammation in zebrafish. Proceedings of the National Academy of Sciences of the United States of America *112*, 2770-2775.

- Martin, A.C., Gelbart, M., Fernandez-Gonzalez, R., Kaschube, M., and Wieschaus, E.F. (2010). Integration of contractile forces during tissue invagination. The Journal of cell biology *188*, 735-749.

- Martin, A.C., Kaschube, M., and Wieschaus, E.F. (2009). Pulsed contractions of an actin-myosin network drive apical constriction. Nature *457*, 495-499.

- Martin-Belmonte, F., Gassama, A., Datta, A., Yu, W., Rescher, U., Gerke, V., and Mostov, K. (2007). PTEN-mediated apical segregation of phosphoinositides controls epithelial morphogenesis through Cdc42. Cell *128*, 383-397.

- Martin-Belmonte, F., and Mostov, K. (2007). Phosphoinositides control epithelial development. Cell cycle *6*, 1957-1961.

- Martin-Belmonte, F., and Mostov, K. (2008). Regulation of cell polarity during epithelial morphogenesis. Current opinion in cell biology *20*, 227-234.

- Martin-Belmonte, F., and Perez-Moreno, M. (2011). Epithelial cell polarity, stem cells and cancer. Nature reviews Cancer *12*, 23-38.

- Martin-Belmonte, F., Yu, W., Rodriguez-Fraticelli, A.E., Ewald, A.J., Werb, Z., Alonso, M.A., and Mostov, K. (2008). Cell-polarity dynamics controls the mechanism of lumen formation in epithelial morphogenesis. Current biology : CB *18*, 507-513.

- Massarwa, R., Schejter, E.D., and Shilo, B.Z. (2009). Apical secretion in epithelial tubes of the Drosophila embryo is directed by the Formin-family protein Diaphanous. Developmental cell *16*, 877-888.

- Matter, K., and Balda, M.S. (2003). Signalling to and from tight junctions. Nature reviews Molecular cell biology *4*, 225-236.

- Mays, R.W., Beck, K.A., and Nelson, W.J. (1994). Organization and function of the cytoskeleton in polarized epithelial cells: a component of the protein sorting machinery. Current opinion in cell biology *6*, 16-24.

- Meder, D., Shevchenko, A., Simons, K., and Fullekrug, J. (2005). Gp135/podocalyxin and NHERF-2 participate in the formation of a preapical domain during polarization of MDCK cells. The Journal of cell biology *168*, 303-313.

- Michael, M., Meiring, J.C.M., Acharya, B.R., Matthews, D.R., Verma, S., Han, S.P., Hill, M.M., Parton, R.G., Gomez, G.A., and Yap, A.S. (2016). Coronin 1B Reorganizes the Architecture of F-Actin Networks for Contractility at Steady-State and Apoptotic Adherens Junctions. Developmental cell *37*, 58-71.

- Michael, M., and Yap, A.S. (2013). The regulation and functional impact of actin assembly at cadherin cell-cell adhesions. Seminars in cell & developmental biology *24*, 298-307.

- Miyata, H., Nishiyama, S., Akashi, K., and Kinosita, K., Jr. (1999). Protrusive growth from giant liposomes driven by actin polymerization. Proceedings of the National Academy of Sciences of the United States of America *96*, 2048-2053.

- Miyoshi, J., and Takai, Y. (2008). Structural and functional associations of apical junctions with cytoskeleton. Biochimica et biophysica acta *1778*, 670-691.

- Morin, X., Jaouen, F., and Durbec, P. (2007). Control of planar divisions by the G-protein regulator LGN maintains progenitors in the chick neuroepithelium. Nature neuroscience *10*, 1440-1448.

- Muller, T., Hess, M.W., Schiefermeier, N., Pfaller, K., Ebner, H.L., Heinz-Erian, P., Ponstingl, H., Partsch, J., Rollinghoff, B., Kohler, H.*, et al.* (2008). MYO5B mutations cause microvillus inclusion disease and disrupt epithelial cell polarity. Nature genetics *40*, 1163-1165.

- Murali, M., and MacDonald, J.A. (2018). Smoothelins and the Control of Muscle Contractility. Advances in pharmacology *81*, 39-78.

- Nambiar, R., McConnell, R.E., and Tyska, M.J. (2010). Myosin motor function: the ins and outs of actin-based membrane protrusions. Cellular and molecular life sciences : CMLS *67*, 1239-1254.

- Naylor, M.J., Li, N., Cheung, J., Lowe, E.T., Lambert, E., Marlow, R., Wang, P., Schatzmann, F., Wintermantel, T., Schuetz, G.*, et al.* (2005). Ablation of beta1 integrin in mammary epithelium reveals a key role for integrin in glandular morphogenesis and differentiation. The Journal of cell biology *171*, 717-728.

- Nelson, W.J., Hammerton, R.W., Wang, A.Z., and Shore, E.M. (1990). Involvement of the membrane-cytoskeleton in development of epithelial cell polarity. Seminars in cell biology *1*, 359-371.

- Ng, A.N., de Jong-Curtain, T.A., Mawdsley, D.J., White, S.J., Shin, J., Appel, B., Dong, P.D., Stainier, D.Y., and Heath, J.K. (2005). Formation of the digestive system in zebrafish: III. Intestinal epithelium morphogenesis. Developmental biology *286*, 114-135.

- Nguyen-Ngoc, K.V., Shamir, E.R., Huebner, R.J., Beck, J.N., Cheung, K.J., and Ewald, A.J. (2015). 3D culture assays of murine mammary branching morphogenesis and epithelial invasion. Methods in molecular biology *1189*, 135-162.

- O'Brien, L.E., Jou, T.S., Pollack, A.L., Zhang, Q., Hansen, S.H., Yurchenco, P., and Mostov, K.E. (2001). Rac1 orientates epithelial apical polarity through effects on basolateral laminin assembly. Nature cell biology *3*, 831-838.

- O'Brien, L.E., Zegers, M.M., and Mostov, K.E. (2002). Opinion: Building epithelial architecture: insights from three-dimensional culture models. Nature reviews Molecular cell biology *3*, 531-537.

- Ohoka, Y., and Takai, Y. (1998). Isolation and characterization of cortactin isoforms and a novel cortactin-binding protein, CBP90. Genes to cells : devoted to molecular & cellular mechanisms *3*, 603-612.

- Oyama, K., Arai, T., Isaka, A., Sekiguchi, T., Itoh, H., Seto, Y., Miyazaki, M., Itabashi, T., Ohki, T., Suzuki, M.*, et al.* (2015). Directional bleb formation in spherical cells under temperature gradient. Biophysical journal *109*, 355-364.

- Pack, M., Solnica-Krezel, L., Malicki, J., Neuhauss, S.C., Schier, A.F., Stemple, D.L., Driever, W., and Fishman, M.C. (1996). Mutations affecting development of zebrafish digestive organs. Development *123*, 321-328.

- Parekh, S.H., Chaudhuri, O., Theriot, J.A., and Fletcher, D.A. (2005). Loading history determines the velocity of actin-network growth. Nature cell biology *7*, 1219-1223.

- Peyre, E., Jaouen, F., Saadaoui, M., Haren, L., Merdes, A., Durbec, P., and Morin, X. (2011). A lateral belt of cortical LGN and NuMA guides mitotic spindle movements and planar division in neuroepithelial cells. The Journal of cell biology *193*, 141-154.

- Pletjushkina, O.J., Rajfur, Z., Pomorski, P., Oliver, T.N., Vasiliev, J.M., and Jacobson, K.A. (2001). Induction of cortical oscillations in spreading cells by depolymerization of microtubules. Cell motility and the cytoskeleton *48*, 235-244.

- Qin, Y., Meisen, W.H., Hao, Y., and Macara, I.G. (2010). Tuba, a Cdc42 GEF, is required for polarized spindle orientation during epithelial cyst formation. The Journal of cell biology *189*, 661-669.

- Rafelski, S.M., and Marshall, W.F. (2008). Building the cell: design principles of cellular architecture. Nature reviews Molecular cell biology *9*, 593-602.

- Rauzi, M., Krzic, U., Saunders, T.E., Krajnc, M., Ziherl, P., Hufnagel, L., and Leptin, M. (2015). Embryo-scale tissue mechanics during Drosophila gastrulation movements. Nature communications *6*, 8677.

- Rauzi, M., Lenne, P.F., and Lecuit, T. (2010). Planar polarized actomyosin contractile flows control epithelial junction remodelling. Nature *468*, 1110-1114.

- Reed, R.A., Womble, M.A., Dush, M.K., Tull, R.R., Bloom, S.K., Morckel, A.R., Devlin, E.W., and Nascone-Yoder, N.M. (2009). Morphogenesis of the primitive gut tube is generated by Rho/ROCK/myosin II-mediated endoderm rearrangements. Developmental dynamics : an official publication of the American Association of Anatomists *238*, 3111-3125.

- Rensen, S., Merkx, G., Doevendans, P., Geurts Van Kessel, A., and van Eys, G. (2000). Structure and chromosome location of Smtn, the mouse smoothelin gene. Cytogenetics and cell genetics *89*, 225-229.

- Rodriguez-Boulan, E., Kreitzer, G., and Musch, A. (2005). Organization of vesicular trafficking in epithelia. Nature reviews Molecular cell biology *6*, 233-247.

- Rodriguez-Boulan, E., and Macara, I.G. (2014). Organization and execution of the epithelial polarity programme. Nature reviews Molecular cell biology *15*, 225-242.

- Rodriguez-Fraticelli, A.E., Auzan, M., Alonso, M.A., Bornens, M., and Martin-Belmonte, F. (2012). Cell confinement controls centrosome positioning and lumen initiation during epithelial morphogenesis. The Journal of cell biology *198*, 1011-1023.

- Rodriguez-Fraticelli, A.E., Bagwell, J., Bosch-Fortea, M., Boncompain, G., Reglero-Real, N., Garcia-Leon, M.J., Andres, G., Toribio, M.L., Alonso, M.A., Millan, J.*, et al.* (2015). Developmental regulation of apical endocytosis controls epithelial patterning in vertebrate tubular organs. Nature cell biology *17*, 241-250.

- Rodriguez-Fraticelli, A.E., and Martin-Belmonte, F. (2013). Mechanical control of epithelial lumen formation. Small GTPases *4*, 136-140.

- Rodriguez-Fraticelli, A.E., Vergarajauregui, S., Eastburn, D.J., Datta, A., Alonso, M.A., Mostov, K., and Martin-Belmonte, F. (2010). The Cdc42 GEF Intersectin 2 controls mitotic spindle orientation to form the lumen during epithelial morphogenesis. The Journal of cell biology *189*, 725-738.

- Roignot, J., Peng, X., and Mostov, K. (2013). Polarity in mammalian epithelial morphogenesis. Cold Spring Harbor perspectives in biology *5*.

- Roland, J.T., Bryant, D.M., Datta, A., Itzen, A., Mostov, K.E., and Goldenring, J.R. (2011). Rab GTPase-Myo5B complexes control membrane recycling and epithelial polarization. Proceedings of the National Academy of Sciences of the United States of America *108*, 2789-2794.

- Roper, K. (2015). Integration of cell-cell adhesion and contractile actomyosin activity during morphogenesis. Current topics in developmental biology *112*, 103-127.

- Rosenblatt, J., Raff, M.C., and Cramer, L.P. (2001). An epithelial cell destined for apoptosis signals its neighbors to extrude it by an actin- and myosin-dependent mechanism. Current biology : CB *11*, 1847-1857.

- Roux, K.J., Kim, D.I., Raida, M., and Burke, B. (2012). A promiscuous biotin ligase fusion protein identifies proximal and interacting proteins in mammalian cells. The Journal of cell biology *196*, 801-810.

- Rubin, D.C. (2007). Intestinal morphogenesis. Current opinion in gastroenterology *23*, 111-114.

- Sahai, E., and Marshall, C.J. (2002). ROCK and Dia have opposing effects on adherens junctions downstream of Rho. Nature cell biology *4*, 408-415.

- Sahai, E., and Marshall, C.J. (2003). Differing modes of tumour cell invasion have distinct requirements for Rho/ROCK signalling and extracellular proteolysis. Nature cell biology *5*, 711-719.

- Sato, T., Vries, R.G., Snippert, H.J., van de Wetering, M., Barker, N., Stange, D.E., van Es, J.H., Abo, A., Kujala, P., Peters, P.J., *et al.* (2009). Single Lgr5 stem cells build crypt-villus structures in vitro without a mesenchymal niche. Nature *459*, 262-265.

- Schaefer, M., Shevchenko, A., Shevchenko, A., and Knoblich, J.A. (2000). A protein complex containing Inscuteable and the Galpha-binding protein Pins orients asymmetric cell divisions in Drosophila. Current biology : CB *10*, 353-362.

- Schmeichel, K.L., and Bissell, M.J. (2003). Modeling tissue-specific signaling and organ function in three dimensions. Journal of cell science *116*, 2377-2388.

- Schottenfeld, J., Song, Y., and Ghabrial, A.S. (2010). Tube continued: morphogenesis of the Drosophila tracheal system. Current opinion in cell biology *22*, 633-639.

- Seiler, C., Davuluri, G., Abrams, J., Byfield, F.J., Janmey, P.A., and Pack, M. (2012). Smooth muscle tension induces invasive remodeling of the zebrafish intestine. PLoS biology *10*, e1001386.

- Sheetz, M.P. (2001). Cell control by membrane-cytoskeleton adhesion. Nature reviews Molecular cell biology *2*, 392-396.

- Sigurbjornsdottir, S., Mathew, R., and Leptin, M. (2014). Molecular mechanisms of de novo lumen formation. Nature reviews Molecular cell biology *15*, 665-676.

- Siller, K.H., and Doe, C.Q. (2009). Spindle orientation during asymmetric cell division. Nature cell biology *11*, 365-374.

- Skau, C.T., Plotnikov, S.V., Doyle, A.D., and Waterman, C.M. (2015). Inverted formin 2 in focal adhesions promotes dorsal stress fiber and fibrillar adhesion formation to drive extracellular matrix assembly. Proceedings of the National Academy of Sciences of the United States of America *112*, E2447-2456.

- Skau, C.T., and Waterman, C.M. (2015). Specification of Architecture and Function of Actin Structures by Actin Nucleation Factors. Annual review of biophysics *44*, 285-310.

- Solon, J., Kaya-Copur, A., Colombelli, J., and Brunner, D. (2009). Pulsed forces timed by a ratchet-like mechanism drive directed tissue movement during dorsal closure. Cell *137*, 1331-1342.

- Sroka, J., von Gunten, M., Dunn, G.A., and Keller, H.U. (2002). Phenotype modulation in non-adherent and adherent sublines of Walker carcinosarcoma cells: the role of cell-substratum contacts and microtubules in controlling cell shape, locomotion and cytoskeletal structure. The international journal of biochemistry & cell biology *34*, 882-899.

- Stossel, T.P., Hartwig, J.H., Yin, H.L., Zaner, K.S., and Stendahl, O.I. (1982). Actin gelation and structure of cortical cytoplasm. Cold Spring Harbor symposia on quantitative biology *46 Pt 2*, 569-578.

- Strilic, B., Eglinger, J., Krieg, M., Zeeb, M., Axnick, J., Babal, P., Muller, D.J., and Lammert, E. (2010). Electrostatic cell-surface repulsion initiates lumen formation in developing blood vessels. Current biology : CB *20*, 2003-2009.

- Strilic, B., Kucera, T., Eglinger, J., Hughes, M.R., McNagny, K.M., Tsukita, S., Dejana, E., Ferrara, N., and Lammert, E. (2009). The molecular basis of vascular lumen formation in the developing mouse aorta. Developmental cell *17*, 505-515.

- Sun, H., Breslin, J.W., Zhu, J., Yuan, S.Y., and Wu, M.H. (2006). Rho and ROCK signaling in VEGF-induced microvascular endothelial hyperpermeability. Microcirculation *13*, 237-247.

- Svitkina, T.M., and Borisy, G.G. (1999). Arp2/3 complex and actin depolymerizing factor/cofilin in dendritic organization and treadmilling of actin filament array in lamellipodia. The Journal of cell biology *145*, 1009-1026.

- Szperl, A.M., Golachowska, M.R., Bruinenberg, M., Prekeris, R., Thunnissen, A.M., Karrenbeld, A., Dijkstra, G., Hoekstra, D., Mercer, D., Ksiazyk, J.*, et al.* (2011). Functional characterization of mutations in the myosin Vb gene associated with microvillus inclusion disease. Journal of pediatric gastroenterology and nutrition *52*, 307-313.

- Takasato, M., Er, P.X., Chiu, H.S., Maier, B., Baillie, G.J., Ferguson, C., Parton, R.G., Wolvetang, E.J., Roost, M.S., Chuva de Sousa Lopes, S.M.*, et al.* (2015). Kidney organoids from human iPS cells contain multiple lineages and model human nephrogenesis. Nature *526*, 564-568.

- Takasato, M., and Little, M.H. (2016). A strategy for generating kidney organoids: Recapitulating the development in human pluripotent stem cells. Developmental biology *420*, 210-220.

- Takeda, T., McQuistan, T., Orlando, R.A., and Farquhar, M.G. (2001). Loss of glomerular foot processes is associated with uncoupling of podocalyxin from the actin cytoskeleton. The Journal of clinical investigation *108*, 289-301.

- Takenawa, T., and Suetsugu, S. (2007). The WASP-WAVE protein network: connecting the membrane to the cytoskeleton. Nature reviews Molecular cell biology *8*, 37-48.

- Tang, V.W., and Brieher, W.M. (2012). alpha-Actinin-4/FSGS1 is required for Arp2/3-dependent actin assembly at the adherens junction. The Journal of cell biology *196*, 115-130.

- Taniguchi, K., Shao, Y., Townshend, R.F., Tsai, Y.H., DeLong, C.J., Lopez, S.A., Gayen, S., Freddo, A.M., Chue, D.J., Thomas, D.J.*, et al.* (2015). Lumen Formation Is an Intrinsic Property of Isolated Human Pluripotent Stem Cells. Stem cell reports *5*, 954-962.

- Theriot, J.A. (2000). The polymerization motor. Traffic *1*, 19-28.

- Thiery, J.P. (2009). [Epithelial-mesenchymal transitions in cancer onset and progression]. Bulletin de l'Academie nationale de medecine *193*, 1969-1978; discussion 1978-1969.

- Thoeni, C.E., Vogel, G.F., Tancevski, I., Geley, S., Lechner, S., Pfaller, K., Hess, M.W., Muller, T., Janecke, A.R., Avitzur, Y., *et al.* (2014). Microvillus inclusion disease: loss of Myosin vb disrupts intracellular traffic and cell polarity. Traffic *15*, 22-42.

- Townley, A.K., Schmidt, K., Hodgson, L., and Stephens, D.J. (2012). Epithelial organization and cyst lumen expansion require efficient Sec13-Sec31-driven secretion. Journal of cell science *125*, 673-684.

- Tozluoglu, M., Tournier, A.L., Jenkins, R.P., Hooper, S., Bates, P.A., and Sahai, E. (2013). Matrix geometry determines optimal cancer cell migration strategy and modulates response to interventions. Nature cell biology *15*, 751-762.

- Trinkaus, J.P. (1973). Modes of cell locomotion in vivo. Ciba Foundation symposium *14*, 233-249.

- Turner, S.R., and MacDonald, J.A. (2014). Novel contributions of the smoothelin-like 1 protein in vascular smooth muscle contraction and its potential involvement in myogenic tone. Microcirculation *21*, 249-258.

- Uetrecht, A.C., and Bear, J.E. (2006). Coronins: the return of the crown. Trends in cell biology *16*, 421-426.

- Ulke-Lemee, A., Ishida, H., Chappellaz, M., Vogel, H.J., and MacDonald, J.A. (2014). Two domains of the smoothelin-like 1 protein bind apo- and calcium-calmodulin independently. Biochimica et biophysica acta *1844*, 1580-1590.

- Ulke-Lemee, A., Turner, S.R., Mughal, S.H., Borman, M.A., Winkfein, R.J., and MacDonald, J.A. (2011). Mapping and functional characterization of the murine smoothelin-like 1 promoter. BMC molecular biology *12*, 10.

- Vasilyev, A., and Drummond, I.A. (2012). Live imaging kidney development in zebrafish. Methods in molecular biology *886*, 55-70.

- Verma, S., Han, S.P., Michael, M., Gomez, G.A., Yang, Z., Teasdale, R.D., Ratheesh, A., Kovacs, E.M., Ali, R.G., and Yap, A.S. (2012). A WAVE2-Arp2/3 actin nucleator apparatus supports junctional tension at the epithelial zonula adherens. Molecular biology of the cell *23*, 4601-4610.

- Vidal-Quadras, M., Holst, M.R., Francis, M.K., Larsson, E., Hachimi, M., Yau, W.L., Peranen, J., Martin-Belmonte, F., and Lundmark, R. (2017). Endocytic turnover of Rab8 controls cell polarization. Journal of cell science *130*, 1147-1157.

- Wallace, K.N., Akhter, S., Smith, E.M., Lorent, K., and Pack, M. (2005). Intestinal growth and differentiation in zebrafish. Mechanisms of development *122*, 157-173.

- Wallace, K.N., and Pack, M. (2003). Unique and conserved aspects of gut development in zebrafish. Developmental biology *255*, 12-29.

- Weaver, A.M., Heuser, J.E., Karginov, A.V., Lee, W.L., Parsons, J.T., and Cooper, J.A. (2002). Interaction of cortactin and N-WASp with Arp2/3 complex. Current biology : CB *12*, 1270-1278.

- Wegner, A., Aktories, K., Ditsch, A., Just, I., Schoepper, B., Selve, N., and Wille, M. (1994). Actin-gelsolin interaction. Advances in experimental medicine and biology *358*, 97-104.

- Williams, S.E., Beronja, S., Pasolli, H.A., and Fuchs, E. (2011). Asymmetric cell divisions promote Notch-dependent epidermal differentiation. Nature *470*, 353-358.

- Wooldridge, A.A., Fortner, C.N., Lontay, B., Akimoto, T., Neppl, R.L., Facemire, C., Datto, M.B., Kwon, A., McCook, E., Li, P.*, et al.* (2008). Deletion of the protein kinase A/protein kinase G target SMTNL1 promotes an exercise-adapted phenotype in vascular smooth muscle. The Journal of biological chemistry *283*, 11850-11859.

- Worthylake, R.A., Lemoine, S., Watson, J.M., and Burridge, K. (2001). RhoA is required for monocyte tail retraction during transendothelial migration. The Journal of cell biology *154*, 147-160.

- Wu, W., Kitamura, S., Truong, D.M., Rieg, T., Vallon, V., Sakurai, H., Bush, K.T., Vera, D.R., Ross, R.S., and Nigam, S.K. (2009). Beta1-integrin is required for kidney collecting duct morphogenesis and maintenance of renal function. American journal of physiology Renal physiology *297*, F210-217.

- Xia, Y., Nivet, E., Sancho-Martinez, I., Gallegos, T., Suzuki, K., Okamura, D., Wu, M.Z., Dubova, I., Esteban, C.R., Montserrat, N.*, et al.* (2013). Directed differentiation of human pluripotent cells to ureteric bud kidney progenitor-like cells. Nature cell biology *15*, 1507-1515.

- Xu, K., and Cleaver, O. (2011). Tubulogenesis during blood vessel formation. Seminars in cell & developmental biology *22*, 993-1004.

- Xu, K., Sacharidou, A., Fu, S., Chong, D.C., Skaug, B., Chen, Z.J., Davis, G.E., and Cleaver, O. (2011). Blood vessel tubulogenesis requires Rasip1 regulation of GTPase signaling. Developmental cell *20*, 526-539.

- Yamada, S., Pokutta, S., Drees, F., Weis, W.I., and Nelson, W.J. (2005). Deconstructing the cadherin-catenin-actin complex. Cell *123*, 889-901.

- Yamanaka, T., and Ohno, S. (2008). Role of Lgl/Dlg/Scribble in the regulation of epithelial junction, polarity and growth. Frontiers in bioscience : a journal and virtual library *13*, 6693-6707.

- Yang, B., Sonawane, N.D., Zhao, D., Somlo, S., and Verkman, A.S. (2008). Small-molecule CFTR inhibitors slow cyst growth in polycystic kidney disease. Journal of the American Society of Nephrology : JASN *19*, 1300-1310.

- Yasuda, T., Saegusa, C., Kamakura, S., Sumimoto, H., and Fukuda, M. (2012). Rab27 effector Slp2-a transports the apical signaling molecule podocalyxin to the apical surface of MDCK II cells and regulates claudin-2 expression. Molecular biology of the cell *23*, 3229-3239.

- Yu, F., Morin, X., Cai, Y., Yang, X., and Chia, W. (2000). Analysis of partner of inscuteable, a novel player of Drosophila asymmetric divisions, reveals two distinct steps in inscuteable apical localization. Cell *100*, 399-409.

- Yu, W., Datta, A., Leroy, P., O'Brien, L.E., Mak, G., Jou, T.S., Matlin, K.S., Mostov, K.E., and Zegers, M.M. (2005). Beta1-integrin orients epithelial polarity via Rac1 and laminin. Molecular biology of the cell *16*, 433-445.

- Zhang, X., Mernaugh, G., Yang, D.H., Gewin, L., Srichai, M.B., Harris, R.C., Iturregui, J.M., Nelson, R.D., Kohan, D.E., Abrahamson, D*., et al.* (2009). beta1 integrin is necessary for ureteric bud branching morphogenesis and maintenance of collecting duct structural integrity. Development *136*, 3357-3366.

- Zheng, Z., Zhu, H., Wan, Q., Liu, J., Xiao, Z., Siderovski, D.P., and Du, Q. (2010). LGN regulates mitotic spindle orientation during epithelial morphogenesis. The Journal of cell biology *189*, 275-288.

- Zhong, T.P. (2005). Zebrafish genetics and formation of embryonic vasculature. Current topics in developmental biology *71*, 53-81.

- Zihni, C., Mills, C., Matter, K., and Balda, M.S. (2016). Tight junctions: from simple barriers to multifunctional molecular gates. Nature reviews Molecular cell biology *17*, 564-580.